

**HYBRID SOLAR/HEAT PIPE/THERMOELECTRIC POWER
GENERATION**

LEE JIE SHENG

**A project report submitted in partial fulfilment of the
requirements for the award of the degree of
Bachelor of Engineering (Hons) Industrial Engineering**

**Faculty of Engineering and Green Technology
Universiti Tunku Abdul Rahman**

May 2015

DECLARATION

I hereby declare that this project report is based on my original work except for citations and quotations which have been duly acknowledged. I also declare that it has not been previously and concurrently submitted for any other degree or award at UTAR or other institutions.

Signature : _____

Name : LEE JIE SHENG

ID No. : 10AGB05198

Date : _____

APPROVAL FOR SUBMISSION

I certify that this project report entitled **“HYBRID SOLAR/HEAT PIPE/THERMOELECTRIC POWER GENERATION”** was prepared by **LEE JIE SHENG** has met the required standard for submission in partial fulfilment of the requirements for the award of Bachelor of Engineering (Hons) Industrial Engineering at Universiti Tunku Abdul Rahman.

Approved by,

Signature : _____

Supervisor : Prof. Ir. Dr. Ong Kok Seng

Date : _____

The copyright of this report belongs to the author under the terms of the copyright Act 1987 as qualified by Intellectual Property Policy of Universiti Tunku Abdul Rahman. Due acknowledgement shall always be made of the use of any material contained in, or derived from, this report.

© 2015, Lee Jie Sheng. All right reserved.

Specially dedicated to
my beloved family

ACKNOWLEDGEMENTS

I would like to thank everyone who had contributed to the successful completion of this project. I would like to express my profound sense of gratitude to my research supervisor, Prof. Ir. Dr. Ong Kok Seng for his invaluable advice, guidance and his enormous patience throughout the development of the research. Prof Ong has been constantly providing me with the knowledge I need to understand and proceed with my project. Despite his busy schedule, he would make time to meet me and discuss on the progress of my project. The regular discussions we had enabled me to gain vital and constructive feedbacks which assisted me in completing my final year project.

Besides that, I would like to express my gratitude to Mr Christopher Li Yi-Jin for guiding me throughout this project on the setup of the experimental apparatus and on writing up my report. Also, thanks to Mr. Tan Choong Foong, who helped me on the basics of thermoelectric, a field in which he is very knowledgeable with.

In addition, I would like thank Multi-precision for the fabrication of parts needed in my project. Multi-precision Industries Sdn. Bhd. helped in the machining of water cooling jackets. Besides that, I would like to thank my seniors, my coursemates and the laboratory assistants, Mr. Khairul and Mr. Syahrul for their constant help offered throughout this project.

Lastly, I would like to thank my family members and friends for their endless support and encouragement which motivated me to finish my final year project and complete the course.

HYBRID SOLAR/HEAT PIPE/THERMOELECTRIC POWER GENERATION

ABSTRACT

Solar energy is a renewable heat source freely and widely available everywhere in Malaysia throughout the year. Heat pipes are passive and very efficient heat transfer devices. Thermoelectric devices can be used for thermoelectric power generation from waste heat. A hybrid system with a combination of heat pipe solar collector and thermoelectric could provide both power and hot water simultaneously. An experimental set up was established that consisted of an evacuated glass tube heat pipe solar collector, four thermoelectric modules and four water cooling jackets. Investigations were conducted under outdoor conditions in order to determine and evaluate the performance of such a hybrid system.

Typical daily experimental results showed that all temperatures and DC output voltage increased as the day progressed and peaked to their maximum values around 15.30 hour and then started to decrease. On a sunny day with very little cloud cover, at the peak around 15.15 hour, the system was able to generate 0.114 W of power albeit at a very low electrical efficiency of only about 0.15 %. Recommendations for future studies are presented in the hope to achieve better results.

TABLE OF CONTENTS

DECLARATION	i
APPROVAL FOR SUBMISSION	ii
ACKNOWLEDGEMENTS	v
ABSTRACT	vi
TABLE OF CONTENTS	vii
LIST OF FIGURES	ix
LIST OF TABLES	xii
LIST OF SYMBOLS	xiii

CHAPTER

1	INTRODUCTION	1
	1.1 Background of Study	1
	1.2 Problem Statements	6
	1.3 Objective of Study	6
	1.4 Outline of Thesis	7
2	LITERATURE REVIEW	8
	2.1 Thermoelectric Modules for Power Generation	8
	2.2 Performance of Heat Pipe	13
	2.3 Solar Energy as Heat Source for Thermoelectric Power Generator	14
	2.4 Hybrid Solar Heat Pipe Thermoelectric Power Generation	17

3	EXPERIMENTAL INVESTIGATION	19
3.1	Experimental Apparatus	19
3.1.1	Evacuated Glass Tube Heat Pipe Solar Collector (ETHPSC)	24
3.1.2	Thermoelectric Modules	25
3.1.3	Water Cooling Jacket	26
3.2	Experimental Procedures	27
3.2.1	Thermocouple Calibration	27
3.2.2	Procedures	27
3.3	Experimental Calculations	28
3.1	Experimental Results	29
4	DISCUSSION OF RESULTS	49
4.1	Experimental Results of Solar Radiation, Ambient Temperature and Thermoelectric Voltage Generated	49
4.2	Experimental Results of Heat Pipe Temperatures	51
4.3	Experimental Results of Thermoelectric Hot and Cold Junction Temperatures and the Temperature Difference Across	52
4.4	Experimental Results of Current, Power and Thermoelectric Efficiencies	53
5	SUGGESTIONS FOR FURTHER STUDIES	55
6	CONCLUSIONS	56
	REFERENCES	57
	APPENDICES	61

LIST OF FIGURES

FIGURE	TITLE	PAGE
Figure 1:	Share of global energy production.	3
Figure 2:	Cross sectional view of a heat pipe [3].	4
Figure 3:	Schematic diagram of a thermoelectric module.	5
Figure 4:	Operation of TEG model (Ferrotec, 2015) [5].	6
Figure 5:	Perspective (a) and side view (b) of proposed TEG (Shiho Kim, et al, 2011).	10
Figure 6:	Experimental Setup of the System (Kim, S.K., et al, 2011).	11
Figure 7:	Concept of combined heat pipes and thermoelectric generators (HPTEG).	12
Figure 8:	Schematic diagram of hybrid generation system (Yuan Deng et al, 2012).	16
Figure 9:	Photograph of experimental setup.	19
Figure 10:	Schematic of SHPTE hybrid system.	20
Figure 11:	Isometric view of aluminium block.	20
Figure 12:	Flowing of energy in SHPTE hybrid system.	21
Figure 13:	Position of thermocouples in the SHPTE system.	23
Figure 14:	Longitudinal view of ETHPSC.	24
Figure 15:	Cross section view of ETHPSC.	24
Figure 16:	Dimensions of ThermoTEC™ Series HT8,12,F2,4040.	25
Figure 17:	Image of water channel within water cooling jacket.	26

Figure 18: Isometric view of water cooling jacket with dimension.	26
Figure 19: Typical experimental results showing solar radiation, ambient temperature and thermoelectric open voltage generated (RUN#1).	300
Figure 20: Typical experimental results showing solar radiation, ambient temperature and thermoelectric voltage generated (RUN#2).	31
Figure 21: Typical experimental results showing solar radiation, ambient temperature and thermoelectric voltage generated (RUN#3).	32
Figure 22: Typical experimental results showing solar radiation, ambient temperature and thermoelectric voltage generated (RUN#4).	33
Figure 23: Typical experimental results showing solar radiation, ambient temperature and thermoelectric voltage generated (RUN#5).	34
Figure 24: Typical experimental results showing heat pipe temperatures (RUN#1).	35
Figure 25: Typical experimental results showing heat pipe temperatures (RUN#2).	36
Figure 26: Typical experimental results showing heat pipe temperatures (RUN#3).	37
Figure 27: Typical experimental results showing heat pipe temperatures (RUN#4).	38
Figure 28: Typical experimental results showing heat pipe temperatures (RUN#5).	39
Figure 29: Typical experimental results showing thermoelectric hot and cold junction temperatures and the temperature difference (RUN#1).	40
Figure 30: Typical experimental results showing thermoelectric hot and cold junction temperatures and the temperature difference (RUN#2).	41
Figure 31: Typical experimental results showing thermoelectric hot and cold junction temperatures and the temperature difference (RUN#3).	42

Figure 32: Typical experimental results showing thermoelectric hot and cold junction temperatures and the temperature difference (RUN#4).	43
Figure 33: Typical experimental results showing thermoelectric hot and cold junction temperatures and the temperature difference (RUN#5).	44
Figure 34: Typical experimental results showing current, power and thermoelectric efficiencies for (RUN#2).	45
Figure 35: Typical experimental results showing current, power and thermoelectric efficiencies for (RUN#3).	46
Figure 36: Typical experimental results showing current, power and thermoelectric efficiencies for (RUN#4).	47
Figure 37: Typical experimental results showing current, power and thermoelectric efficiencies for (RUN#5).	48

LIST OF TABLES

TABLE	TITLE	PAGE
1a	Raw Data of Run #1	62
1b	Raw Data of Run #1	64
2a	Raw Data of Run #2	65
2b	Raw Data of Run #2	66
3a	Raw Data of Run #3	67
3b	Raw Data of Run #3	68
4a	Raw Data of Run #4	69
4b	Raw Data of Run #4	70
5a	Raw Data of Run #5	71
5b	Raw Data of Run #5	72
6	Summary of Run #1	73
7	Summary of Run #2	74
8	Summary of Run #3	74
9	Summary of Run #4	75
10	Summary of Run #5	75

LIST OF SYMBOLS

A_{al}	total mean surface area of aluminium block over condensing section [m^2]
A_{SC}	horizontal surface area of ETHPSC exposed to solar radiation [= $D_o L_{hp, evap}$, m^2]
c_{pw}	specific heat of water [= 4.183 J/g K]
D_o	diameter of outer glass tube [= 0.058 m]
D_i	diameter of inner glass tube [= 0.048 m]
H	solar radiation intensity [W/m^2]
I_{TE}	current developed in each TE [amp]
k_{al}	thermal conductivity of aluminium block [= 200 W/m K]
L_{al}	length of aluminium block over condenser section [= 0.105 m]
$L_{hp, evap}$	length of heat pipe evaporator section [= 1.645 m]
\dot{m}_w	total coolant water flow rate in each cooling jacket [g/s]
P_L	power developed by each TE module [W]
R_L	total load resistance for each TE module [= 5.3 ohm]
T_a	ambient temperature [K]
T_{cond}	heat pipe condenser temperature [K]
T_c	TE cold side junction temperature [K]
T_h	TE hot side junction temperature [K]
T_{fin}	temperature of aluminum fin and inner glass tube of ETHPSC [K]
T_w	mean coolant water temperature [K]
T_{wi}	coolant water inlet temperature [K]
T_{wo}	coolant water outlet temperature [K]
V_L	voltage developed in each TE under load [volt]
W_{al}	width of aluminium block over condenser section [= 0.07 m]
W_{wc}	width of cooling water jacket [= 0.06 m]

CHAPTER 1

INTRODUCTION

1.1 Background of Study

1.1.1 Solar Energy as Renewable Energy Source

As mankind are facing energy and environmental problems caused by rapid industrialization and high consumption of fossil fuel all over the world, research on renewable energy such as solar, wind, hydro, etc. have been widely conducted. With regard to solar energy, solar energy to generate electricity is becoming more crucial because it is the most abundant renewable energy source available and is pollution free. Solar energy is the sun's energy that can be converted into both thermal and electrical energy. Every hour, the sun radiates more energy into the earth than the entire human population uses in one whole year. (American Energy Independence, 2012) [1]

Solar power generation is the cleanest form of energy generation. There are no emissions from lengthy transportation and delivery, no environmental damage from open-pit mines, and it eliminates the need of waste storage on potential hazardous waste. Besides that, unlike conventional power generation from renewable energy such as tidal and wind, solar power generation does not require any moving mechanical parts, as there is no need of spinning turbines. Therefore, the need for maintenance is very low and extended lifetimes yield long-term economic profit in return. Although solar power generation required large land area but when the lifetime is expired, the land may be returned to its original use since it is free from residual stains of pollution.

The greatest need for energy consumption which is known as the peak times is during the day when businesses, offices and factories consume tremendous amounts of power to operate all kind of appliances such as air-conditioners, lighting, computers and manufacturing equipment. It is during these peak times where solar power is maximally available.

With the presence of modern technology, the utilization of solar energy for a variety of uses including generating electricity and heating water is made possible. Active solar systems use electrical devices to convert sunlight and heat from the sun to another form of usable energy include photovoltaics, solar thermal heating and cooling. On the other hand, passive solar systems eliminates the usage of any moving parts or electronics. These systems are being utilized in buildings where they are designed to collect, store, and distribute the heat energy from sunlight to provide comfort to the resident.

The main problem that come up against solar power is the current setup cost which is higher than most alternative forms of energy. However, this is changing quickly because governments from around the globe have acknowledged the advantages of solar power, and started getting involve with economic incentives and subsidies. The basic concept is that by scaling up the production and encouraging the development of solar power, improved technologies and innovations will reduce the cost. In the long run, at some point the cost of solar power will be on par with the cost of conventional power generators.

Figure 1 below from German Advisory Council on Global Change shows how the world will obtain its energy over the next century. While solar power accounts less than 1% of worldwide energy consumption right now but with the tremendous growth of solar power, it is expected to provide more than half of all the world's energy needs by the by the end of the century and become the world's leading energy resource. (German Advisory Council, 2003) [2]

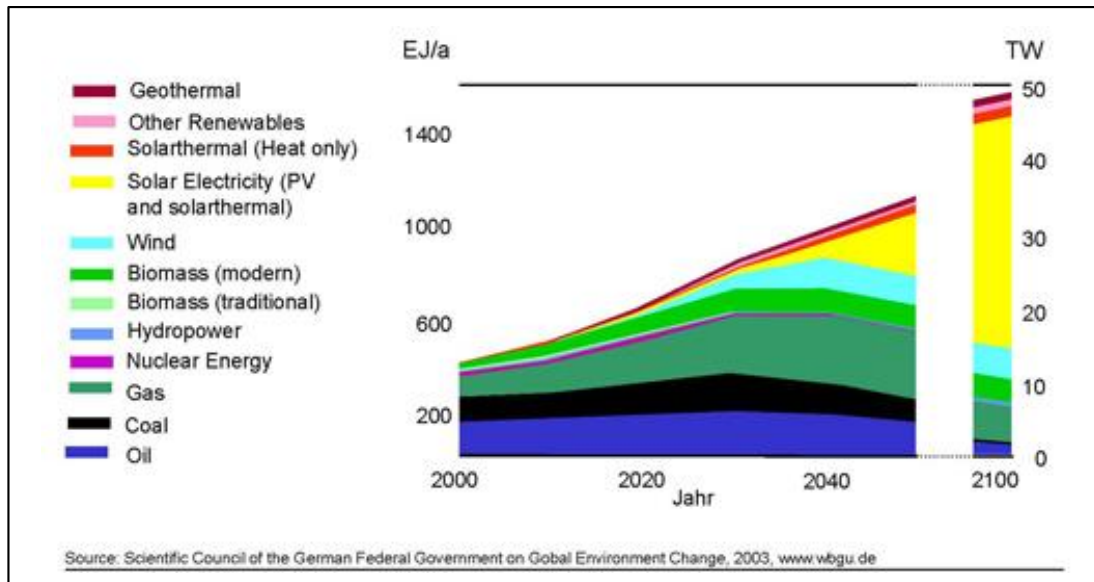


Figure 1: Share of global energy production
(German Advisory Council, 2003). [2]

1.1.2 Heat Pipe

A Heat pipe is a simple heat transfer device with high thermal conductivity that is able of transferring huge amounts of heat efficiently through the process of evaporation and condensation. Due to its simple design and economical manufacturing process, the application of heat pipe can be found widely such as in electronic equipment, solar energy systems, heat recovery systems and air conditioning systems.

A heat pipe shown in Figure 2 consists of three main sections, which are the evaporator, adiabatic and condenser. Heat pipe is a sealed and hollow tube whose inside walls are lined with wick to improve its performance. When the heat pipe is exposed to heat, the coolant in the wick absorb heats and evaporates. Due to a drop in the molecular density, the vaporized coolant is forced upwards to the cold end of the heat pipe. Condensation of vapour take place at the condenser section when the temperature is lower than the evaporation section. The coolant then releases the latent heat it acquired during evaporation and condenses back into liquid state. During the condensation of coolant, its molecular density increase again which caused the gravitational forces to pull the coolant down to the lower end of the heat pipe.

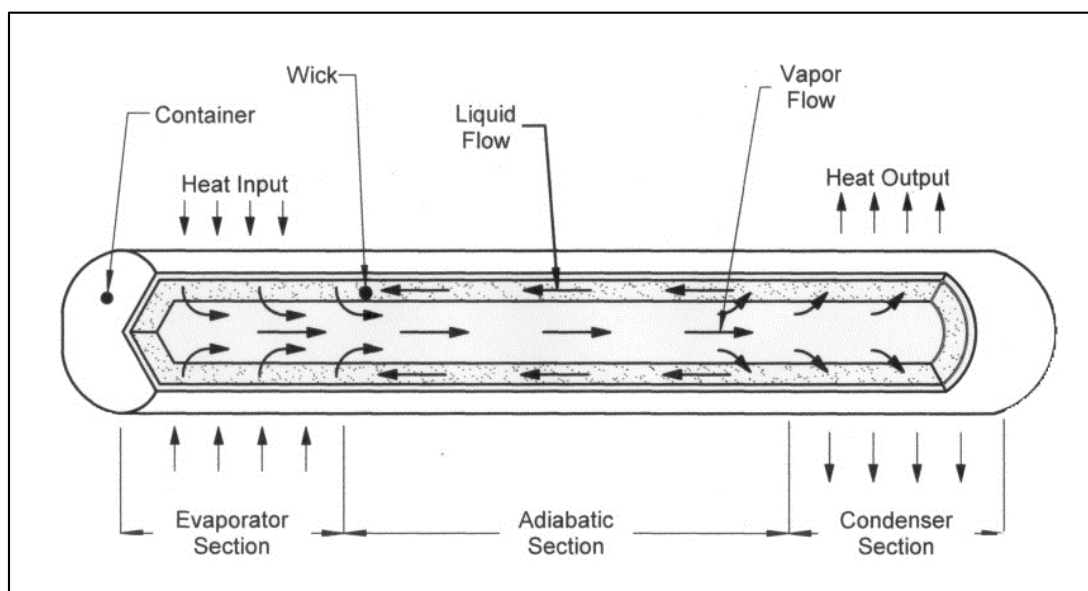


Figure 2: Cross sectional view of a heat pipe. [3]

1.1.3 Thermoelectricity

Thermoelectricity is the electricity produced from heat. Thermoelectricity is a two-way process, which is known as the Seebeck effect and Peltier effect. In the 1820's, Thomas J. Seebeck discovered the Seebeck effect where a temperature difference between one side of a material and the other can produce electricity. On the other hand, in 1830's, a French physicist Jean C. A. Peltier discovered the reverse of Seebeck effect whereby applying an electricity current through the material can create a temperature difference between its two sides. This phenomenon is known as Peltier effect, which is use to cool or heat things.

These discoveries led to the introduction of thermoelectric (TE) modules. TE modules consists of an array of *p*-type and *n*-type semiconductors elements, usually Bismuth Telluride (Bi_2TE_3), that are heavily doped with electrical carriers. The *p*-type and *n*-type elements are configured to be electrically connected in series but thermally connected in parallel to ensure a maximum power generation output. The elements are then sandwiched between two ceramic plates, one side covers the hot joins while the

side other covers the cold joins. The schematic of thermoelectric module is shown in Figure 3.

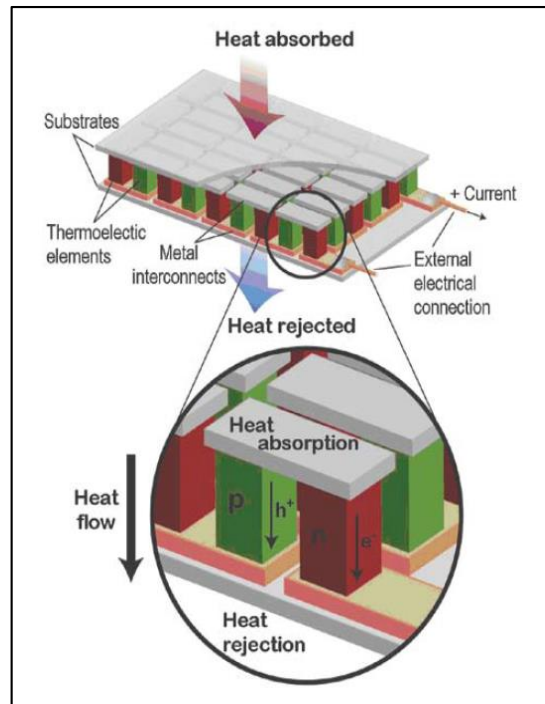


Figure 3: Schematic diagram of a thermoelectric module
(Snyder, G. and Toberer, E., 2008). [4]

By utilizing the Seebeck effect, TE module can act as a thermoelectric power generator (TEG). The conversion of heat into electricity is made possible by thermoelectric generators (TEG) which are solid-state energy converters that combine thermal, electrical, and also semiconductor properties. When one side of a TEG module absorbs heat, the mobile charge carriers start to diffuse, producing an even concentration distribution in the TEG along the temperature gradient, and this results in an electrical potential difference on both sides of the TE. Due to the thermoelectric effect, electrons flow through the *n-type* element to the colder side whereas in the *p-type* elements, the positive charge carriers flow to the cold side, and thus producing electricity. Figure 4 below demonstrate the operation of TEG module.

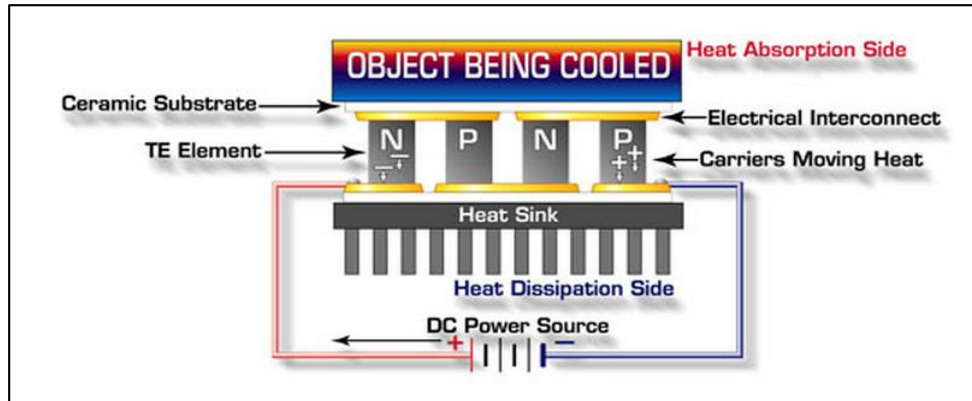


Figure 4: Operation of TEG model (Ferrotec, 2015). [5]

1.2 Problem Statements

Solar energy is a renewable heat source freely and widely available everywhere in Malaysia throughout the year. Heat pipes are passive and very efficient heat transfer devices. Thermoelectric modules can be used for thermoelectric power generation. A hybrid system which combines solar, heat pipe and thermoelectric could provide both power and hot water simultaneously. The purpose of this study is to evaluate the performance of a hybrid solar heat pipe collector coupled to a thermoelectric power generator module

1.3 Objective of Study

The objective of the study is to design and evaluate the performance of a hybrid solar/heat pipe/thermoelectric power generator.

1.4 Outline of Thesis

Chapter 1 introduces solar energy as a renewable energy source together with the working principles and application of heat pipes and thermoelectric. A literature survey on past works of thermoelectric power generation and solar heat pipe are presented in Chapter 2. Next, experimental investigations are presented in Chapter 3 and discussed in Chapter 4. Chapter 5 lists several suggestions recommended for further studies. The thesis is concluded in Chapter 6..

CHAPTER 2

LITERATURE REVIEW

2.1 Thermoelectric Modules for Power Generation

Suvit Punnachaiya et al (2013) [6] developed a 50 watt thermoelectric power generator by making use of low grade waste heat as his source of heat to retrieve and take advantage of the waste heat that are available in the cooling systems of industrial processes. The developed power generator is made up of 4 modules and each module can generate 15 watts. A total power output of 60 W was generated with the configuration of two modules connected in series and then attaching the two-module sets in parallel. Each module of 96 TEC devices had been connected in series to generate 15 W. Water steam was chosen as the heat source. With a temperature difference of 25 °C, the system was capable of generating an open-circuit DC of 250 V and short-circuit current of 1.2A. The generated power output was converted into AC power source of 50 W at 220 V with 50 Hz frequency using an inverter,. This system was able to achieve an electrical efficiency of 0.47%.

Risha Mal et al (2014) [7] developed a prototype for thermoelectric power generator module integrated with a double chambered forced draft cookstove. A module of an appropriate rating is chosen for the testing and then power generation is observed. The voltage generated is further stepped-up using a DC-DC step-up converter to run a DC brushless fan of 5V, 0.3A. The fan is to cool the one side of thermoelectric power generator and to supply the air to the combustion chamber of cookstove. The air is directed to the combustion chamber through a duct which increases the air-to-fuel ratio

which helps for a cleaner combustion. A net output of 4W is generated from the thermoelectric power generator.

A.M. Goudarzi et al (2013) [8] enhanced the combustion chamber of the stove by using electric fan and 56 mm × 56 mm thermoelectric generators (TEGs) as the drawback of traditional fire stoves is low in efficiency. Electrical fan was used to increase the air-to-fuel ratio. This in return improves the system efficiency and at the same time decreases air pollution by providing complete combustion of wood. On top of that the thermoelectric generators (TEGs) can produce power for the basic needs. A water-based cooling system were used to increase TEG efficiency of the as well as to provide hot water. The results achieved an average of 7.9 W and 14.7 W of output power can be produce at the maximum matched load. The stove generated a total power of 166W. The presented prototype was designed to meet the basic needs of domestic usage of electricity, hot water, and fulfilling the need of essential heating for warming the room and cooking.

Singh, R., et al (2011) [9] designed a power generation module made up 2 meter long copper-water thermosyphon with 100 mm in diameter, and 16 thermoelectric modules, attached the condenser. The combination of thermosyphon and thermoelectric modules enables it to create a fully passive and simple power supply system for remote area applications using the temperature differences that exists in a typical solar pond. In solar ponds, temperature difference ranges from 40 °C to 60 °C between the lower and upper convective zone. The highest power that could be provided by the designed TTM module was of 3.2 W when temperature difference of 27 °C was maintained across 16 thermoelectric modules. In this case, the open-circuit voltage of 26 V and the short circuit current of 0.4 A were obtained. The proposed system suits the profile for small-scale applications of solar ponds for power generation most ideally. Another plus point of this system is the thermal heat storage capability of the solar pond because the system is capable of supplying valuable electrical power continuously during the night or under cloudy conditions.

Shiho Kim, et al (2011) [10] developed a thermoelectric power generator (TEG) that uses the engine coolant of a 2 Litre engine. The conventional radiator was replaced with the proposed TEG without additional water pumps or mechanical devices. Figure 5 illustrates the schematic of proposed TEG. The system of proposed thermoelectric power generator is made up of hot side and cold side block. The cold side block consisted of heat pipes and heat sinks for the cooling purpose. 128 units of heat pipes installed was built, where thermoelectric modules were mounted on both sides of the hot and cold side block. Attached to the thermoelectric generator were 72 units of 4 mm by 4 mm bismuth telluride (Bi_2Te_3) thermoelectric modules. Based on the experimental results, the greatest amount of power output from the proposed TEG was estimated to be 75 W with module efficiency of 2.1%. The power generated from the waste heat of engine coolant during the driving mode at 80km/h has an overall efficiency of 0.3%. Conventional radiators can be substituted with the proposed TEG without the needs of additional water pumps or mechanical components in the existing water cooling structure of radiators.

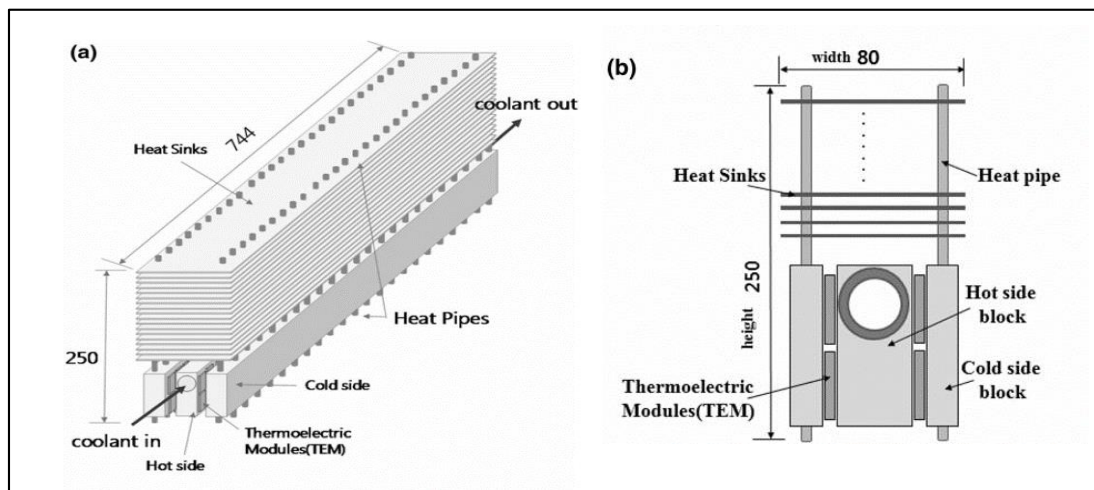


Figure 5: Perspective (a) and side view (b) of proposed TEG (Shiho Kim, et al, 2011).

With the help of a thermoelectric module (TEM) and heat pipes to generate electricity, Kim, S.K., et al. (2011) [11] performed a research on the recovery of waste heat from the exhaust gas system of hybrid vehicles. The system as shown in Figure 6 has a heat pipe thermal transporter, a thermoelectric converter, a cold fluid loops, a hot plate, and a data acquisition system. The cold fluid loops serve to cool the TEMs and they include

a fluid bath with temperature-controlled electrical heaters and pump. 112 units of bismuth telluride (Bi_2Te_3) thermoelectric modules (TEM) with dimension of 40 mm×40 mm×4.2 mm were located between the hot plate and cold fluid loop plate in two separate layers, with one heat pipe hot plate. All the TEM were electrically connected in series with a diode to ensure the current flows in a single direction. The compact design of this system makes it ideal for a more number of modules. Besides that it can easily be scaled to suit power generation purpose in an efficient system to regain thermal energy. When evaporator of the heat pipe was heated by the hot exhaust gas to 170 °C, the new waste heat recovery system can produce power as much as 350W. The great prospects for the application of this technology offer a more promising future for energy-efficient hybrid vehicles.

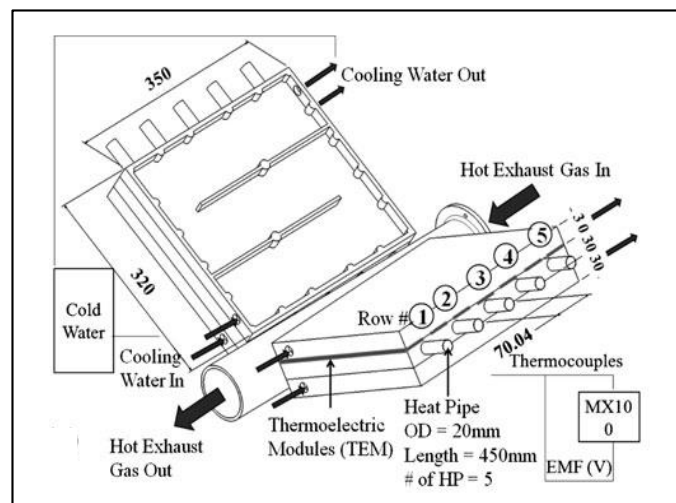


Figure 6: Experimental Setup of the System (Kim, S.K., et al, 2011).

Muhammad Fairuz Remeli et al (2015) [12] proposed a concept of fully passive and stand-alone cogeneration system based on the use of recovering industrial waste heat and converting it to electricity using heat pipes and thermoelectric power generators (HPTEG), Figure 7. The TEG is located between two finned heat pipes whereby heat pipe 1 heats the surface of the TEG and heat pipe 2 cools it. This creates a temperature gradient across TEG for generating electric current. Based on the outcome of the theoretical simulation it showed that a heat input of 1.9kW thermal energy can be recovered by eight modules of HPTEG. At the same time 27W of electric power could be produced.

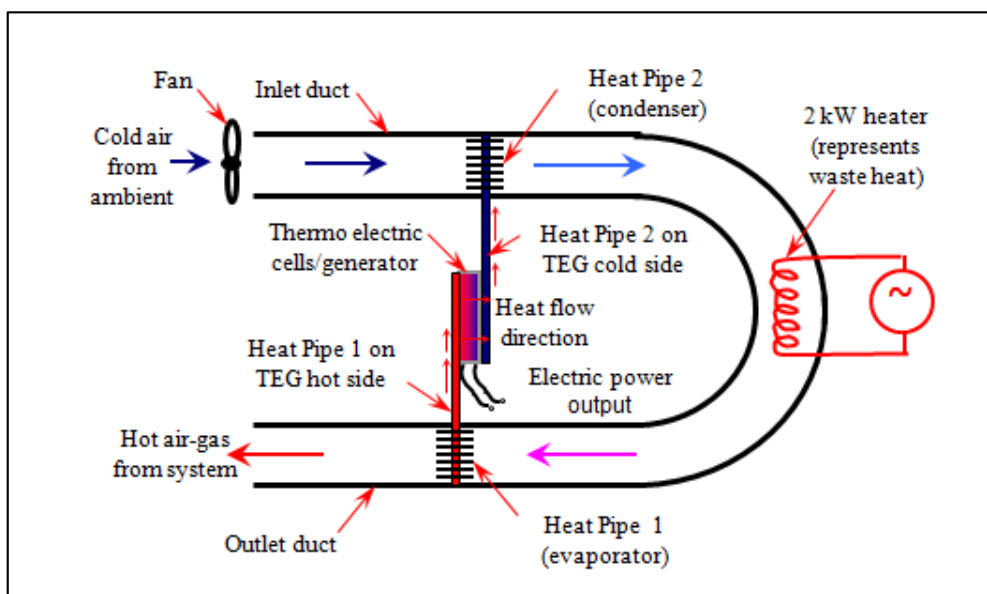


Figure 7: Concept of combined heat pipes and thermoelectric generators (HPTEG)
(Muhammad Fairuz Remeli et al, 2015).

2.2 Performance of Heat Pipe

Wei-Keng (2012) [13] studied the performance of the Laminar Heat Pipe Heat Exchanger. The experimental setup consists of two samples, one is the metal corrugated sheet with heat pipe, while another sample is without heat pipe. These two samples were dipped into hot water and an infrared thermal imager was used to observe the thermal image. The results showed that the temperature of the metal corrugated sheet with heat pipe increased at a faster pace than the temperature of the metal corrugated sheet without heat pipe. When the temperature of water and ambient were 30 °C and 20 °C respectively, the temperature of the metal corrugated sheet with heat pipe increased rapidly to 26 °C in one minute, whereas the one without heat pipe rises to 22 °C only. When the temperature of hot water increased to around 50 °C, the metal corrugated sheet with heat pipe increases rapidly to 33 °C within one minute, whereas the one without heat pipe maintained at 22 °C. The temperature difference is more pronounced when the water temperature is hotter. From the results, it is obvious that heat pipe affects the rising speed of temperature, suggesting that heat pipe plays a significant role in heat transfer process.

Mantelli, M. et al (2004) [14] conducted an experimental study on vertical thermosyphon for industrial heat exchangers applications. A carbon steel with 2.2m in length was used with evaporator and condenser section length of 1m and adiabatic section length of 0.2m. The carbon steel has an outer diameter dimension of 50.80mm. In order to examine the thermal performance of vertical thermosyphon, heat was supplied from a thermal bath. The results revealed that the thermal performance of thermosyphon is the most ideal when more heat was supplied. Besides that, the area of condenser section has no influence on the thermal performance. Throughout the experiment, the internal heat transfer coefficient of the condenser is minimally one order of the magnitude higher than evaporator. They also discovered that thermal performance of a heat exchanger relies on the tube external heat transfer conditions by using thermosyphon technology.

2.3 Solar Energy as Heat Source for Thermoelectric Power Generator

Ning Zhu et al (2013) [15] conducted a research on small solar power generation system. A small parabolic collector was used to collect both the light and heat. A thermoelectric generator (TEG) consisting of 4 Peltier modules was designed. The TEG was mounted to the focus part of parabolic collector. A test was conducted to identify the performance of electricity generation by the solar power generation system and found that with a temperature difference of 40 °C, the system is able to produce an open voltage up to 3.9V.

Concentrating solar power (CSP) is a special renewable energy technology. It is a method to increase the solar power density. Taleb M. Maslamani (2014) [16] carried out studies on the design of the solar thermoelectric generators (STG), focusing mainly on systems with high optical concentration that use multiple material systems to maximize efficiency over a large temperature difference. A single-stage generators are considered, over an optical concentration range of 0.1 to 1000X. The results showed that in high concentration STG, it is possible to achieve conversion efficiencies up to 13% with current thermoelectric materials and selective surfaces. The assembled system as the concentrator thermoelectric generator (CTEG) is capable of generating electric power output of around 5.5 W when the temperature difference is about 35 °C. The experimental results agreed with the mathematical model. In summary, further testing about the full understanding of the CTEG should be studied.

E. A. Ch'avez Urbiola and Y. Vorobiev (2013) [17] performed a study on solar-concentrating system based on thermoelectric generators (TEGs). The TEG array has six electricity generating elements connected in series. Solar radiation was concentrated on one side while the other side was cooled by running water. A sun-tracking concentrator with a mosaic set of mirrors was orientated towards the sun by using two pairs of radiation sensors, a differential amplifier and two servomotors. The hot side and cold side temperature of TEGs during midday is about 200 °C and 50 °C respectively. The system produced an average of 20 W electrical power and 200 W of thermal power stored in water with a temperature of around 45 °C.

Hasan Nia et al (2014) [18] presented a design, whereby Fresnel lens and thermoelectric module were used to focus solar beam and produce electrical power, respectively. The design consisted of a mono-axial adjustable structure, a thermoelectric generator (TEG) and a Fresnel lens with an area of 0.09 m^2 . An array of Fresnel lenses concentrate the solar radiation in their focal points to increase the intensity of radiation. In addition, oil reservoirs were located at the center of each lens. There, the heat absorbed by the oil was transferred to the water reservoir which is attached with thermoelectric module. The heat transfer in between the oil and water reservoir create a temperature difference across both sides of the thermoelectric module and thus generated electricity. The experimental results revealed that under solar radiation of 705.9 W/m^2 , the power output is 1.08 W at an electrical efficiency of 51.33% . Finally, it is recommended to employ an array of Fresnel lenses that transfer heat to thermoelectric module by an intermediate fluid in order for the thermoelectric module to generate electricity optimally.

L. Miao et al (2015) [19] designed a prototype solar thermoelectric cogenerator (STECG) consisted of solar-selective absorber (SSA) slab, thermoelectric modules (TE), a depressed water flow tube (multichannel cooling heat sink, MCS), and a $2 \text{ m} \times 2 \text{ m}$ east–west focal axis parabolic trough concentrator. Six Bi_2Te_3 thermoelectric modules were arranged in series and bonded directly to the rear surface of the solar absorber slab. The maximum temperature on the hot-side of the TE module was $152 \text{ }^\circ\text{C}$. Under the best environmental and solar radiation conditions, the system achieved an electrical efficiency of 1.14% , heat exchange coefficient of the MCS of 56.1% , and overall system efficiency of 49.5% . To justify these values, an equivalent thermal network diagram based on a single-temperature-node heat transfer model representing the respective system components was used to analyse the thermal transfer and losses of the system. Finally, power output of 18 W was generated, with 2 Litre per min of hot water at $37 \text{ }^\circ\text{C}$ were produced and stored in an insulated tank.

Yuan Deng et al (2012) [20] developed a hybrid generation system (HGS) driven by solar energy was with the help of an integrated design, where it comprised of a silicon thin-film solar cell (STC), thermoelectric generators (TEGs) and a heat collector to enhance the power generation efficiency. Figure 8 shows the schematic diagram of HGS. The STC serves two purposes where it converts parts of the solar energy

absorbed into electric energy. The STC can also produce thermoelectric conversion whereby the heat collector collects parts of the solar energy and conducts to TEG. The total power generated by the HGS is twice as large as the one generated by a single STC. In other words, the developed HGS is a promising power system because it has more potential at broadening the usage of the solar spectrum and improving the photoelectric conversion efficiency. Under an illumination intensity of $60\text{mW}/\text{cm}^2$, the STC can only achieve a photovoltaic conversion efficiency of only 4.55%. The temperature difference across the TEG influences the performance of TEG. For this reason, there are a few alternatives available to improve the performance of HGS such as by using TEG with higher ZT material, PV with better efficiency, and by optimizing thermal management design of HGS.

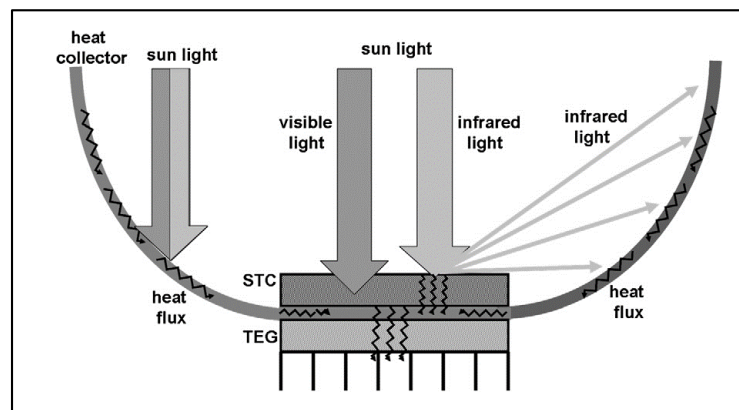


Figure 8: Schematic diagram of hybrid generation system (Yuan Deng et al, 2012).

Hongnan Fan (2011) [21] built a concentrator thermoelectric generator consisted of a parabolic dish concentrator (CTEG) of 1.8 m diameter, two-axes linear tracking system, liquid cooled system and Bi_2Te_3 thermoelectric modules. Laboratory tests were conducted under controlled experimental conditions. At a temperature difference of $110\text{ }^\circ\text{C}$ a single thermoelectric generator was able to produce a maximum power output of 4.8W with conversion efficiency of 2.9%. Besides that, a few tests have been carried out in order to get the actual capacity of the parabolic dish. The CTEG was capable of producing an electrical power of up to 5.9W with a temperature difference of $35\text{ }^\circ\text{C}$, the receiver achieved a maximum temperature of $143\text{ }^\circ\text{C}$ and the overall efficiency is 11.4%.

2.4 Hybrid Solar Heat Pipe Thermoelectric Power Generation

In pursuance of further improve on the efficiency of a TEG system, integration of various technologies has been carried out by researchers in order to provide the TE modules with ample heat absorption and heat rejection. With solar energy as an abundant source of heat energy and the heat transfer capabilities of heat pipe technologies, many have worked to achieve the maximum performance out of the currently available TE devices.

Wei He et al (2012) [22] conducted an experimental study on integrating the evacuated glass tube heat pipe solar collectors with thermoelectric modules to heat water and generate electricity. The thermoelectric modules were sandwiched between the condenser of heat pipe and a water channel. The heat from solar absorbed within the evacuated glass tube was transferred to the condenser of heat pipe and subsequently to thermoelectric module. They also presented a mathematical model to predict the electrical and thermal performance of the system. The results illustrated that the SHP-TE unit is able to achieve an electrical efficiency more than 1% and thermal efficiency of around 55% when the solar radiation is larger than 600 W/m^2 and water temperature of $45 \text{ }^\circ\text{C}$. The SHP-TE system has about 1-2% of electrical efficiency.

Ming Zhang et al (2013) [23] designed a solar thermoelectric cogenerator (STECG) system, which incorporate an evacuated tube heat pipe solar collector to the thermoelectric modules. This system is able to supply both electric power and heat simultaneously. A preliminary experimental results showed that when the solar radiation, velocity of wind, temperatures of ambient and water were 1000 W/m^2 , 1.3 m/s , $25 \text{ }^\circ\text{C}$ and $25 \text{ }^\circ\text{C}$ respectively, for the figure of merit of thermoelectric modules, $ZT_M = 0.59$, the generated power output reached 41.3 W at an electrical efficiency of 1.06%. The STECG is capable of generating 0.19 kWh of electricity. Meanwhile, the STECG also heated up about 300 litres of hot water from $25 \text{ }^\circ\text{C}$ to $55 \text{ }^\circ\text{C}$. For thermoelectric modules with $ZT_M = 1$, the power output was 64.80 W with the collector efficiency and electrical efficiency of 47.54% and 1.59%, respectively. The results imply that STECGs are economical and practical.

Lertsatitthanakorn et al (2008) [24] investigated a hybrid thermoelectric solar air collector which generates both electrical energy and thermal energy simultaneously. In this experiment, a double-pass thermoelectric solar air collector was developed where a heat absorber plate was heated up by the incident solar radiation to create a temperature difference across the thermoelectric modules. Ambient air flows through the heat sink which is located at the lower channel, this allows the flowing air to gain heat while cooling the thermoelectric module hence providing heat to the air flow. Results showed that thermal efficiency increases when the flow rate of the air is faster. The electrical efficiency is dependent on the temperature difference. When the temperature difference is 22.8°C, the power output generated by the system is 2.13 W at an efficiency of 6.17%. This concept of a solar collector for supplying heat source is widely anticipated to increase the output of TE power generating systems due to its abundance.

Sathawane N.S. and Dr. Walke P.V. (2015) [25] presented the development, experimentation and performance of the solar thermoelectric cogeneration system (STECG) which is proposed to be cost efficient. This system was based on the integration of evacuated glass tube solar collector with thermoelectric modules (TEMs) that is capable of producing electricity and heat simultaneously. The outcome from the experiment was excellent. The system produced a maximum power output of 1.4344 W when the temperature difference is 34°C. Within the temperature range of 329 K to 346 K, the maximum achievable value for Z_{Tm} is 0.2898 with a conversion efficiency of 1.1217 %. It is possible to mount more than 20 thermoelectric generating modules on this prototype. This will improve the power, figure of merit of the generator and thus the conversion efficiency for the same generator and corresponding to same temperature difference. They proposed that by having more evacuated tube solar collectors, the hot side temperature can be increased causing the power produced by the thermoelectric generator to increase. A higher temperature resistance thermoelectric module and a better generator design are solutions to improving power output.

CHAPTER 3

EXPERIMENTAL INVESTIGATION

3.1 Experimental Apparatus

A photograph of the SHPTE system is shown in Figure 9. This design combines an evacuated heat pipe solar collector (ETHPSC) with a thermoelectric power generation (TEG) module with water cooled heat sink to provide both power and hot water simultaneously. The schematic of the system can be seen in Figure 10. The system consists essentially of four units of thermoelectric modules together with four units of water cooling jackets with an aluminium block fitted over the end of the condenser section of the ETHPSC. The aluminium block shown in Figure 11 is machined to fit over the condenser end of the heat pipe. The thermoelectric (TE) modules is placed on the outer surfaces of all four sides of the aluminium block. Then the water cooling jackets are placed over the TE modules, sandwiching the TE.

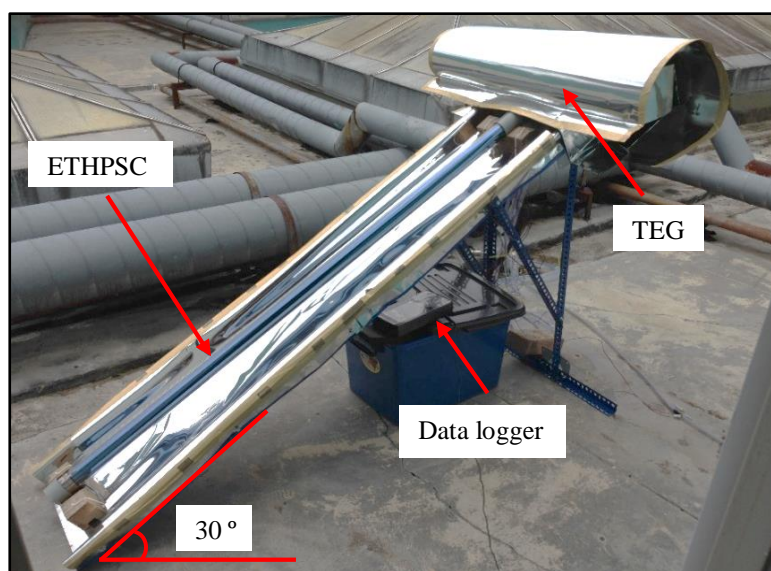


Figure 9: Photograph of experimental setup.

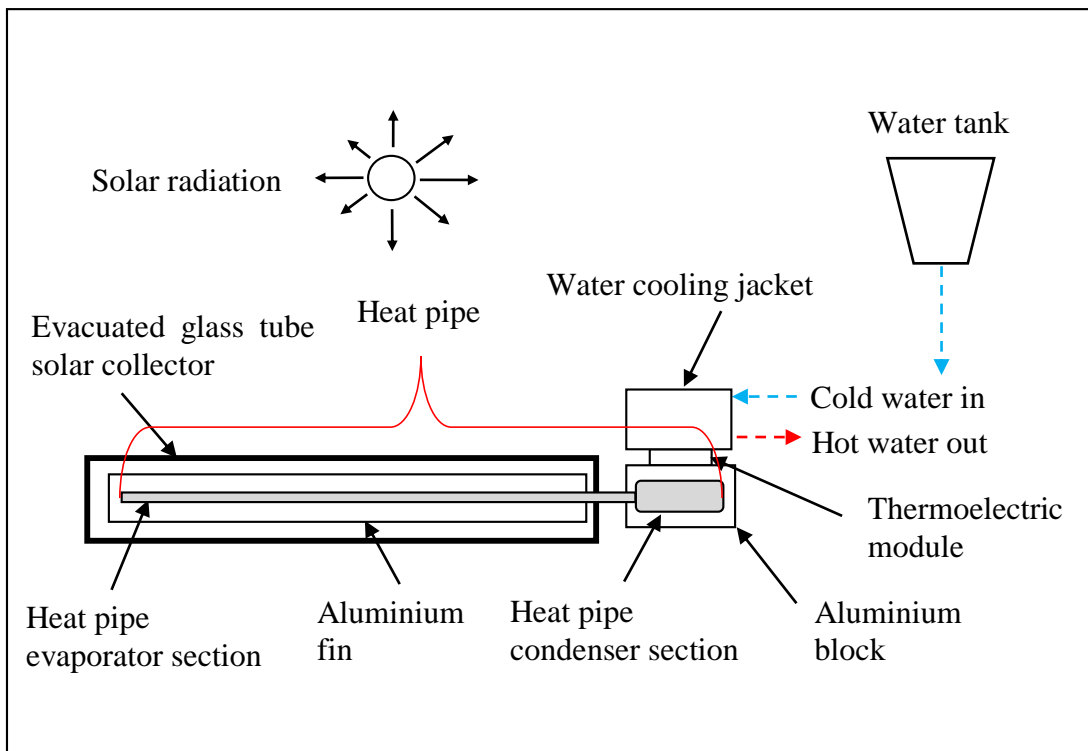


Figure 10: Schematic of SHPTE hybrid system.

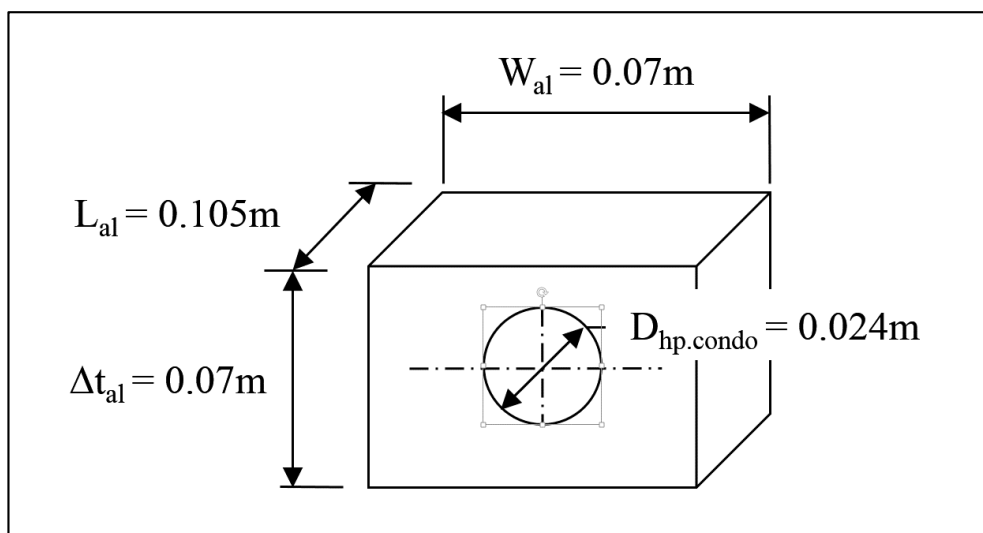


Figure 11: Isometric view of aluminium block.

When the ETHPSC is exposed to sunlight, incident solar energy is absorbed by the aluminium fin. A major portion of heat absorbed by the aluminium fin in the evaporator section of the heat pipe is conveyed to the condenser section at the end of the heat pipe. The rest is transmitted through the inner tube to the outer tube and is release into the the atmosphere. Heat transfers occurred within the condenser and the aluminium block and eventually heated up the aluminium block. Heat is then conducted across the heat spreader aluminium block to the hot junctions of the four units of thermoelectric modules and rejected at the cold junction. On the other hand, the cold junction of TE module is in close contact with the water cooling jacket. The rejected heat heats up the water flowing through the water cooling jackets. The temperature difference across both the hot and cold surfaces of the thermoelectric module and resulted in DC power being generated. In addition, the heat energy absorbed by the water is used as water heating thus increase the overall usefulness of the system. Figure 12 shows the flow of heat energy throughout in the system.

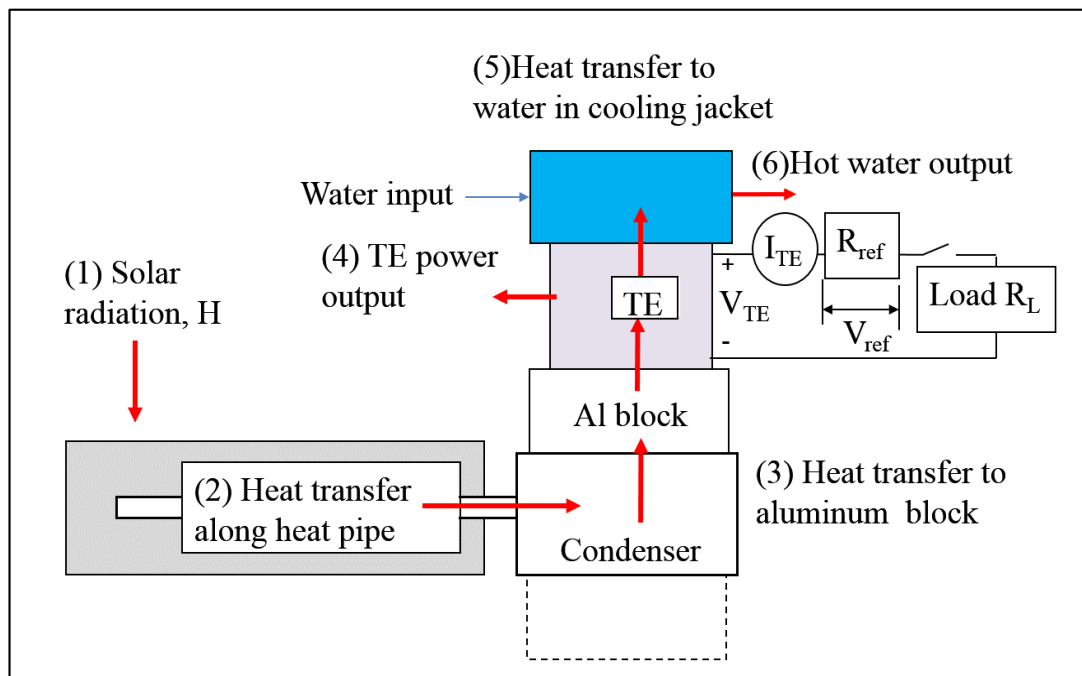


Figure 12: Flowing of energy in SHPTE hybrid system.

Thermocouples are used to measure the temperatures of water, heat pipe and ambient. The temperatures and voltages were recorded by a data logger, which is connected to the terminals that hold all the thermocouple wires. There were 38 thermocouple wires in total that were attached in the whole system. Three thermocouples were attached on the wall of heat pipe at the evaporator section and one at the adiabatic section. Then, another four thermocouples were inserted into the aluminium spreader to measure the temperature of the condenser. Besides that, 24 thermocouple wires were positioned evenly at all four sides of aluminium spreader and heat sink to measure their respective temperature. After that, another one thermocouple is located in ambient. Furthermore, the water distribution is in 1 to 4 configuration, whereby one input of water will be distribute to four water cooling jackets. One thermocouple wires was inserted at the main water input while the remaining four were inserted at the water outlet of all the four water cooling jackets to measure input and output the water temperature. Figure 13 is the schematic diagram that show the position of thermocouple wires to measure the temperature at each respective section of the system.

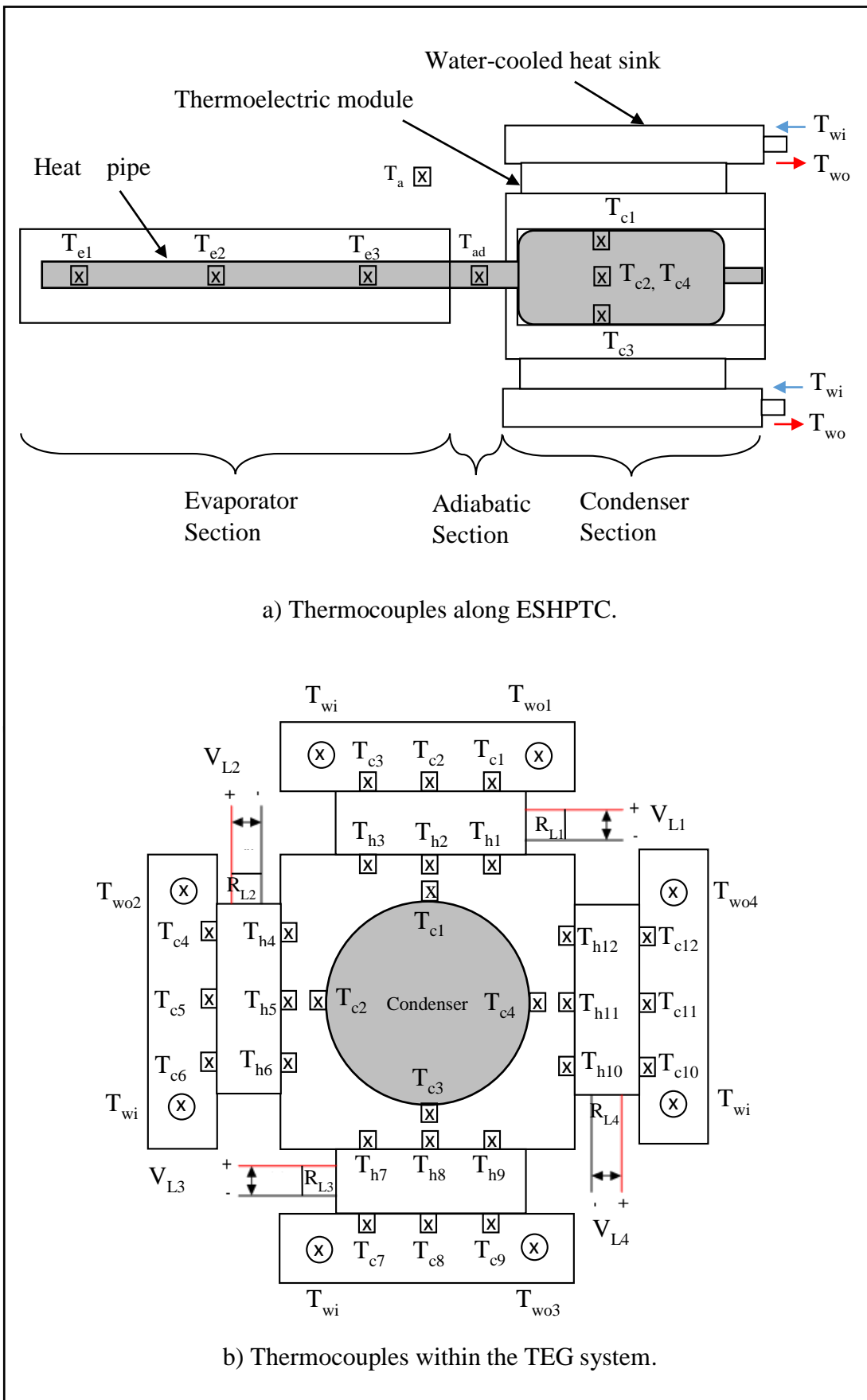


Figure 13: Position of thermocouples in the SHPTE system.

3.1.1 Evacuated Glass Tube Heat Pipe Solar Collector (ETHPSC)

The ETHPSC consists of a heat pipe tightly wrapped by an aluminium fin. The aluminium fin is placed in a very close contact with the inside surface of the inner glass tube. The evacuated glass tube consists of the outer glass tube and inner glass tube. The outer surface of the inner glass tube is coated with a selective coating. Figure 14 and Figure 15 show the detailed drawing of ETHPSC.

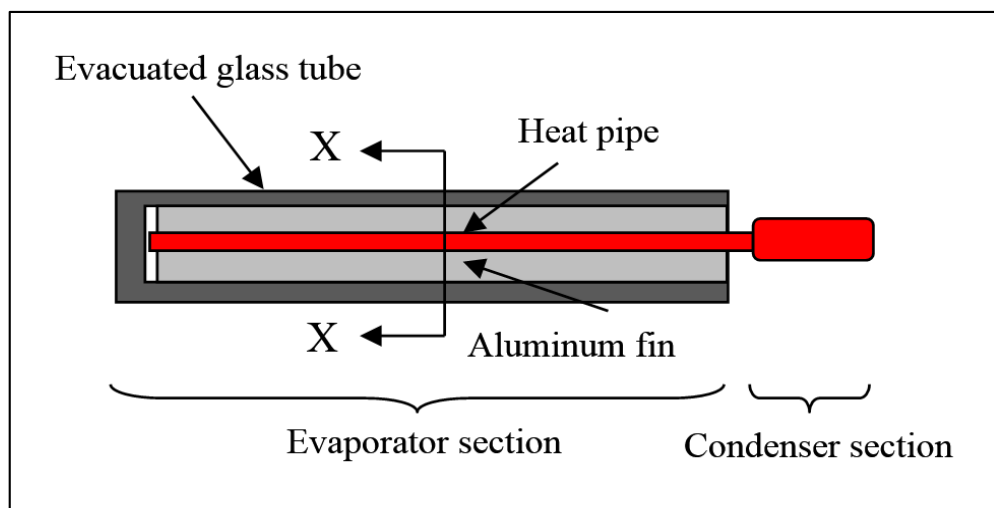


Figure 14: Longitudinal view of ETHPSC.

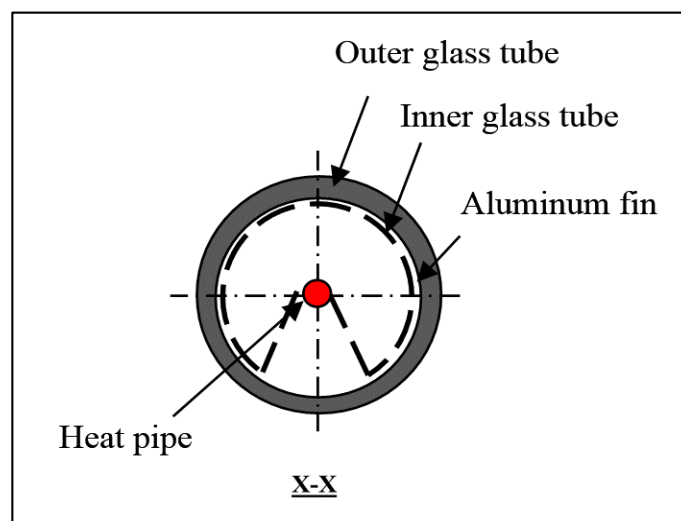


Figure 15: Cross section view of ETHPSC.

3.1.2 Thermoelectric Modules

The 4 thermoelectric modules used in the thermoelectric power generation (TEG) system are the ThermaTEC™ Series HT8,12,F2,4040. The thermoelectric series are designed to operate under high temperature applications. The ThermaTEC™ Series is assembled with proprietary solder construction, Bismuth Telluride (Bi_2Te_3) semiconductor material and thermally conductive Aluminium Oxide (Al_2O_3) ceramics, making these TE modules suitable for higher current application. These modules have a maximum operating temperature of $175\text{ }^\circ\text{C}$. The TE modules dimensions is $43.9\text{mm} \times 39.9\text{mm} \times 3.5\text{mm}$ as shown in Figure 16.

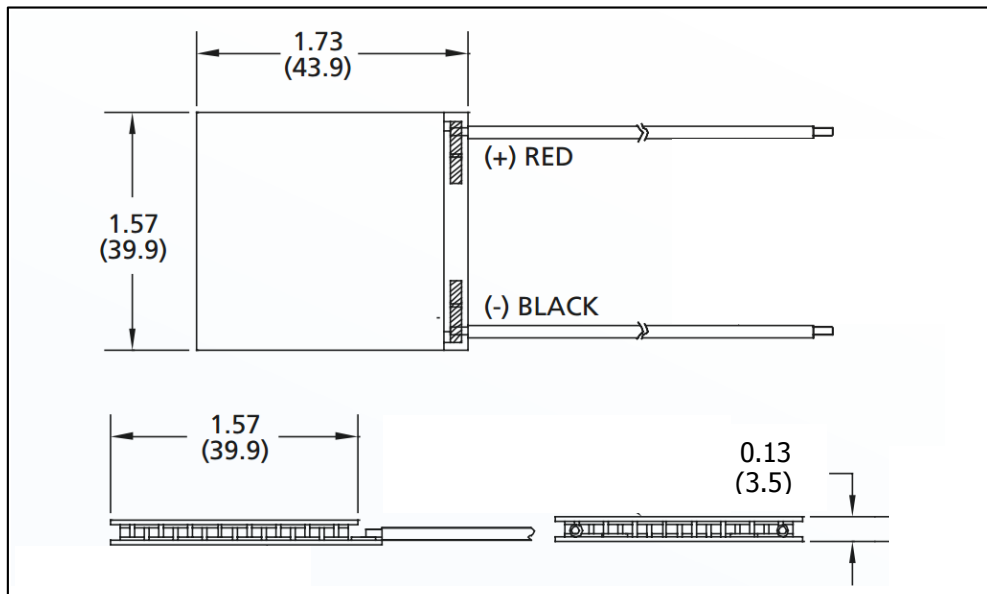


Figure 16: Dimensions of ThermaTEC™ Series HT8,12,F2,4040.

The thermoelectric modules are sandwiched between the aluminium heat spreader which spreads heat from the condenser and the water cooling jacket that provide heat to create a temperature difference on both faces. Non-hardening thermal paste is applied on both the surfaces of aluminium heat spreader and water cooling jacket to remove any small air gap, and increase the thermal conductivity. The temperatures of both hot and cold side are measured independently and the location of the thermocouple are shown in Figure 13 above.

3.1.3 Water Cooling Jacket

The water cooling system consists of four units of flat rectangular shaped aluminium water jackets each measuring $70\text{mm} \times 70\text{mm} \times 10\text{mm}$ thick with six 1mm diameter water channels machined inside and connected to two 5mm diameter common manifolds for water flow into and out of the jacket, Figure 17. This type of water cooling jacket is able to provide even cooling over a large surface area. An isometric sketch of the cooling water jacket with dimension is shown in Figure 18.

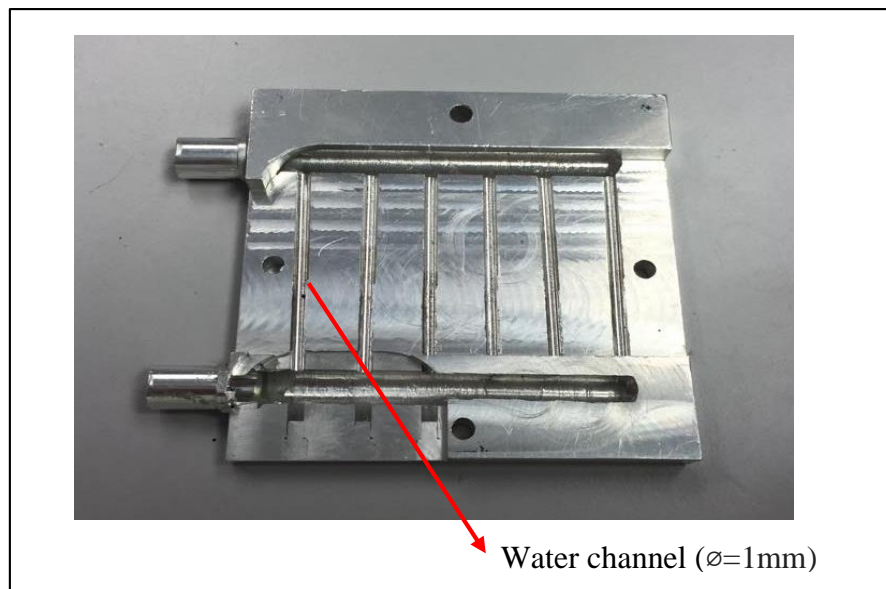


Figure 17: Image of water channel within water cooling jacket.

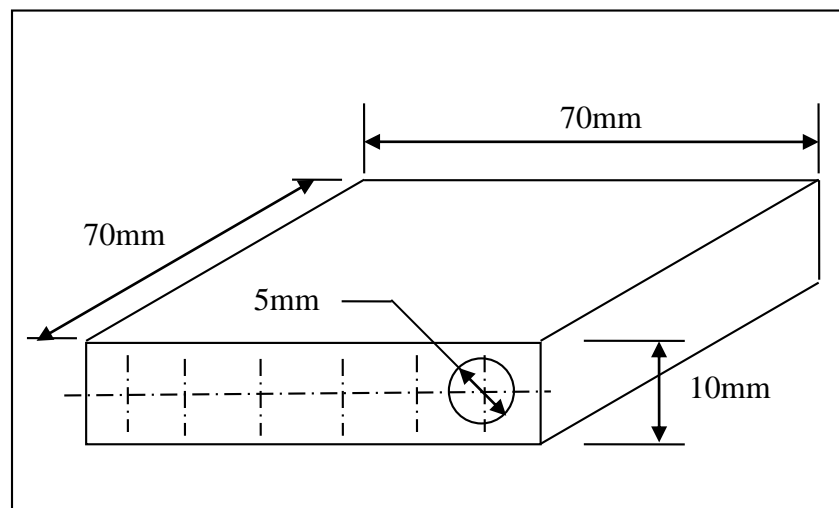


Figure 18: Isometric view of water cooling jacket with dimension.

3.2 Experimental Procedures

3.2.1 Thermocouple Calibration

Thermocouples were calibrated to examine the accuracy of each thermocouple before attaching them to the SHPTE hybrid system. 38 thermocouples were used in conducting this experiment and those thermocouples were ensured with high accuracy within ± 1 °C. Some equipment and apparatus were used to conduct the calibration of thermocouples. Including a stopwatch, thermos bath, terminal extension, data logger, distilled water, and calibrated thermometer. Before commencing the calibration, adequate distilled water was filled into the thermos bath. Then, the thermocouples were connected to terminal extension, which attached with the data logger. The end of the thermocouples was immersed into the water. After that, the water was heated up 30 °C and waited for 10 minutes to achieve steady state. The readings of thermos bath and calibrated thermometer were recorded. Calibrations were repeated by raising the distilled water temperature by 10 °C for every 20 minutes interval until the temperature reached 100 °C.

3.2.2 Procedures

The SHPTE hybrid system is placed outdoor to be exposed to solar radiation and the water valve is turned on at 10 in the morning and left to run for 7 hours. Before commencing the experiment, the water valve was turned on fully to maximize the flow rate in order to remove the stagnated water and air bubbles trapped within the water channel. This is to avoid the performance of thermoelectric module from affected by the uneven supply of water due to air bubbles.

Once the water flows are constant, the water flow rate is varied at different value to investigate the effect of water flow rate on the performance of thermoelectric power generation. Beakers were placed at water output channel and volume of water collected within a minute was measured to determine the water velocity. To ensure accurate water flow rate, the measurement were carried out twice and the average water velocity was determined.

In the meantime, a Kipp-and-Zonen pyranometer was placed under the direct sunlight and away from shadow to obtain maximum solar radiation. The pyranometer is connected to a computer where an installed software will record all the value of solar radiation and generate a graph of solar radiation vs time. In addition, the temperatures and voltage generated of the system are measured by the type T (Cu-con) thermocouples and recorded by a data logger on per minute basic to ascertain the steady-state of the system. From the accumulated data, the electrical and thermal efficiency of the system was calculated and several graphs are plotted in order to determine the overall performance of system.

Lastly, it is crucial to make sure that there is no water leakage from the piping as any leakage in piping could result in uneven water supply.

3.3 Experimental Calculations

By measuring the voltage, power generated can be calculated:

The current can be calculated from:

$$I = \frac{V}{R}$$

The power generated is calculated from:

$$P = \frac{V^2}{R}$$

and the efficiency to TE power generation is:

$$\eta_{TE} = \frac{4 \times P}{H \times A_{sc}} \times 100\%$$

3.1 Experimental Results

RUN#1 was conducted with an open-circuit to obtain the open voltage. RUN#2 to RUN#5 were conducted to investigate the performance of the system with external load connected. Power generated can be measured and the electrical efficiency of the hybrid system determined. A load resistance of 5.3Ω was incorporated into the system. In these experiment runs, the average water mass flowrate for RUN#2, RUN#3, RUN#4 and RUN#5 were kept at 0.9g/s, 1.5g/s, 1.6g/s and 8.3g/s respectively. Figure 19 shows the typical experimental results of solar radiation, ambient temperature and thermoelectric open voltage generated for RUN#1. Figure 20 to Figure 23 shows the typical experimental results of solar radiation, ambient temperature and thermoelectric voltage generated for RUN#2 to RUN#5. Figure 24 to Figure 28 shows the typical experimental results of heat pipe temperatures from RUN#1 to RUN#5. Figure 29 to Figure 33 shows the typical experimental results showing thermoelectric hot and cold junction temperatures and the temperature difference for RUN#1 to RUN#5. Figure 34 to Figure 37 shows the typical experimental results showing current, power and TE efficiencies for Run#2 to RUN#5

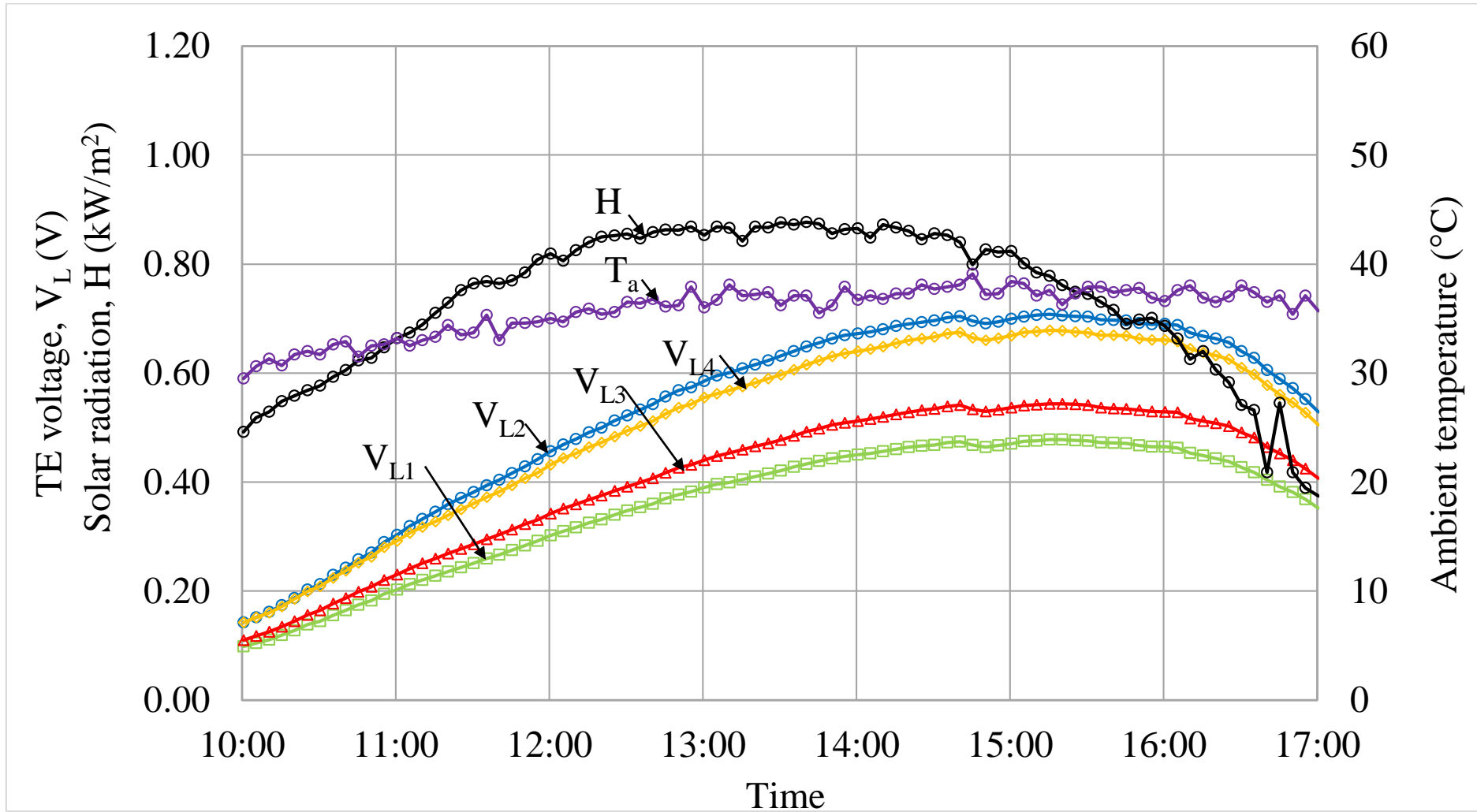


Figure 19: Typical experimental results showing solar radiation, ambient temperature and thermoelectric open voltage generated (RUN#1).

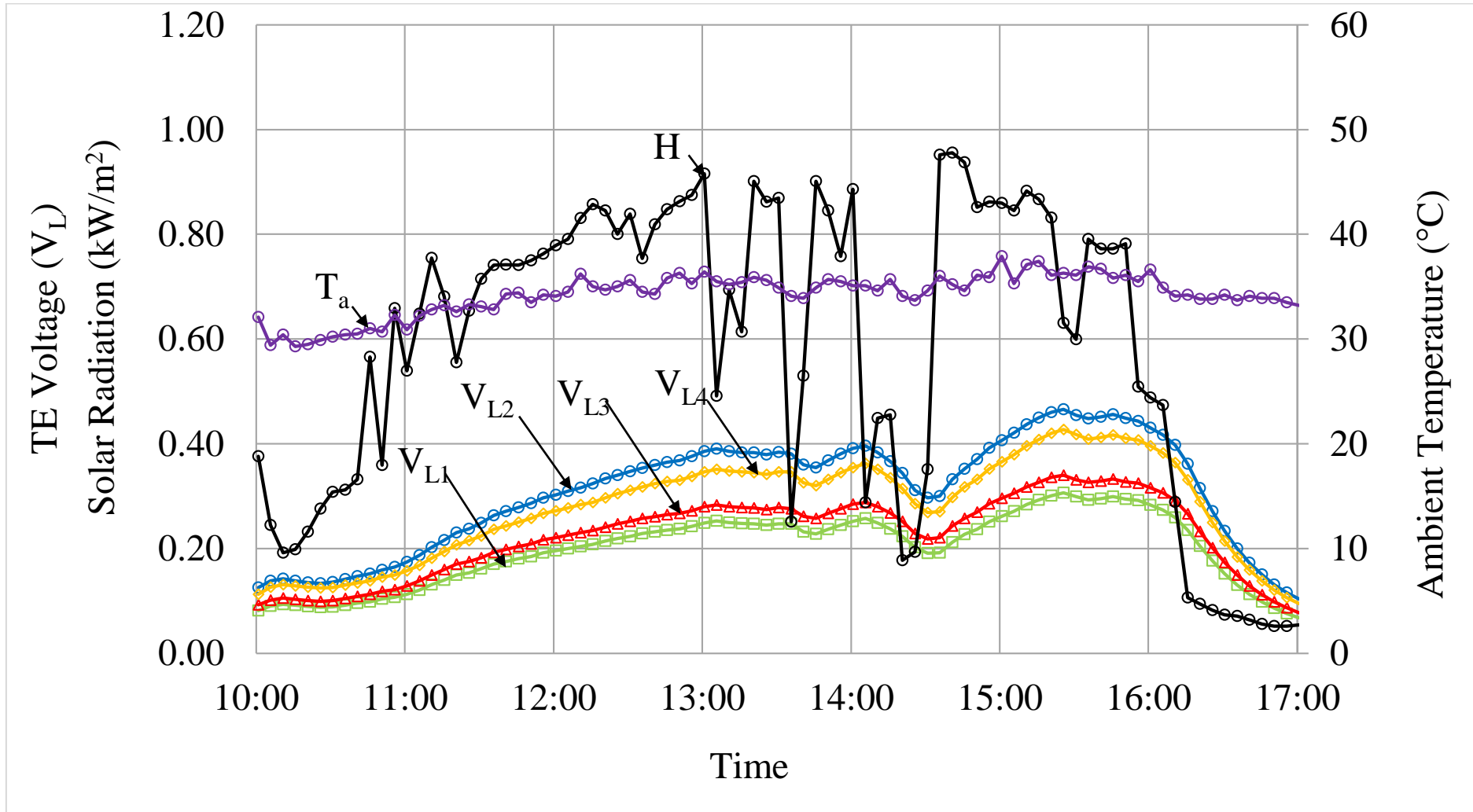


Figure 20: Typical experimental results showing solar radiation, ambient temperature and thermoelectric voltage generated (RUN#2).

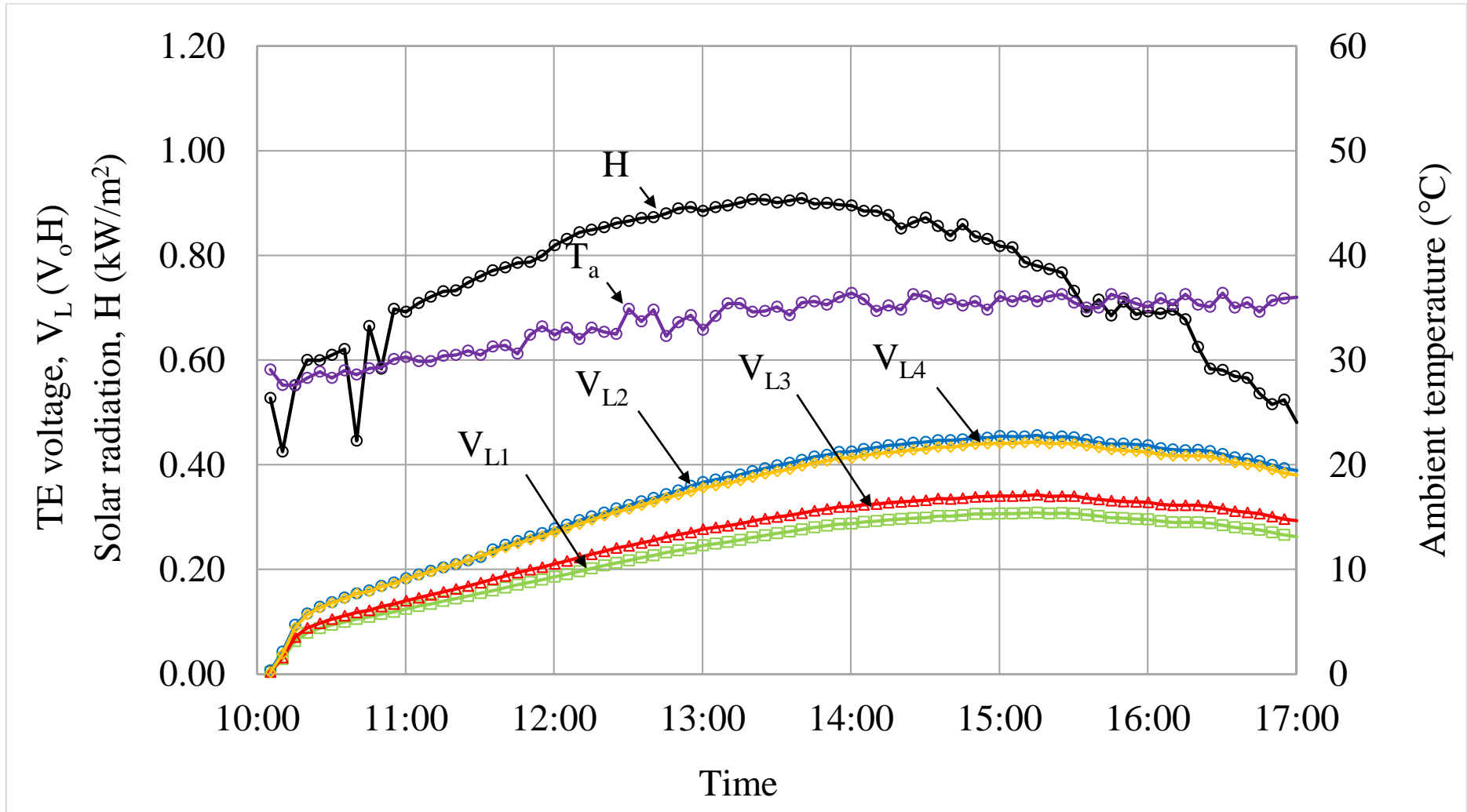


Figure 21: Typical experimental results showing solar radiation, ambient temperature and thermoelectric voltage generated (RUN#3).

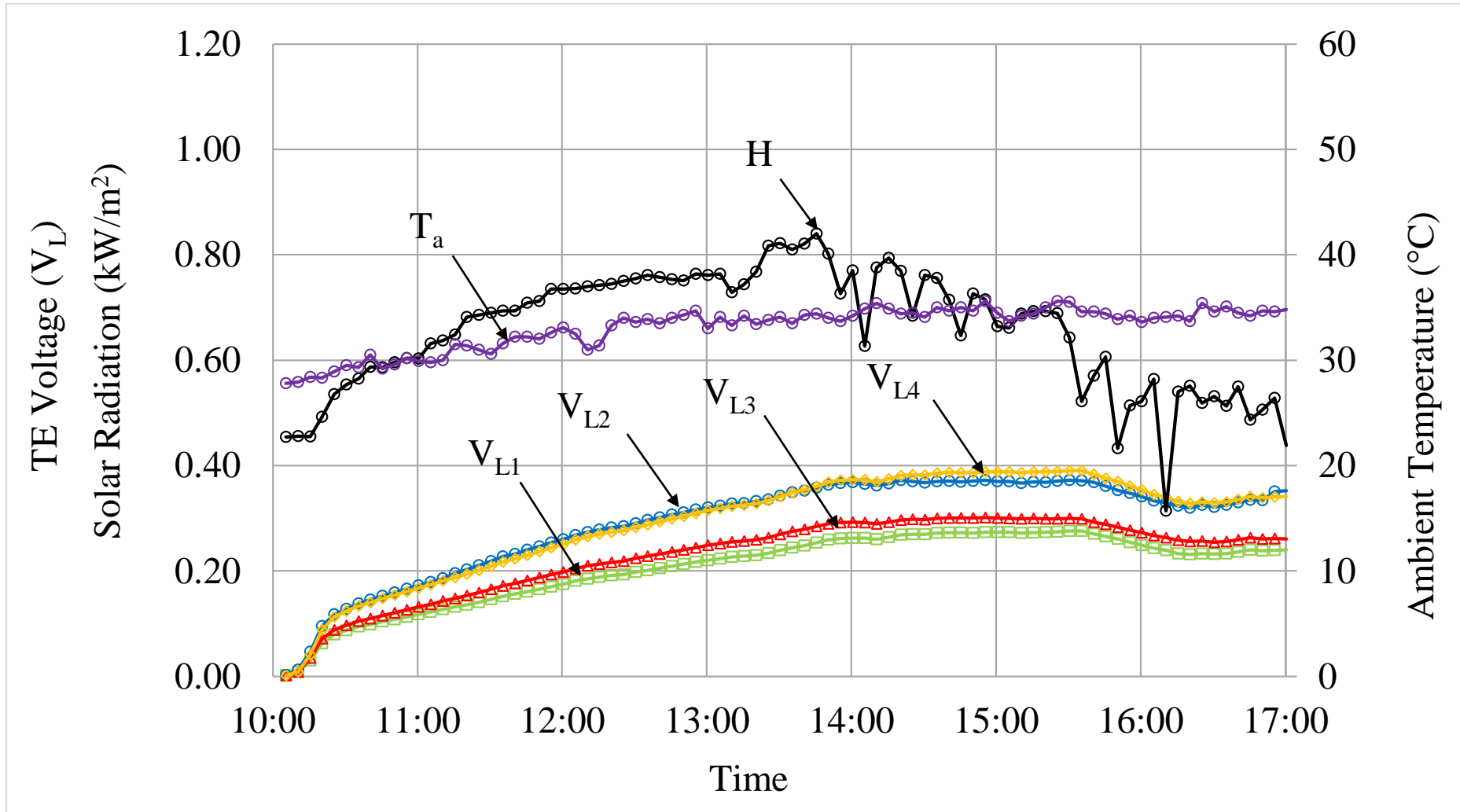


Figure 22: Typical experimental results showing solar radiation, ambient temperature and thermoelectric voltage generated (RUN#4).

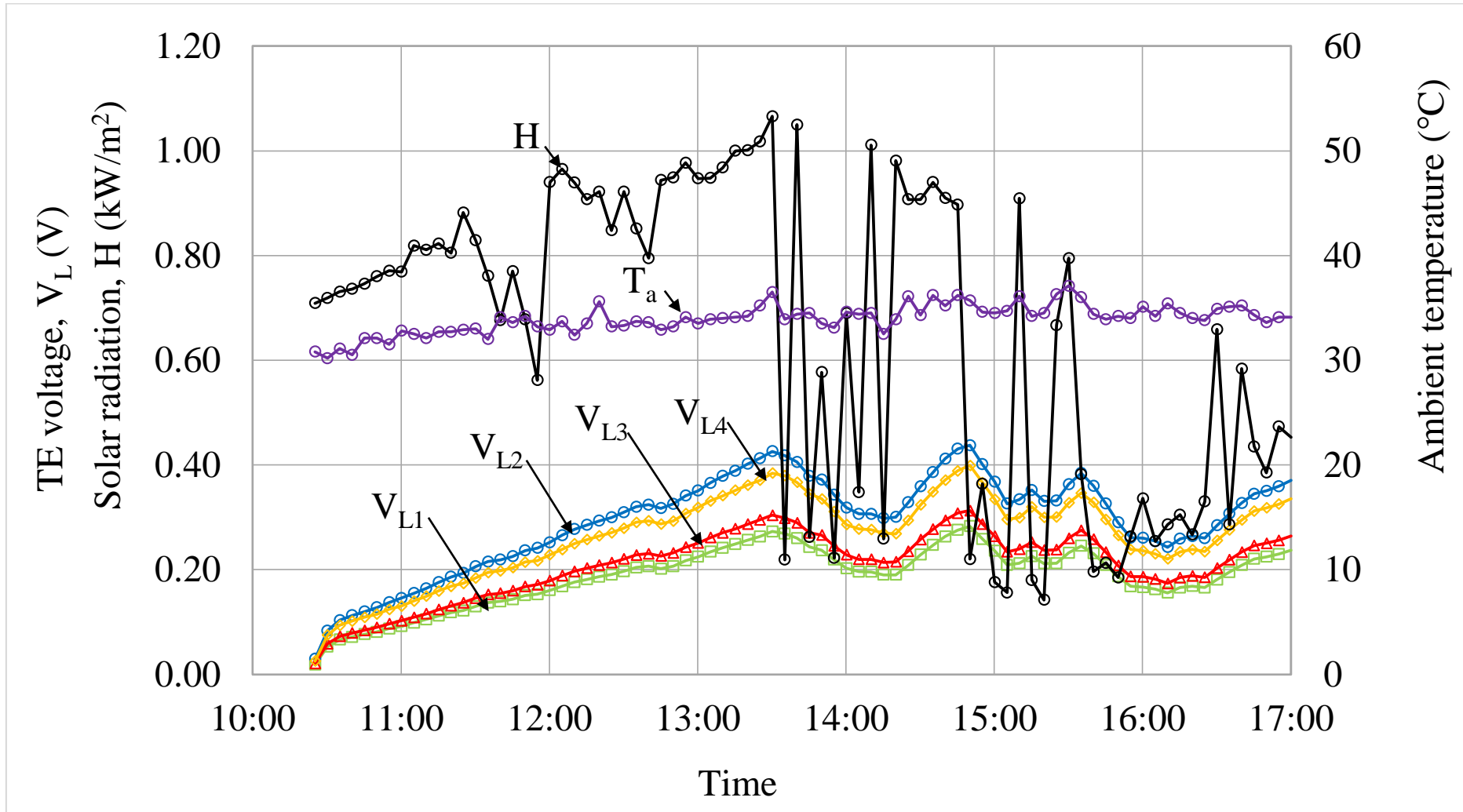


Figure 23: Typical experimental results showing solar radiation, ambient temperature and thermoelectric voltage generated (RUN#5).

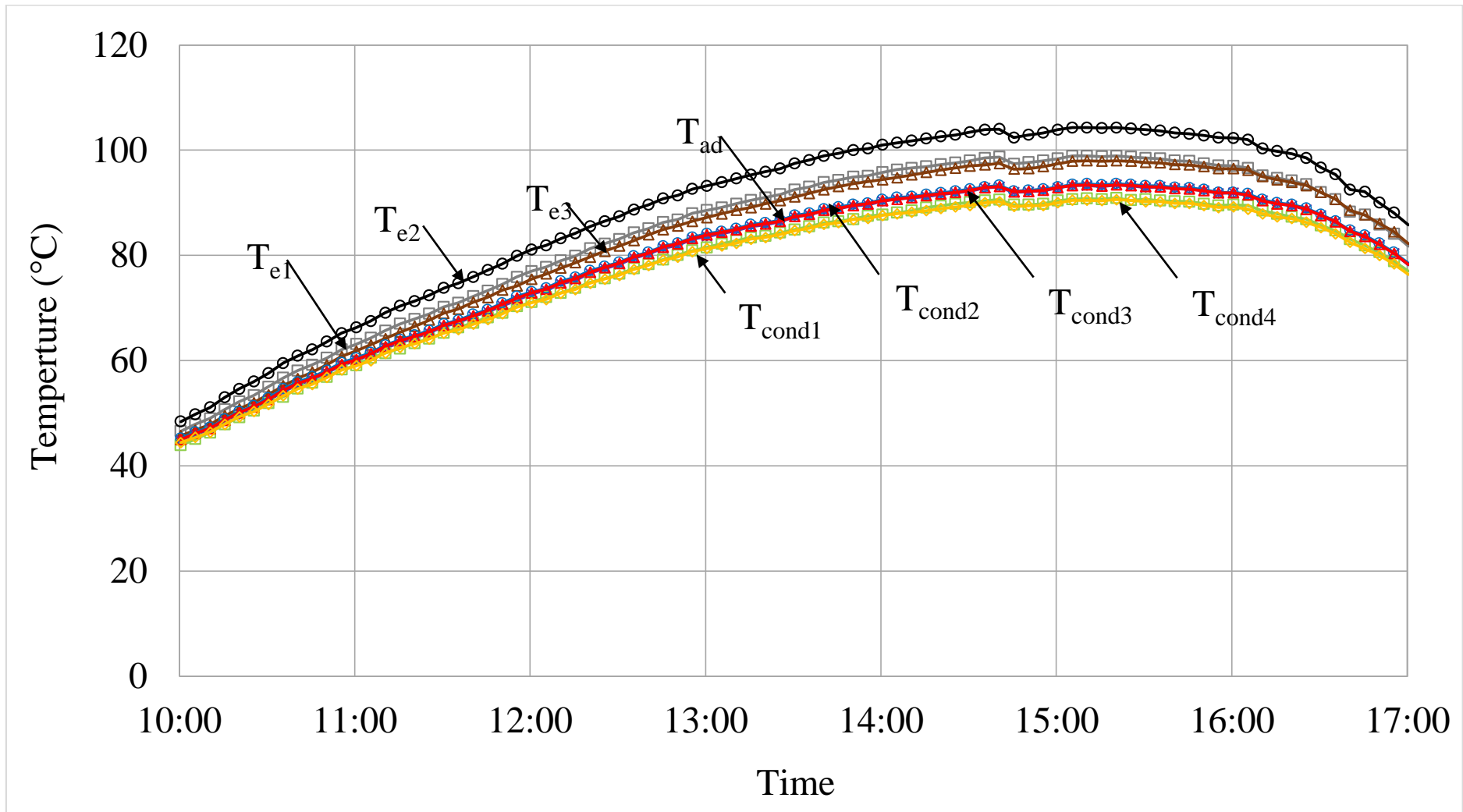


Figure 24: Typical experimental results showing heat pipe temperatures (RUN#1).

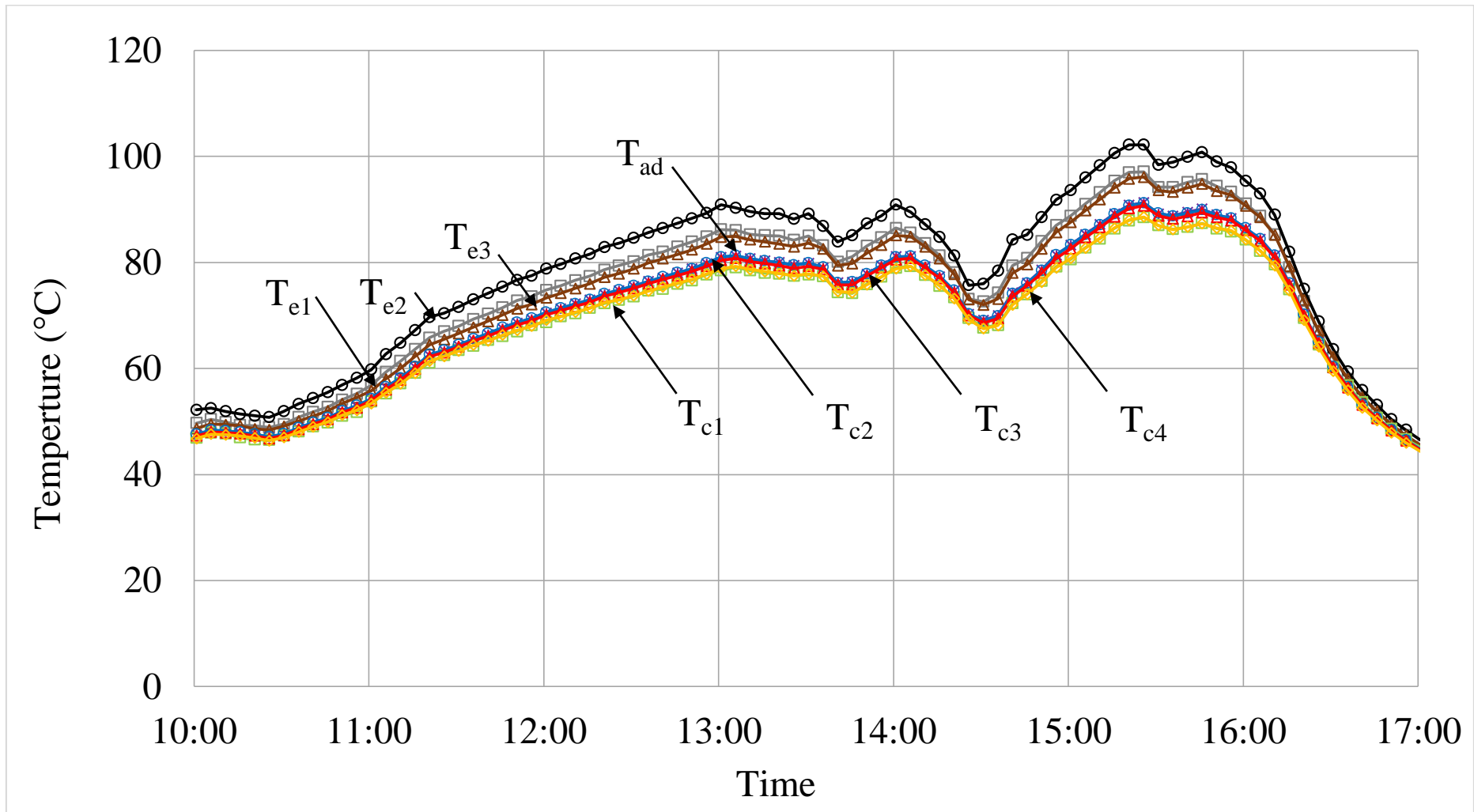


Figure 25: Typical experimental results showing heat pipe temperatures (RUN#2).

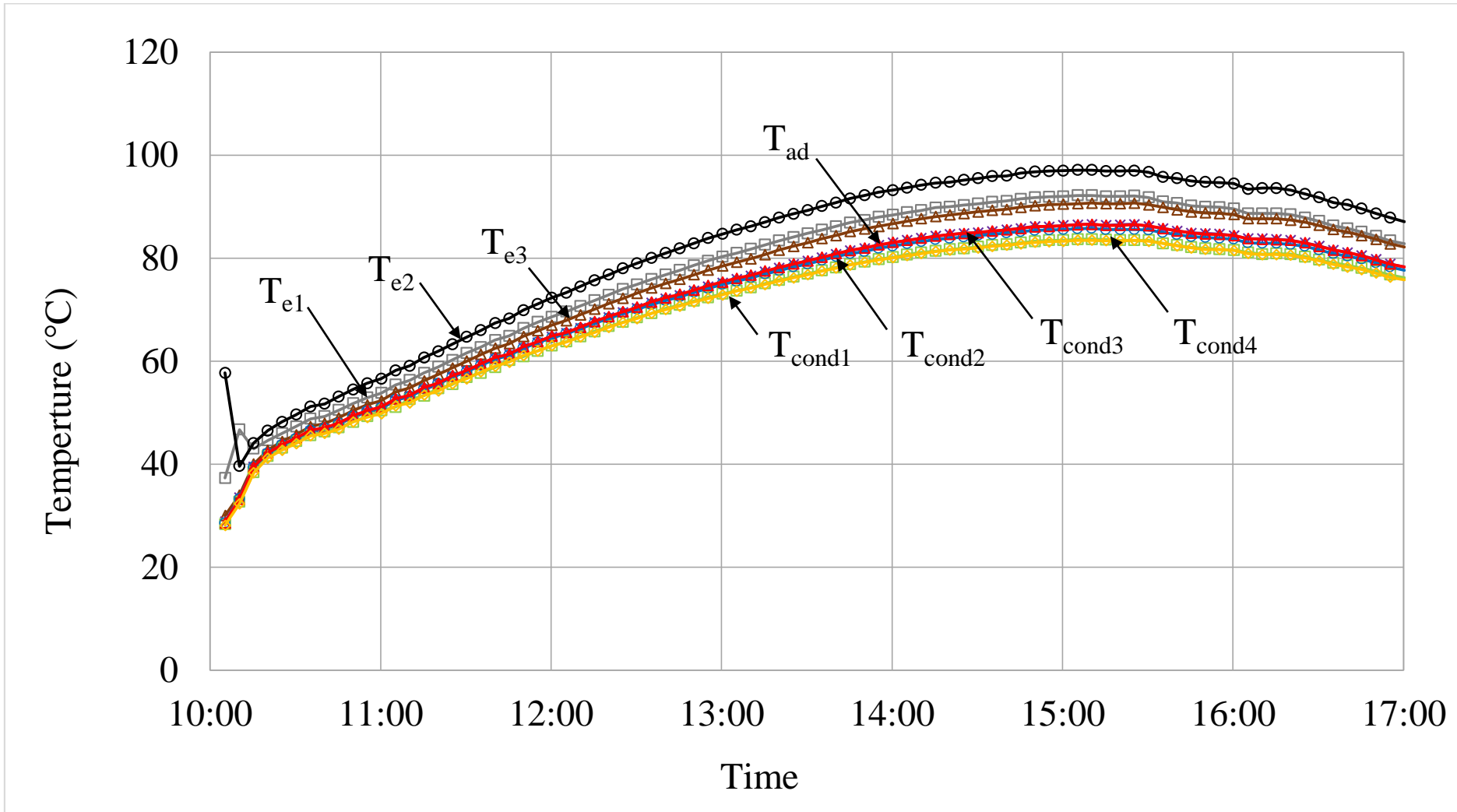


Figure 26: Typical experimental results showing heat pipe temperatures (RUN#3).

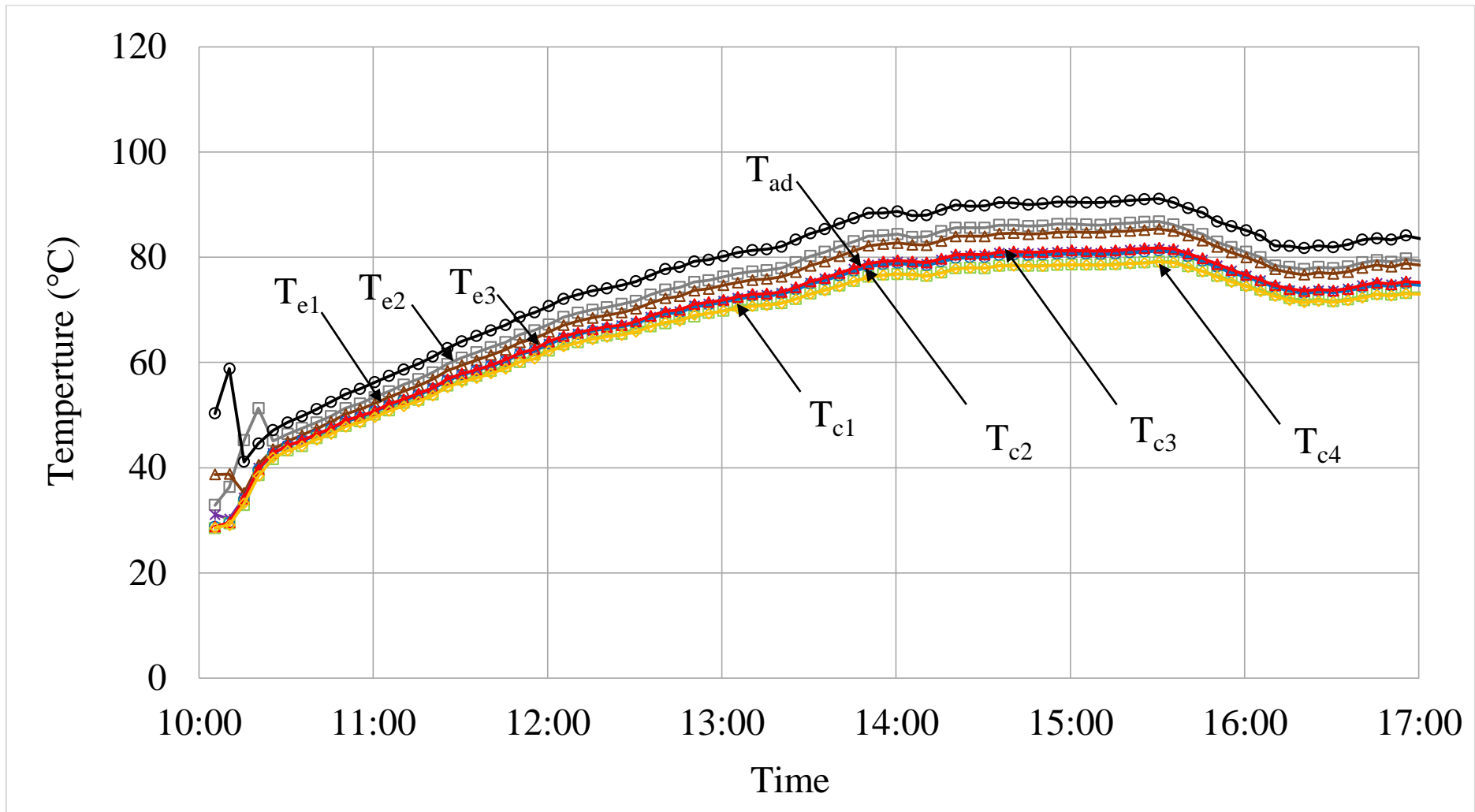


Figure 27: Typical experimental results showing heat pipe temperatures (RUN#4).

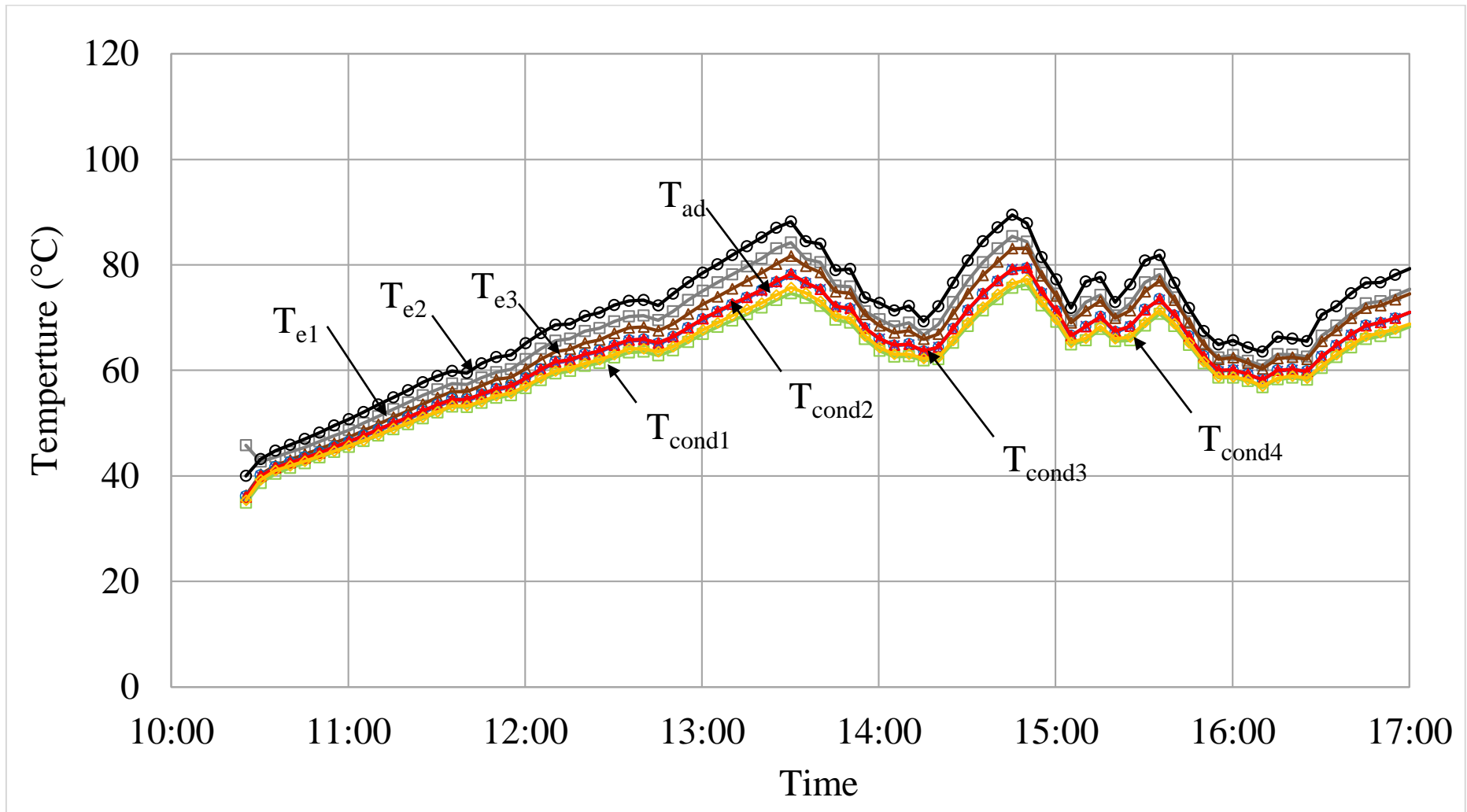


Figure 28: Typical experimental results showing heat pipe temperatures (RUN#5).

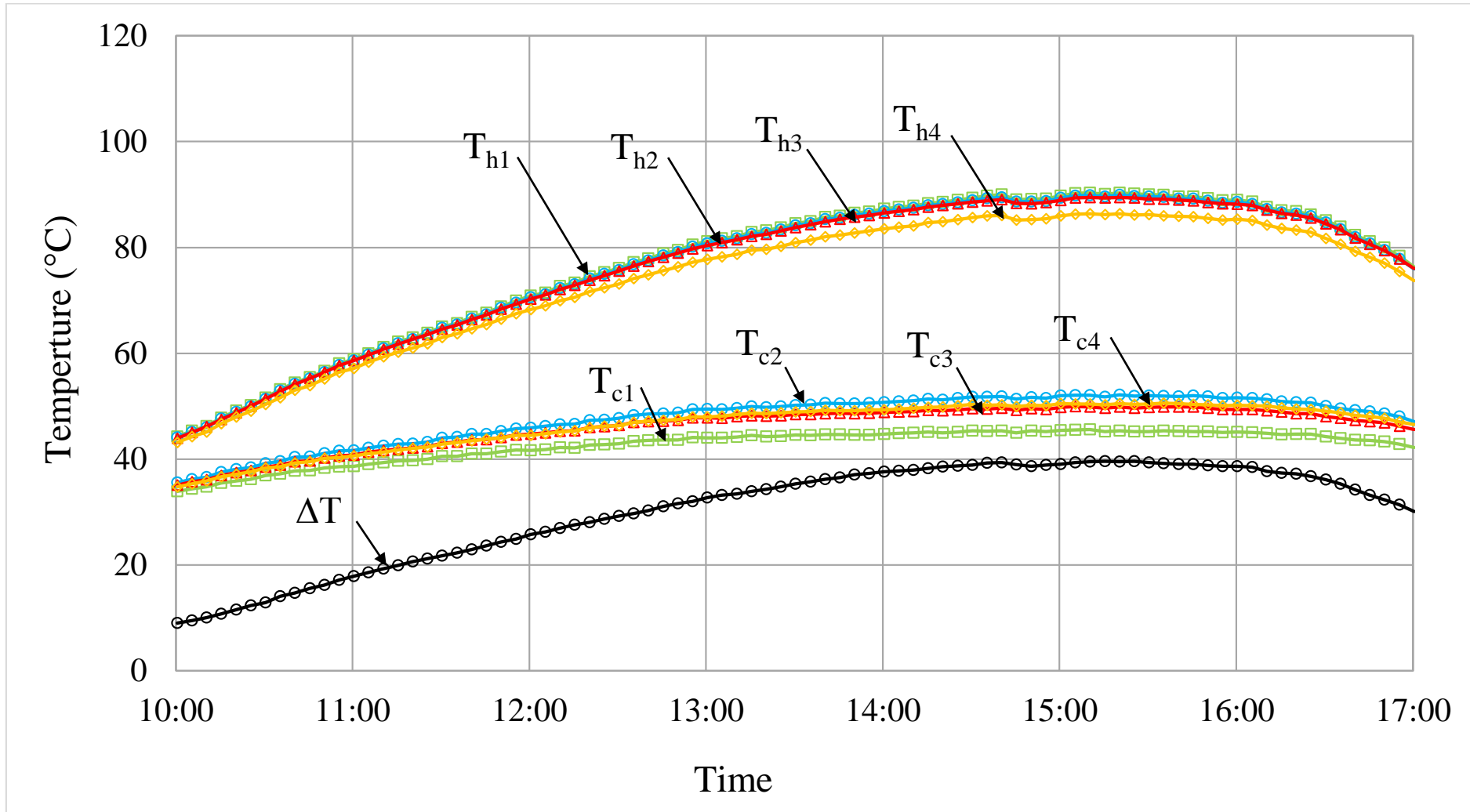


Figure 29: Typical experimental results showing thermoelectric hot and cold junction temperatures and the temperature difference (RUN#1).

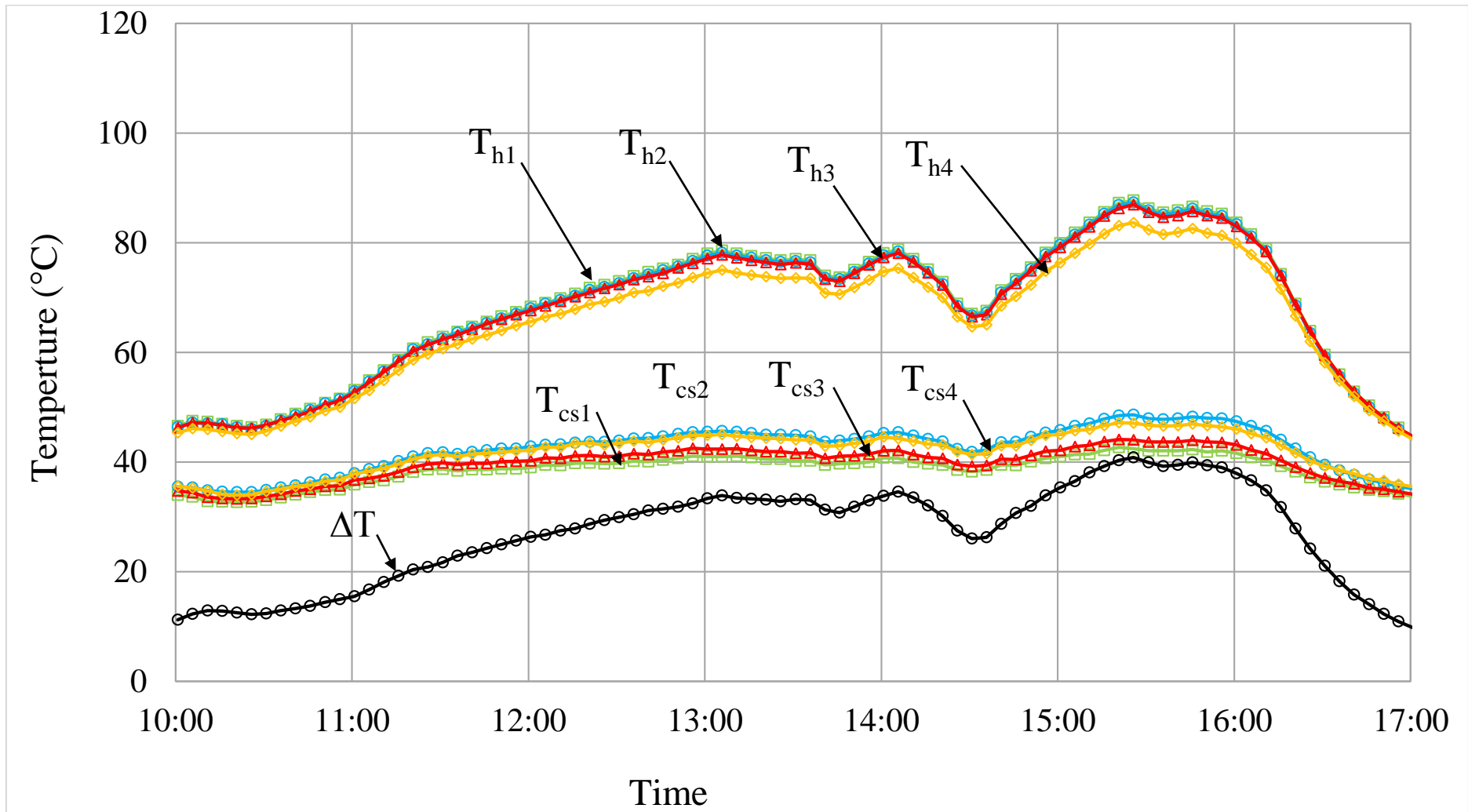


Figure 30: Typical experimental results showing thermoelectric hot and cold junction temperatures and the temperature difference (RUN#2).

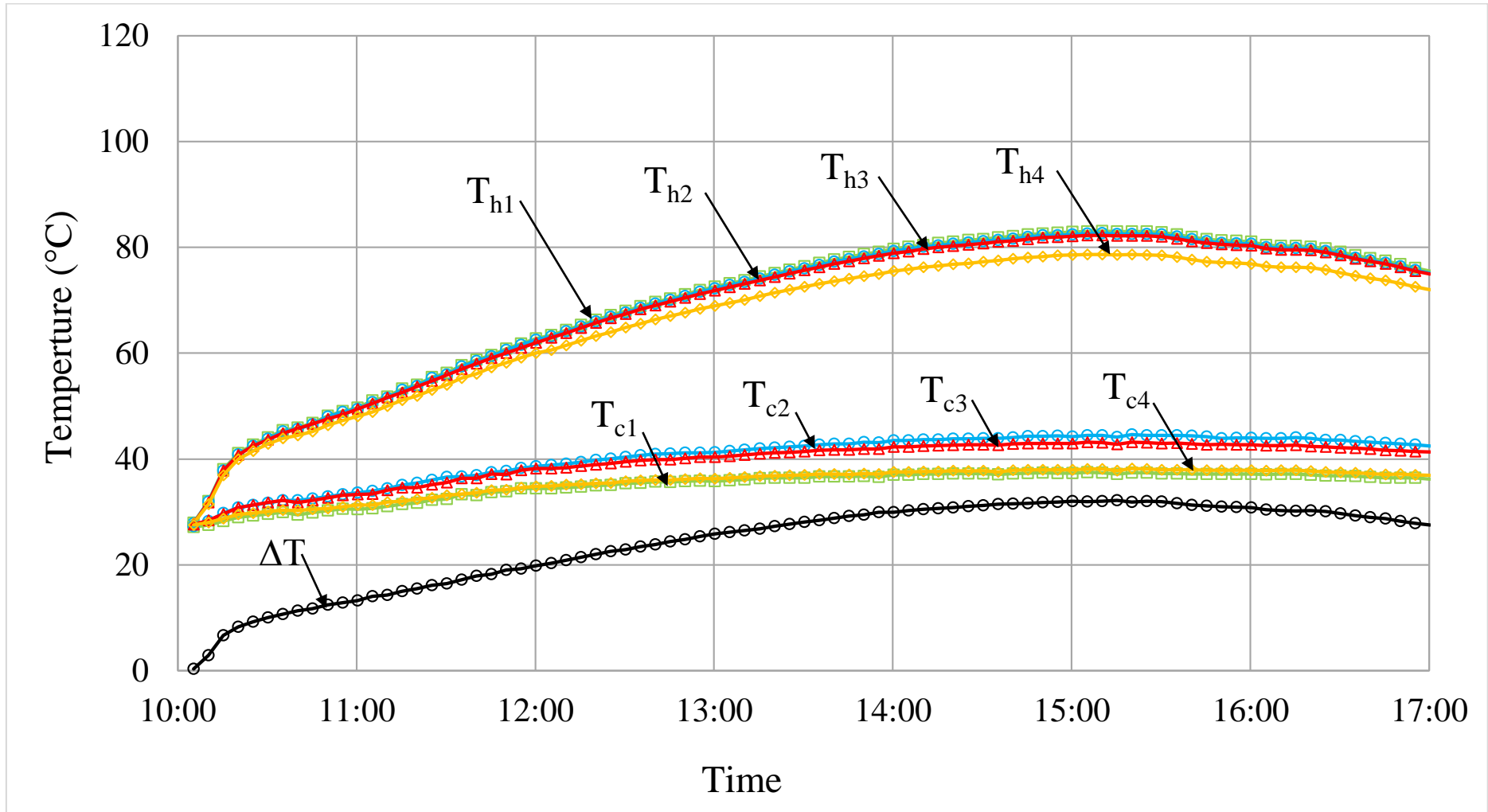


Figure 31: Typical experimental results showing thermoelectric hot and cold junction temperatures and the temperature difference (RUN#3).

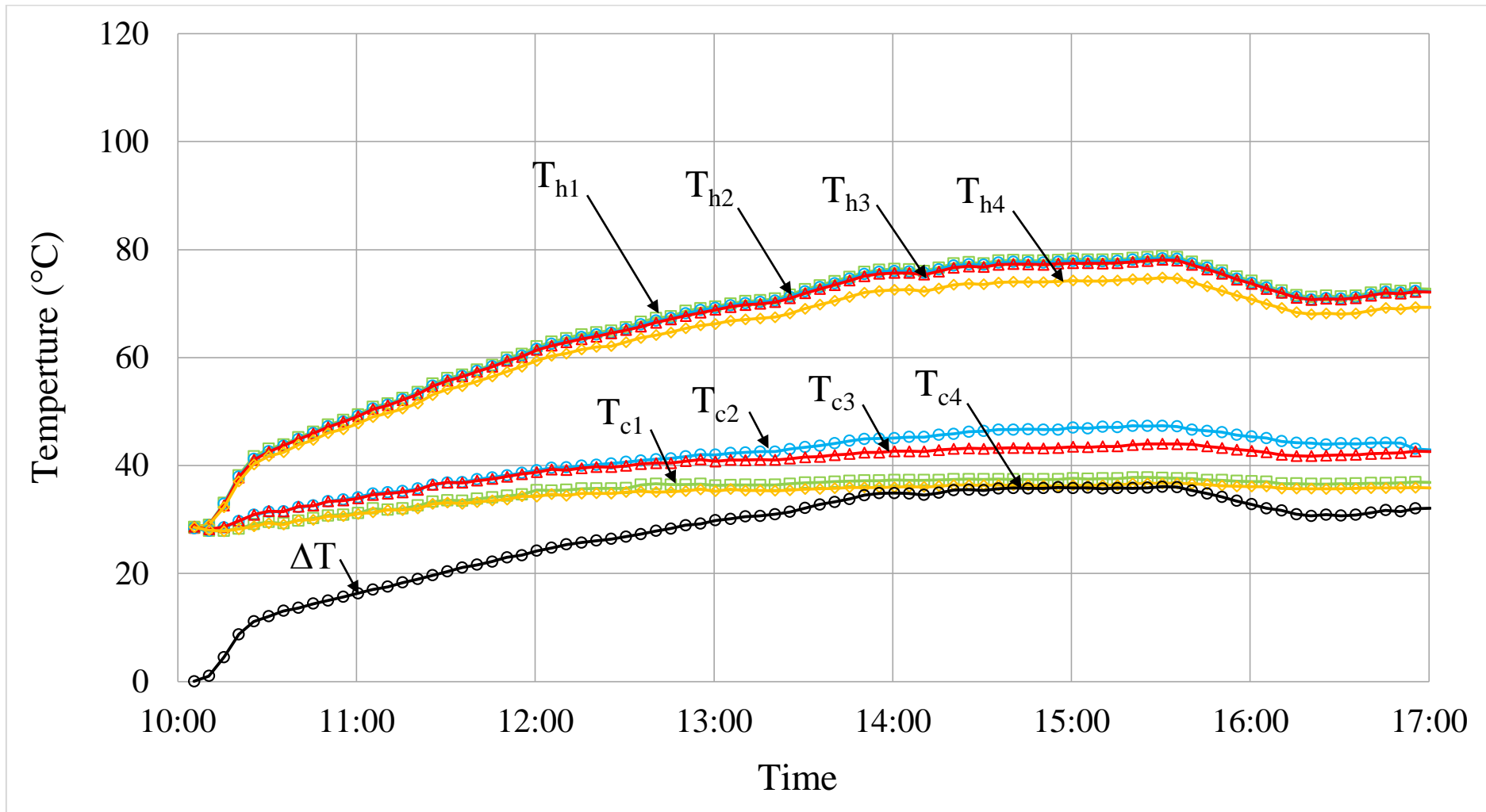


Figure 32: Typical experimental results showing thermoelectric hot and cold junction temperatures and the temperature difference (RUN#4).

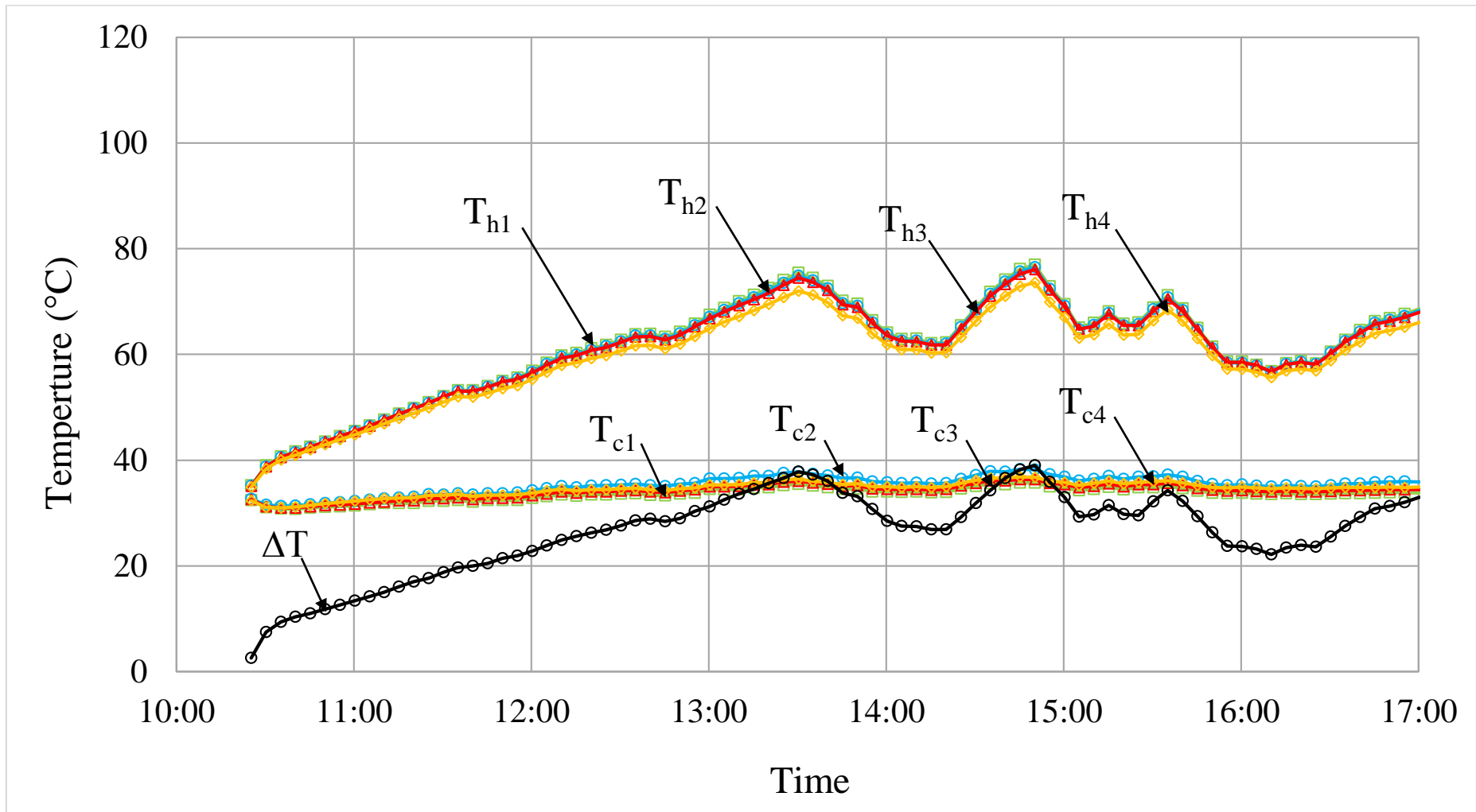


Figure 33: Typical experimental results showing thermoelectric hot and cold junction temperatures and the temperature difference (RUN#5).

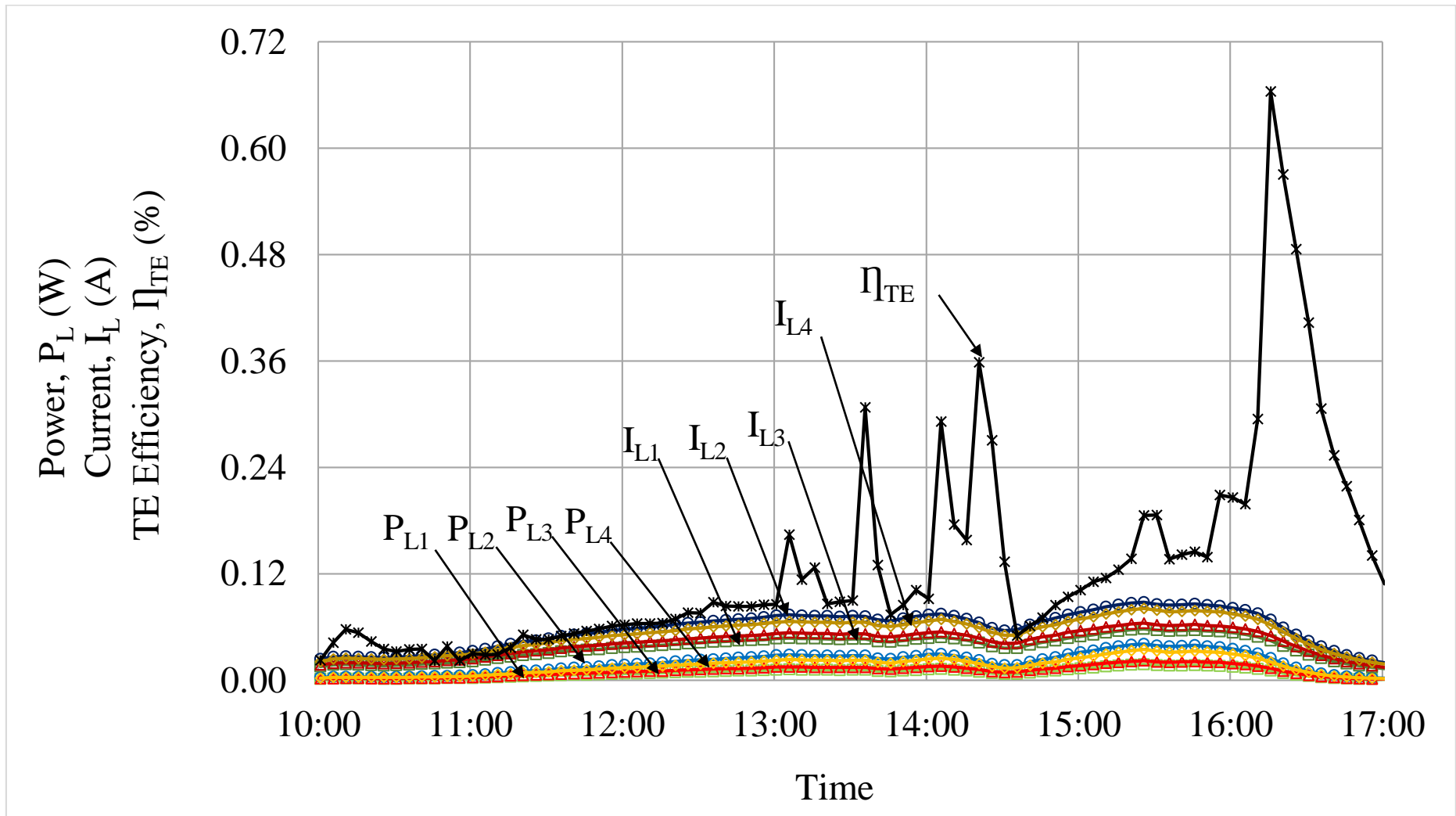


Figure 34: Typical experimental results showing current, power and thermoelectric efficiencies for (RUN#2).

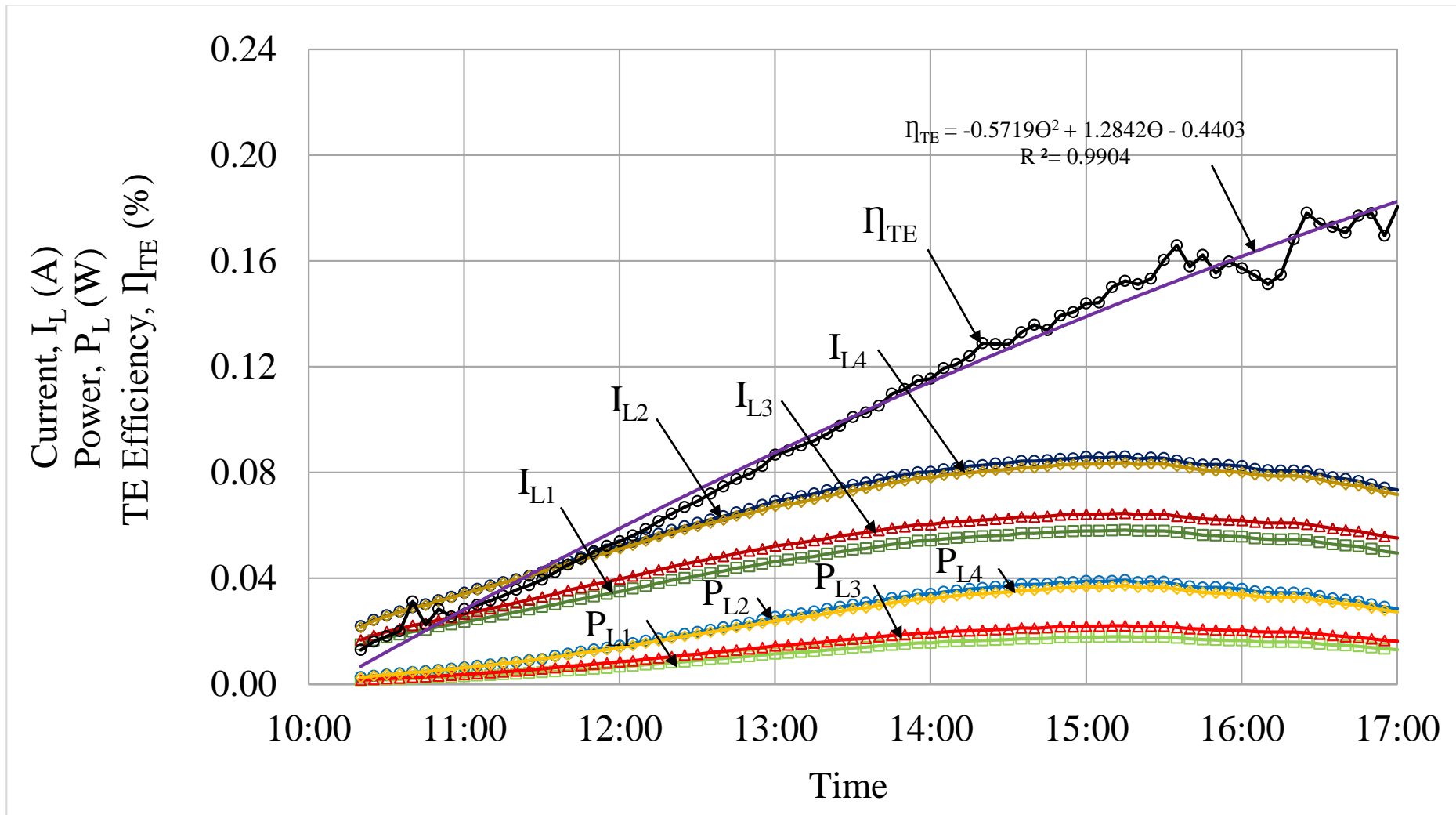


Figure 35: Typical experimental results showing current, power and thermoelectric efficiencies for (RUN#3).

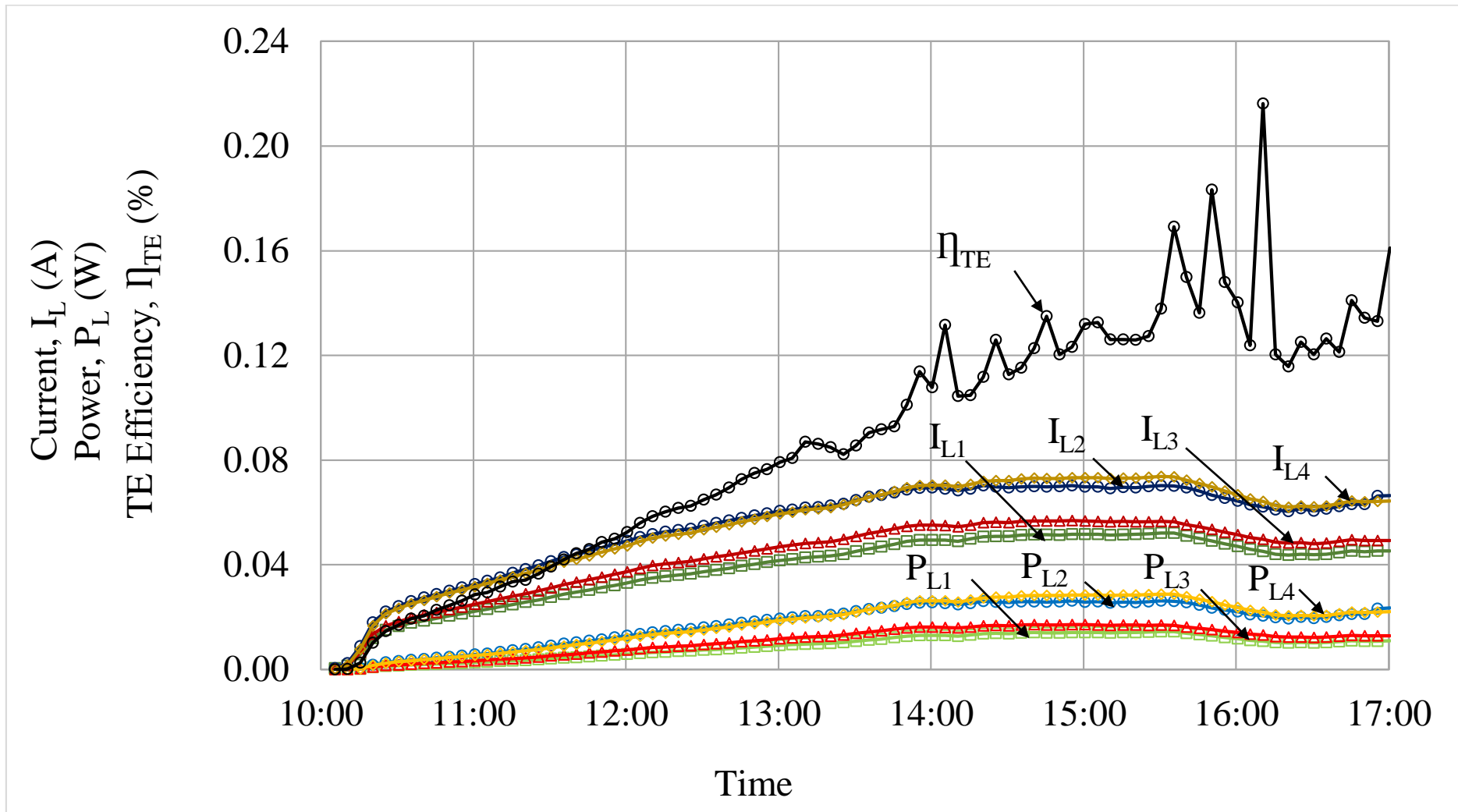


Figure 36: Typical experimental results showing current, power and thermoelectric efficiencies for (RUN#4).

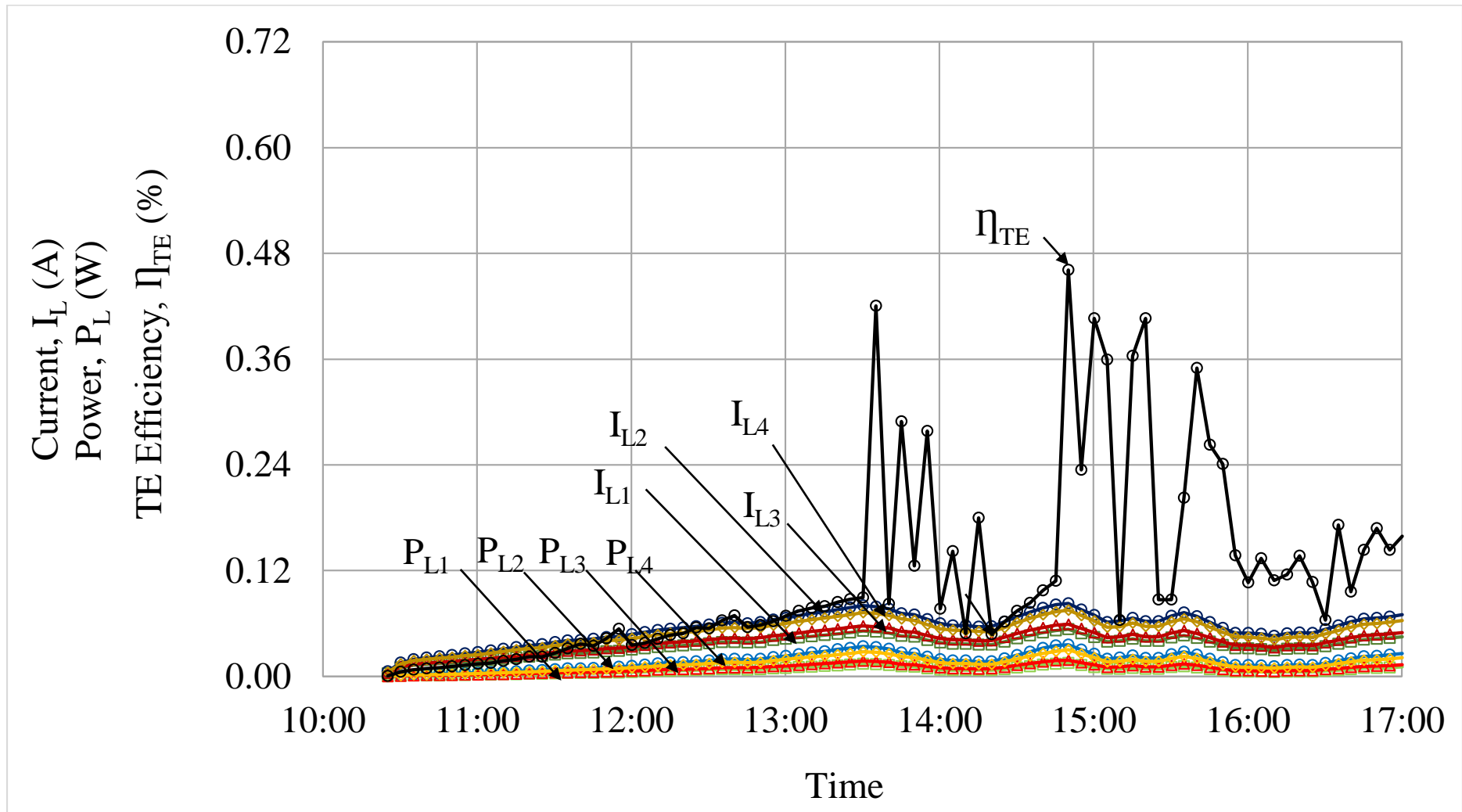


Figure 37: Typical experimental results showing current, power and thermoelectric efficiencies for (RUN#5).

CHAPTER 4

DISCUSSION OF RESULTS

4.1 Experimental Results of Solar Radiation, Ambient Temperature and Thermoelectric Voltage Generated

Figure 4.10 to figure 4.14 shows the solar radiation pattern, ambient temperature and the voltage generated for RUN#1 to RUN#5. RUN#1 and RUN#3 were conducted on a sunny day and the solar radiation pattern both run is smooth throughout the day. In both runs, the solar radiation increased smoothly, peaked around 13.40 hour with solar radiation of 877 W/m^2 and 909 W/m^2 , respectively and then decreased towards the evening. RUN#4 was conducted on a partially hazy and cloudy day and the solar radiation pattern is considerably smooth until 13.45 hour where, the solar radiation starts to decrease and fluctuate due to the presence of cloud in the afternoon. Due to the hazy condition during RUN#4, the peaked solar radiation at 13.45 hour only managed to reach 840 W/m^2 , which is considerably low among all 5 runs. RUN#2 and RUN#5 were conducted during a cloudy day, as a result the solar radiation fluctuated throughout the day. The presence of clouds cause the instantaneous radiation measured to be erratic and weather will greatly affect the level of instantaneous radiation. The level of solar radiation intensifies as the time of day approaches 13.00 hour due to the cloudy sky that hinder direct sunlight. A common similarities for all 5 runs is that the maximum solar radiation peaked in between 13.00 – 15.00 hours in all 5 runs. Besides that, the maximum ambient temperature of the day was achievable at around 14.00 – 15.00 hours ranging from $35.6 \text{ }^\circ\text{C}$ to $39.1 \text{ }^\circ\text{C}$.

Next, the open voltage generated in open circuited RUN#1 peaked at 15.15 hour with one of the thermoelectric modules achieved up to 0.78 V. The recorded peaked open voltage generated by all 4 thermoelectric modules varied by 0.23 V. The average voltage produced from 10.00– 17.00 hours is 1.68 V. For RUN#2 to RUN#5, a load resistance of 5.3 Ω were applied. RUN#2 to RUN#5 were conducted with different water mass flow rate to investigate the effect on water velocity on the voltage generated. RUN#3 was carried out with average water velocity of 1.5g/s and a smooth solar radiation pattern achieved during the run. The load voltage generated peaked around 15.25 hour and the maximum load voltage recorded range from 0.30 V to 0.46 V. The voltage decreased as the amount of radiation decreased as the time of day approaches the evening thus causing the temperature difference between the TE module junctions to decrease. The average voltage produced from 10.00 – 17.00 hours is 1.16 V. The voltage generated on all 5 runs recorded a variation of 0.14 V to 0.23 V. These differences could be due to the manufacturing tolerances, mounting procedure (pressure), thermal contact resistance and the water mass flow rate into each water cooling jacket.

RUN#2, Run#4 and RUN#5 were conducted with water velocity of 0.9 g/s, 1.625 g/s and 8.333 g/s respectively. Theoretically, a higher water velocity is capable providing more cooling to the water cooling jacket, lowering the temperature, increase the temperature difference across the thermoelectric hot and cold junction, and thus generating higher voltage. However, in our experimental runs, it can be seen that the velocity of water did not reflect on the performance of the system as the voltage generated did not increase with higher water mass flow rate. RUN#2 was conducted with water velocity of 0.9 g/s achieved a peaked voltage of 0.46 V. Run#4 was conducted with water velocity of 1.625 g/s achieved a peaked voltage of 0.39 V, while RUN#5 was conducted with water velocity 8.333 g/s achieved a peaked voltage of 0.44 V. This scenario could be due to the inconsistent solar radiation that are not capable of providing sufficient thermal. Therefore, even though the system was supplied with a higher water velocity, but the heat pipe was unable to provide adequate heat to create a bigger temperature for the TE hot and cold junction and hence generating lower voltage.

4.2 Experimental Results of Heat Pipe Temperatures

Figure 4.15 to figure 4.19 shows the temperature along the heat pipe for RUN#1 to RUN#5. The heat pipe temperatures were categorised as fin temperature which is also the evaporator part of the heat pipe ($T_{e1} - T_{ce4}$), adiabatic temperature (T_{ad}) and condenser temperatures ($T_{cond1} - T_{cond4}$). The temperature of heat pipe is correlated with the solar radiation as it is directly affected by the solar radiation pattern.

For RUN#2 and RUN#5, the temperatures along the heat pipe fluctuated in a pattern that is exactly same as the solar radiation pattern. RUN#2 was conducted on a cloudy day and as from the graph it can be seen that the temperature of the heat pipe dropped from 14.00 – 14.30 hour when the solar radiation dipped from 886 W/m^2 to 177 W/m^2 and increased from 14.30 – 15.00 hour when the solar radiation rose sharply to 952 W/m^2 . As expected for RUN#5 which was conducted on a cloudy weather, the temperatures of heat pipe faced the similar phenomenon, where the temperature suffered a drop when the solar radiation dipped. For RUN#1 and RUN#3 which were conducted on a sunny weather, the temperature of the heat pipe increased, peaked with a maximum evaporator temperature of $104.3 \text{ }^\circ\text{C}$ and $97.1 \text{ }^\circ\text{C}$ respectively, and decreased as the day approached evening. Throughout these two runs, there were no drop in heat pipe temperature as the solar radiation for both runs is smooth without any spike and dip.

Besides that, from all 5 graphs, it can be seen that the evaporator temperature varied by about $6 \text{ }^\circ\text{C}$, while the condenser temperature varied by about $3 \text{ }^\circ\text{C}$. The degree of variation in temperature is similar for the all 5 runs. The variation in evaporator and condenser section could be due to the imperfect internal structure of the heat pipe that caused the uneven distribution of temperature throughout the heat pipe.

Next, from the graphs of all 5 runs, all temperatures along the heat pipe increased throughout the day and peaked at around 14.30 – 15.30 hours. The temperatures of heat pipe peaked after the solar radiation hit the peak, which is relevant as the heat pipe got heated up more as the solar radiation is higher. The maximum temperature of condenser recorded in RUN#2, RUN#3, RUN#4, RUN#5 is $91.2 \text{ }^\circ\text{C}$, $85.8 \text{ }^\circ\text{C}$, $81.8 \text{ }^\circ\text{C}$ and $79.2 \text{ }^\circ\text{C}$ respectively. The decrease of condenser's temperature from

RUN#2 to RUN#4 is due to the increase of water mass flow rate for each run. The higher water flow rate increased the heat transfer rate from hot side to cold side, thus lowering the condenser temperature and subsequently lowering the temperature of the whole heat pipe.

4.3 Experimental Results of Thermoelectric Hot and Cold Junction Temperatures and the Temperature Difference Across

Figure 4.20 to figure 4.24 shows the thermoelectric hot side and cold side junction and temperature difference across these two side for RUN#1 to RUN#5. The thermocouple wires were located on the groove of the aluminium block which serve as a heat spreader that distribute the heat from the condenser to the TE hot side. So as a result, the TE hot side temperatures is almost similar with the condenser temperature because both parts were in contact with each other and aluminium has a good thermal conductivity.

The hot side temperature is directly influenced by the solar radiation. From the graphs, it can be seen that both hot side (T_h) and cold side temperature (T_c) increases with the increasing solar radiation, but the increase in the hot side is larger than that of cold side, causing temperature difference between hot side and cold side to increase. A larger temperature difference across the thermoelectric generator modules, which is proportional to the heat transfer rate, improved the thermal electromotive force generated by the Seebeck effect and increases the output electrical power. Next, the temperatures of heat pipe and hot side increased as there is temperature built up due to the lack of cooling provided at the condenser section of the heat-pipe. However, as the radiation levels drop instantaneously, the temperature difference however dissipates slowly as the amount of cooling provided by the water channel begins to overtake the heat input from the solar radiation.

In RUN#4, the maximum TE hot side temperatures ($T_{h1} - T_{h4}$) varied by about 4 °C with maximum of 78.8 °C, while TE cold side temperatures ($T_{c1} - T_{c4}$) varied by about 10 °C with maximum of 47.3 °C. The high variation on the cold side is due to the

uneven distribution of water flow into each water cooling jacket. The side with slower water velocity will have higher temperature because there is insufficient water to cool down the hot side and heat transfer rate is also lower. The average temperature difference between TE hot side and TE cold side at maximum was 36 °C.

RUN#5 was conducted with water velocity of 8.333 g/s ensured that the water that entered each water cooling jacket is distributed more evenly than the previous 4 runs. This is proven as the temperature of the cold side varied by about 2 °C which is lower compared to other runs. It can be seen that with higher water velocity, the maximum hot side temperature is 75.8 °C, while the average and maximum cold side temperature is only 34.4 °C and 38.2 °C respectively. Those values are significantly lower than the other 4 runs indicating that high water mass flow rate is capable of providing more cooling to the system due to higher heat transfer rate.

In RUN#1, a peaked voltage of 0.60 V was achieved with an average temperature difference of 39.6 °C. In RUN#2, a peaked voltage of 0.39 V was achieved with an average temperature difference of 40.5 °C, In RUN#3, a peaked voltage of 0.39 V was achieved with an average temperature difference of 32.2 °C, In RUN#4, a peaked voltage of 0.34 V was achieved with an average temperature difference of 36 °C, In RUN#5, a peaked voltage of 0.36 V was achieved with an average temperature difference of 39 °C. That is obvious that the voltage generated in RUN#1 is far higher than the following runs. This is due to the absence of load resistance in the open circuit run. The average temperature difference for all 5 runs is within the range of 24 °C to 30 °C producing an average voltage of around 0.24 V to 0.29 V.

4.4 Experimental Results of Current, Power and Thermoelectric Efficiencies

Figure 4.25 to figure 4.28 shows the current ($I_{L1} - I_{L4}$) and power generated ($P_{L1} - P_{L4}$) and also the electrical efficiency (η_{TE}) of RUN#2 to RUN#5. RUN#1 was open circuited and only open voltages were recorded, thus power generated cannot be measured hence the electrical efficiency of the hybrid system cannot be determined.

In RUN#2, the system achieved a peaked current and power at 15.25 hour generating a total of 0.2904A and 0.112W respectively with a low instantaneous electrical power efficiency of only 0.19%. There is a sudden surge in instantaneous electrical efficiencies at 16.05 hour when the solar radiation suffered a sudden dipped. However, this did not reflect the performance of system. This is due to theoretical calculation we used. This phenomenon happened when there is a high thermal heat storage, and the solar radiation is too low.

In RUN#4, the system achieved a peaked current and power at 15.30 hour generating a total of 0.2527A and 0.085 W respectively with a low instantaneous electrical power efficiency of only 0.14%. Although the water flowrate is faster compared to RUN#2 and RUN#3 but the power generated and electrical. In RUN#5, the system achieved a peaked current and power at 14.50 hour generating a total of 0.2703A and 0.097 W respectively. The instantaneous electrical efficiencies fluctuated throughout the day due to the fluctuated solar radiation. Although the water flowrate in RUN#5 was the fastest compared to RUN#2, RUN#3 and RUN#4 but and electrical efficiency is the lowest among these 4 runs. This is due to a less sunny day with lower overall solar radiation and fluctuated solar radiation pattern.

RUN#3 was conducted on a sunny day with minimal cloud that might affect the solar radiation reading. The instantaneous electrical efficiencies increased continuously beyond 17.00 hour due to the thermal energy storage. The results showed that during the peak at 15.15 hour, the system was able to generate 0.114 W of power with very low electrical efficiency at only about 0.15 %. Of the all 4 runs, RUN#3 was able to achieve a most consistent electrical efficiency because of the stable solar radiation. A polynomial graph was plotted to determine the exact efficiency pattern. Comparing the efficiency obtain from calculation with the exact efficiency, the biggest percentage error is less than 9 percent.

From the all graphs, it can be seen that, the voltages varies directly from the temperature difference. The increase in voltage results in the increase in electrical power output from thermoelectric generator. The rate of rise is high at the beginning due to rapid increase in solar radiation. The drop in power output is gradual with the drop in temperature difference.

CHAPTER 5

SUGGESTIONS FOR FURTHER STUDIES

The following are some suggestions on improvement for further studies:

1. Increase the number of heat pipes to increase the thermal performance of ETHPSC.
2. Conduct the experimental runs with a wider range of water flow rates to investigate the effect of water velocity on TE power generation.
3. Use a more accurate method to control and determine the water flow rate.
4. Add an insulated water storage tank to system to enable a recirculating flow system between the ETHPSC and the tank.
5. Set up the ETHPSC with different degrees of inclination to investigate their performance.

CHAPTER 6

CONCLUSIONS

The performance of a hybrid solar heat pipe collector coupled to a thermoelectric power generator module was investigated under outdoor conditions. Typical daily experimental results showed that all temperatures and TEG output voltage increased as the day progressed and peaked to their maximum values around 15.30 hour and then started to decrease. On a sunny day with very little cloud cover, at the peak around 15.15 hour, the system was able to generate 0.114 W of power with very low electrical efficiency at only about 0.15 %.

REFERENCES

- [1] Americanenergyindependence.com, (n.d.). *Solar Energy and Energy Independence*. [online] Available at: <http://www.americanenergyindependence.com/solarenergy.aspx> [Accessed 23 Apr. 2015].
- [2] German Advisory Council on Global Change. (2003). *World in Transition Towards Sustainable Energy System*. [online] Available at: http://www.wbgu.de/fileadmin/templates/dateien/veroeffentlichungen/hauptgutachten/jg2003/wbgu_jg2003_engl.pdf [Accessed 23 Apr. 2015].
- [3] High-end PC System, n.d.. *Heat Pipe Concept*. [image] Available at: http://i-am-fast.com/Pictures/heat_pipe_concept.jpg [Accessed 27 Mar. 2015].
- [4] Snyder, G. and Toberer, E. (2008). Complex thermoelectric materials. *Nature Materials*, 7(2), pp.105-114.
- [5] Ferrotec, ,n.d.. *Thermoelectric Modules*. [online] Available at: <https://www.ferrotec.com/technology/thermoelectric/> [Accessed 23 Mar. 2015].
- [6] Suvit, P., Paiboon, K. and Decho, T., 2010. Development of Low Grade Waste Heat Thermoelectric Power Generator. *Songklanakarinn J. Sci. Technol.*, 32(3), pp.307-313.
- [7] Risha, M., Rajendra P., Virendra K. V., Amit R. V., Ratnesh T. (2014). Thermoelectric Power Generation Integrated Cookstove: A Sustainable Approach of Waste Heat to Energy. *IJRET*, 03(24), pp.35-39.

- [8] Goudarzi, A., Mazandarani, P., Panahi, R., Behsaz, H., Rezaia, A. and Rosendahl, L. (2013). Integration of Thermoelectric Generators and Wood Stove to Produce Heat, Hot Water, and Electrical Power. *Journal of Electronic Materials*, 42(7), pp.2127-2133.
- [9] Singh, R., Tundee, S. and Akbarzadeh, A. (2011). Electric power generation from solar pond using combined thermosyphon and thermoelectric modules. *Solar Energy*, 85(2), pp.371-378.
- [10] Kim, S., Park, S., Kim, S. and Rhi, S. (2011). A Thermoelectric Generator Using Engine Coolant for Light-Duty Internal Combustion Engine-Powered Vehicles. *Journal of Electronic Materials*, 40(5), pp.812-816.
- [11] Kim, S., Won, B., Rhi, S., Kim, S., Yoo, J. and Jang, J. (2011). Thermoelectric Power Generation System for Future Hybrid Vehicles Using Hot Exhaust Gas. *Journal of Electronic Materials*, 40(5), pp.778-783.
- [12] Remeli, M., Tan, L., Date, A., Singh, B. and Akbarzadeh, A. (2015). Simultaneous power generation and heat recovery using a heat pipe assisted thermoelectric generator system. *Energy Conversion and Management*, 91, pp.110-119.
- [13] Wei-Keng Lin., 2012. Heat Transport Study of the Laminar Heat Pipe Heat Exchanger. *SGRE*, 03(04), pp.348-354.
- [14] Mantelli, M., Martins, G., Reis, F., Zimmermann, R. Rocha, G. (2004). Experimental study of vertical thermosyphon for industrial heat exchangers applications, *Proc. 13IHPC Shanghai China*, pp. 531-536.
- [15] Zhu, N., Matsuura, T., Suzuki, R. and Tsuchiya, T., 2014. Development of a Small Solar Power Generation System based on Thermoelectric Generator. *Energy Procedia*, 52, pp.651-658.

- [16] Taleb M. Maslamani. and A.I.Omer., 2014. Development of Solar Thermoelectric Generator. *European Scientific Journal*, 10(9).
- [17] Chávez Urbiola, E. and Vorobiev, Y., 2013. Investigation of Solar Hybrid Electric/Thermal System with Radiation Concentrator and Thermoelectric Generator. *International Journal of Photoenergy*, 2013, pp.1-7.
- [18] Hasan Nia, M., Abbas Nejad, A., Goudarzi, A., Valizadeh, M. and Samadian, P., 2014. Cogeneration solar system using thermoelectric module and fresnel lens. *Energy Conversion and Management*, 84, pp.305-310.
- [19] Miao, L., Kang, Y., Li, C., Tanemura, S., Wan, C., Iwamoto, Y., Shen, Y. and Lin, H. (2015). Experimental Performance of a Solar Thermoelectric Cogenerator Comprising Thermoelectric Modules and Parabolic Trough Concentrator without Evacuated Tube. *Journal of Electronic Materials*, 44(6), pp.1972-1983.
- [20] Deng, Y., Zhu, W., Wang, Y. and Shi, Y. (2013). Enhanced performance of solar-driven photovoltaic–thermoelectric hybrid system in an integrated design. *Solar Energy*, 88, pp.182-191.
- [21] Fan, H., Singh, R. and Akbarzadeh, A. (2011). Electric Power Generation from Thermoelectric Cells Using a Solar Dish Concentrator. *Journal of Electronic Materials*, 40(5), pp.1311-1320.
- [22] He, W., Su, Y., Wang, Y., Riffat, S. and Ji, J., 2012. A study on incorporation of thermoelectric modules with evacuated-tube heat-pipe solar collectors. *Renewable Energy*, 37(1), pp.142-149.
- [23] Zhang, M., Miao, L., Kang, Y., Tanemura, S., Fisher, C., Xu, G., Li, C. and Fan, G., 2013. Efficient, low-cost solar thermoelectric cogenerators comprising evacuated tubular solar collectors and thermoelectric modules. *Applied Energy*, 109, pp.51-59.

- [24] Lertsatitthanakorn, C., Khasee, N., Atthajariyakul, S., Soponronnarit, S., Therdyothin, A. and Suzuki, R. (2008). Performance analysis of a double-pass thermoelectric solar air collector. *Solar Energy Materials and Solar Cells*, 92(9), pp.1105-1109.
- [25] Sathawane, N. and Walke, P. (2015). Development Of Cost Effective Solar Thermoelectric Cogenerator with Evacuated Tube solar Collector. *Advance Research In Science And Engineering*, [online] 4(01). Available at: <http://www.ijarse.com>.

APPENDICES

Table 1a: Raw Data of Run #1

Time	H	T _a	T _{e1}	T _{e2}	T _{e3}	T _{fin}	T _{ad}	T _{cond1}	T _{cond2}	T _{cond3}	T _{cond4}	T _{cond}	V _{L1}	V _{L2}	V _{L3}	V _{L4}	V _L
10:00	492	29.5	46.6	48.4	45.7	46.9	44.9	43.9	45.2	45	44.4	44.6	0.098	0.143	0.110	0.142	0.123
10:10	529	31.3	49	51.1	47.8	49.3	46.9	46.3	47.3	47.1	46.4	46.8	0.111	0.162	0.125	0.161	0.140
10:20	558	31.7	52.2	54.6	50.8	52.5	49.8	49.2	50.3	50.1	49.3	49.7	0.128	0.187	0.145	0.185	0.161
10:30	577	31.7	55	57.6	53.5	55.4	52.4	51.9	52.9	52.6	51.7	52.3	0.145	0.213	0.165	0.209	0.183
10:40	605	32.9	58.1	60.9	56.6	58.5	55.4	54.7	55.9	55.7	54.6	55.2	0.165	0.242	0.187	0.237	0.208
10:50	628	32.5	60.5	63.6	59.2	61.1	57.7	56.9	58.1	57.9	56.8	57.4	0.183	0.270	0.208	0.263	0.231
11:00	664	33.2	63.1	66.3	61.8	63.7	60	59.1	60.5	60.2	59	59.7	0.203	0.303	0.231	0.292	0.257
11:10	689	33	65.7	69.1	64.2	66.3	62.4	61.4	62.9	62.7	61.4	62.1	0.221	0.333	0.251	0.318	0.280
11:20	729	34.4	67.9	71.3	66.5	68.6	64.3	63.3	64.8	64.6	63.2	64	0.236	0.359	0.269	0.339	0.301
11:30	764	33.7	70.2	73.8	69	71	66.5	65.3	67	66.7	65.2	66.1	0.251	0.381	0.286	0.360	0.320
11:40	764	33	72.2	75.9	71.1	73.1	68.4	67.2	68.8	68.5	66.9	67.9	0.267	0.404	0.304	0.382	0.339
11:50	784	34.6	74.5	78.4	73.4	75.4	70.4	69.1	70.9	70.7	68.9	69.9	0.284	0.429	0.323	0.407	0.361
12:00	819	35	77	81.1	75.5	77.9	72.7	71.1	73.1	72.9	71	72	0.302	0.456	0.342	0.432	0.383
12:10	825	35.6	79	83.2	77.6	79.9	74.6	72.9	75.1	74.8	72.8	73.9	0.317	0.479	0.359	0.453	0.402
12:20	850	35.4	81.3	85.5	79.7	82.2	76.6	74.9	77.1	76.8	74.7	75.9	0.331	0.500	0.375	0.473	0.420
12:30	855	36.5	83.1	87.4	81.8	84.1	78.3	76.5	78.7	78.5	76.2	77.5	0.347	0.522	0.392	0.494	0.439
12:40	858	36.8	85.1	89.6	83.9	86.2	80.3	78.3	80.6	80.4	78.1	79.4	0.360	0.543	0.407	0.512	0.455
12:50	862	36.2	86.8	91.4	85.6	87.9	81.9	80.1	82.3	82.2	79.7	81.1	0.377	0.568	0.427	0.536	0.477
13:00	853	36	88.6	93.2	87.2	89.7	83.6	81.5	84.1	83.9	81.3	82.7	0.390	0.585	0.440	0.555	0.493
13:10	866	38.1	89.8	94.6	88.6	91	84.7	82.8	85.1	84.9	82.3	83.8	0.400	0.601	0.453	0.568	0.505
13:20	868	37.2	91	95.9	89.8	92.2	85.8	83.7	86.2	86	83.4	84.8	0.410	0.616	0.466	0.583	0.519
13:30	876	36.2	92.5	97.5	91.1	93.7	87.3	84.9	87.6	87.4	84.7	86.2	0.421	0.631	0.477	0.597	0.532
13:40	877	37.1	93.9	98.9	92.5	95.1	88.5	86.2	88.8	88.6	85.9	87.4	0.433	0.649	0.493	0.615	0.547
13:50	856	36.2	94.9	100	93.6	96.2	89.4	86.9	89.7	89.5	86.8	88.2	0.444	0.663	0.505	0.630	0.560
14:00	865	36.7	95.8	101	94.4	97.1	90.3	87.7	90.6	90.4	87.6	89.1	0.451	0.672	0.512	0.640	0.569
14:10	872	36.8	96.6	102	95.3	97.9	90.9	88.5	91.2	91	88.2	89.7	0.456	0.681	0.520	0.649	0.576
14:20	861	37.3	97.3	103	96.2	98.7	91.6	89.4	91.9	91.7	88.9	90.5	0.464	0.690	0.529	0.660	0.586
14:30	856	37.7	98	103	97	99.5	92.2	90.1	92.6	92.4	89.5	91.2	0.468	0.696	0.534	0.666	0.591
14:40	840	38.1	98.7	104	97.5	100	93	90.6	93.3	93.1	90.2	91.8	0.475	0.704	0.541	0.675	0.599
14:50	827	37.2	97.7	103	96.5	99	92.1	89.6	92.4	92.2	89.4	90.9	0.464	0.691	0.530	0.660	0.586
15:00	824	38.4	98.4	104	97.4	99.9	92.8	90.4	93	92.9	90	91.6	0.471	0.699	0.537	0.669	0.594
15:10	784	37.1	98.9	104	98	100	93.3	90.8	93.6	93.4	90.5	92.1	0.476	0.706	0.542	0.676	0.600
15:20	761	36.3	98.9	104	98	100	93.4	90.9	93.6	93.4	90.6	92.1	0.478	0.706	0.544	0.678	0.601

15:30	745	37.9	98.5	104	97.7	100	92.9	90.7	93.2	93.1	90.2	91.8	0.476	0.703	0.541	0.674	0.598
15:40	716	37.4	98	103	97.3	99.5	92.7	90.3	92.9	92.7	89.9	91.5	0.472	0.697	0.535	0.669	0.593
15:50	698	37.8	97.5	103	96.9	99.1	92.3	89.8	92.5	92.3	89.5	91	0.467	0.692	0.532	0.663	0.589
16:00	686	36.6	97	102	96.5	98.6	91.9	89.6	92	91.9	89.2	90.7	0.465	0.690	0.529	0.661	0.586
16:10	625	38	95.2	100	95	96.8	90.4	88.5	90.6	90.4	87.9	89.4	0.453	0.674	0.517	0.645	0.572
16:20	606	36.5	94.2	99.3	93.9	95.8	89.4	87.3	89.7	89.5	87	88.4	0.443	0.663	0.508	0.632	0.562
16:30	541	38	92	96.7	92	93.6	87.6	85.7	87.8	87.6	85.3	86.6	0.427	0.640	0.491	0.610	0.542
16:40	418	36.5	88.3	92.5	88.6	89.8	84.5	83.1	84.8	84.6	82.5	83.8	0.404	0.605	0.464	0.577	0.513
16:50	418	35.4	85.8	90	86.1	87.3	82	80.6	82.3	82.1	80	81.3	0.382	0.572	0.440	0.546	0.485
17:00	375	35.7	81.8	85.8	82.2	83.3	78.2	77	78.5	78.3	76.4	77.6	0.353	0.529	0.407	0.505	0.449

Table 1b: Raw Data of Run #1

Time	T _{h1}	T _{h2}	T _{h3}	T _{h4}	T _{h5}	T _{h6}	T _{h7}	T _{h8}	T _{h9}	T _{h10}	T _{h11}	T _{h12}	T _h	T _{e1}	T _{e2}	T _{e3}	T _{e4}	T _{e5}	T _{e6}	T _{e7}	T _{e8}	T _{e9}	T _{e10}	T _{e11}	T _{e12}	T _e
10:00	44.2	44.3	44.2	44.1	44.1	44.0	43.5	44.0	44.4	43.6	42.7	43.2	43.9	33.6	34.2	33.9	35.3	35.6	35.7	34.4	35.4	35.4	34.2	35.2	34.3	34.8
10:10	46.2	46.4	46.2	46.0	46.1	46.0	45.8	46.2	46.4	45.5	44.9	45.1	45.9	34.6	35.0	34.8	36.3	36.7	36.8	35.3	36.6	36.5	35.2	36.3	35.4	35.8
10:20	49.1	49.3	49.1	48.9	49.0	48.9	48.3	48.8	49.3	48.3	47.7	47.9	48.7	35.5	36.2	36.0	37.8	38.2	38.3	36.6	37.7	38.0	36.2	37.6	36.7	37.1
10:30	51.5	51.8	51.5	51.3	51.5	51.3	50.9	51.4	51.8	50.6	50.2	50.3	51.2	36.6	37.2	37.0	38.9	39.4	39.4	37.5	39.0	39.1	37.3	38.9	37.8	38.2
10:40	54.4	54.6	54.4	54.2	54.3	54.2	53.6	54.1	54.7	53.4	52.8	53.0	54.0	37.3	38.2	37.9	40.0	40.6	40.6	38.4	40.0	40.2	38.0	39.9	38.7	39.2
10:50	56.6	56.8	56.6	56.4	56.5	56.3	56.0	56.5	56.8	55.4	55.0	55.0	56.2	38.0	38.6	38.3	40.7	41.3	41.3	38.9	41.0	40.9	38.9	40.9	39.4	39.9
11:00	58.8	59.0	58.8	58.6	58.7	58.5	58.2	58.7	59.0	57.5	57.0	57.0	58.3	38.4	39.0	38.6	41.1	41.8	42.0	39.4	41.5	41.5	39.4	41.5	39.8	40.3
11:10	61.1	61.3	61.1	60.9	61.1	60.8	60.1	60.7	61.4	59.7	59.1	59.2	60.5	38.8	39.8	39.4	41.9	42.7	43.0	40.2	42.1	42.6	39.8	42.2	40.5	41.1
11:20	62.9	63.1	62.9	62.6	62.8	62.6	62.1	62.7	63.1	61.3	60.9	60.8	62.3	39.4	40.1	39.7	42.2	43.1	43.5	40.6	42.7	43.0	40.5	43.1	41.0	41.6
11:30	65.0	65.2	65.0	64.7	64.9	64.7	63.9	64.5	65.3	63.3	62.7	62.9	64.3	40.0	41.1	40.6	43.3	44.1	44.6	41.4	43.5	44.0	41.0	43.9	41.7	42.4
11:40	66.7	67.1	66.7	66.5	66.7	66.5	65.7	66.4	67.0	65.0	64.5	64.5	66.1	40.5	41.5	41.0	44.0	44.9	45.2	42.0	44.2	44.7	41.5	44.6	42.3	43.0
11:50	68.8	69.0	68.8	68.5	68.8	68.5	67.7	68.3	69.0	66.8	66.3	66.3	68.1	40.9	42.0	41.4	44.6	45.5	45.8	42.3	44.8	45.2	41.9	45.3	42.7	43.5
12:00	70.8	70.9	70.9	70.5	70.7	70.4	69.5	70.2	71.0	68.6	68.1	68.1	70.0	41.1	42.2	41.7	45.1	46.1	46.5	42.8	45.4	45.9	42.2	45.9	43.1	44.0
12:10	72.7	72.7	72.6	72.2	72.5	72.2	71.3	72.0	72.8	70.2	69.8	69.7	71.7	41.6	42.8	42.2	45.7	46.8	47.2	43.3	46.0	46.5	42.8	46.7	43.6	44.6
12:20	74.5	74.5	74.5	74.1	74.3	74.0	73.1	73.8	74.6	71.9	71.7	71.4	73.5	42.1	43.3	42.7	46.5	47.6	47.9	43.9	46.7	47.3	43.3	47.4	44.4	45.3
12:30	76.1	76.1	76.1	75.6	75.9	75.6	74.9	75.6	76.2	73.3	73.2	72.8	75.1	42.5	43.5	42.8	46.8	48.0	48.3	44.1	47.4	47.6	43.7	48.1	44.6	45.6
12:40	77.9	77.9	77.9	77.4	77.7	77.4	76.6	77.4	78.0	75.0	74.9	74.5	76.9	43.1	44.1	43.5	47.5	48.8	49.2	44.8	48.1	48.4	44.4	49.1	45.3	46.4
12:50	79.5	79.5	79.5	79.0	79.3	79.0	78.2	79.0	79.6	76.5	76.5	75.9	78.5	43.1	44.2	43.6	47.8	49.1	49.4	44.9	48.4	48.7	44.5	49.5	45.5	46.6
13:00	81.1	81.1	81.2	80.7	81.0	80.6	79.5	80.4	81.3	78.0	77.9	77.4	80.0	43.3	44.7	44.0	48.5	49.8	50.1	45.4	48.8	49.3	44.6	50.0	45.9	47.0
13:10	82.1	82.1	82.1	81.6	82.0	81.6	80.7	81.5	82.2	78.8	79.1	78.3	81.0	43.6	44.8	44.1	48.7	50.0	50.2	45.4	49.2	49.5	45.0	50.6	46.3	47.3
13:20	83.2	83.1	83.2	82.7	83.0	82.6	81.7	82.6	83.3	79.8	79.9	79.3	82.0	43.8	44.9	44.2	48.8	50.3	50.3	45.3	49.5	49.5	45.2	50.9	46.3	47.4
13:30	84.5	84.5	84.6	84.0	84.4	84.0	82.9	83.8	84.6	81.1	81.0	80.6	83.3	43.9	45.3	44.5	49.2	50.7	50.7	45.6	49.8	49.9	45.5	51.3	46.5	47.7
13:40	85.7	85.6	85.8	85.2	85.5	85.2	84.0	84.8	85.8	82.1	82.3	81.6	84.5	44.0	45.4	44.6	49.6	51.1	51.0	45.7	50.0	50.2	45.4	51.6	46.8	48.0
13:50	86.5	86.4	86.6	86.0	86.4	85.9	84.9	85.8	86.5	82.8	83.0	82.4	85.3	44.0	45.3	44.5	49.6	51.2	50.8	45.5	50.3	50.0	45.4	51.7	46.6	47.9
14:00	87.4	87.2	87.4	86.8	87.1	86.7	85.6	86.5	87.4	83.6	83.8	83.1	86.1	44.1	45.5	44.6	49.8	51.4	51.1	45.7	50.5	50.3	45.5	51.8	46.8	48.1
14:10	87.9	87.8	87.9	87.3	87.7	87.3	86.3	87.2	87.9	84.1	84.5	83.7	86.6	44.4	45.6	44.8	50.1	51.7	51.3	45.8	50.9	50.4	45.8	52.3	47.0	48.3
14:20	88.6	88.6	88.6	88.1	88.4	88.0	87.1	88.0	88.7	84.8	85.4	84.4	87.4	44.4	45.6	44.8	50.4	51.9	51.4	45.8	51.1	50.6	45.8	52.5	47.2	48.5
14:30	89.3	89.4	89.3	88.8	89.2	88.7	87.7	88.6	89.5	85.6	86.1	85.2	88.1	44.6	46.1	45.3	50.9	52.5	51.9	46.2	51.4	51.1	46.1	53.0	47.7	48.9
14:40	90.0	89.9	90.0	89.4	89.8	89.1	88.2	89.1	89.9	86.1	86.5	85.6	88.6	44.6	46.2	45.3	51.0	52.6	52.0	46.2	51.5	51.1	46.1	53.0	47.6	48.9
14:50	89.1	89.1	89.2	88.6	89.0	88.4	87.4	88.3	89.2	85.3	85.6	84.9	87.8	44.6	46.1	45.3	50.8	52.4	51.8	46.2	51.3	51.1	46.1	52.8	47.5	48.8
15:00	89.7	89.7	89.8	89.2	89.6	89.2	88.0	88.9	89.8	85.9	86.4	85.5	88.5	44.7	46.2	45.4	51.1	52.7	52.1	46.4	51.6	51.3	46.3	53.2	47.8	49.1
15:10	90.3	90.3	90.4	89.8	90.1	89.7	88.5	89.4	90.4	86.4	86.7	86.0	89.0	44.8	46.4	45.5	51.2	52.9	52.2	46.5	51.7	51.5	46.3	53.2	47.7	49.2
15:20	90.3	90.3	90.3	89.8	90.2	89.7	88.5	89.4	90.4	86.4	86.8	86.0	89.0	44.6	46.2	45.4	51.3	52.9	52.2	46.4	51.8	51.4	46.3	53.2	47.8	49.1
15:30	90.0	90.0	90.0	89.5	89.8	89.4	88.2	89.2	90.1	86.1	86.7	85.8	88.7	44.5	46.0	45.2	51.1	52.8	52.0	46.3	51.7	51.3	46.2	53.1	47.8	49.0
15:40	89.6	89.6	89.6	89.1	89.5	89.0	88.1	89.0	89.7	85.8	86.4	85.4	88.4	44.7	46.0	45.1	51.0	52.6	52.0	46.4	51.8	51.4	46.4	53.2	47.8	49.0
15:50	89.3	89.3	89.3	88.7	89.1	88.7	87.6	88.5	89.4	85.5	85.9	85.1	88.0	44.5	46.0	45.1	51.0	52.6	51.9	46.3	51.5	51.2	46.1	53.0	47.6	48.9
16:00	88.9	89.0	89.0	88.5	88.8	88.4	87.3	88.2	89.1	85.3	85.7	84.9	87.8	44.4	45.9	45.1	50.7	52.4	51.8	46.1	51.2	51.0	46.0	52.8	47.5	48.7
16:10	87.6	87.7	87.7	87.1	87.5	87.0	86.2	87.2	87.8	84.1	84.8	83.7	86.5	44.3	45.5	44.8	50.4	52.0	51.4	45.9	50.9	50.7	45.9	52.6	47.4	48.5
16:20	86.7	86.9	86.8	86.3	86.6	86.2	85.2	86.1	87.0	83.3	83.6	82.9	85.6	44.0	45.5	44.7	49.9	51.5	50.9	45.5	50.3	50.1	45.5	52.0	46.9	48.1
16:30	85.0	85.2	85.2	84.6	85.0	84.5	83.6	84.5	85.4	81.7	82.1	81.3	84.0	43.7	44.9	44.1	49.2	50.7	50.2	44.9	49.8	49.4	45.3	51.6	46.6	47.5
16:40	82.2	82.5	82.3	81.9	82.2	81.7	80.9	81.8	82.7	79.2	79.6	78.9	81.3	43.0	44.4	43.6	48.4	49.8	49.4	44.4	48.8	48.8	44.6	50.6	46.0	46.8
16:50	79.8	80.1	79.9	79.5	79.8	79.2	78.6	79.4	80.2	77.0	77.4	76.7	79.0	42.7	43.9	43.3	47.9	49.2	48.8	44.1	48.2	48.2	44.2	49.9	45.6	46.3
17:00	76.2	76.6	76.3	75.8	76.1	75.8	75.3	76.1	76.7	73.7	74.0	73.4	75.5	41.8	42.7	42.1	46.4	47.6	47.4	42.9	47.1	46.7	43.3	48.6	44.5	45.1

Table 2a: Raw Data of Run #2

Time	H	T _a	T _{e1}	T _{e2}	T _{e3}	T _{in}	T _{ad}	T _{cond1}	T _{cond2}	T _{cond3}	T _{cond4}	T _{cond}	V _{L1}	V _{L2}	V _{L3}	V _{L4}	V _L	I _L	P _L	η _{TE}
10:00	376	35.0	49.7	52.2	48.7	50.2	47.5	46.9	47.6	47.3	46.8	47.2	0.081	0.126	0.092	0.113	0.103	0.019	0.002	0.022
10:10	192	34.1	49.9	51.9	49.4	50.4	48.0	47.7	48.2	47.9	47.5	47.8	0.093	0.142	0.105	0.131	0.118	0.022	0.003	0.057
10:20	232	33.7	49.2	51.1	48.6	49.6	47.4	46.6	47.6	47.3	46.9	47.1	0.089	0.135	0.101	0.127	0.113	0.021	0.002	0.043
10:30	308	34.2	49.5	51.9	49.1	50.2	47.6	47.3	47.7	47.4	47.0	47.4	0.089	0.136	0.101	0.125	0.113	0.021	0.002	0.033
10:40	332	35.1	51.8	54.4	51.0	52.4	49.6	49.1	49.8	49.5	49.0	49.4	0.096	0.147	0.109	0.134	0.121	0.023	0.003	0.035
10:50	359	36.1	54.1	56.9	53.4	54.8	51.9	51.1	52.0	51.7	51.2	51.5	0.104	0.159	0.118	0.145	0.131	0.025	0.003	0.038
11:00	539	37.2	56.8	59.8	55.8	57.5	54.3	53.8	54.3	54.0	53.4	53.9	0.113	0.174	0.128	0.157	0.143	0.027	0.004	0.030
11:10	755	38.2	61.4	64.8	60.0	62.1	58.2	57.2	58.2	57.8	57.1	57.6	0.131	0.202	0.150	0.181	0.166	0.031	0.005	0.029
11:20	555	39.8	65.8	69.7	64.5	66.7	62.4	61.1	62.6	62.2	61.4	61.8	0.149	0.230	0.170	0.207	0.189	0.036	0.007	0.051
11:30	715	40.6	68.0	71.6	66.6	68.7	64.3	63.5	64.5	64.1	63.3	63.9	0.161	0.249	0.182	0.224	0.204	0.038	0.008	0.046
11:40	742	40.6	70.3	74.2	68.9	71.1	66.4	65.4	66.6	66.1	65.2	65.8	0.175	0.271	0.198	0.243	0.222	0.042	0.009	0.053
11:50	750	40.9	72.8	76.7	71.3	73.6	68.6	67.0	68.7	68.2	67.2	67.8	0.185	0.286	0.209	0.257	0.234	0.044	0.010	0.058
12:00	779	41.2	74.8	78.8	73.3	75.6	70.5	68.7	70.6	70.1	69.1	69.6	0.196	0.302	0.221	0.272	0.248	0.047	0.012	0.062
12:10	831	41.7	76.6	80.7	75.1	77.5	72.2	70.4	72.2	71.7	70.6	71.2	0.204	0.316	0.231	0.284	0.259	0.049	0.013	0.064
12:20	845	42.2	78.6	82.9	77.2	79.6	74.0	72.3	74.1	73.6	72.4	73.1	0.214	0.333	0.241	0.297	0.271	0.051	0.014	0.069
12:30	839	42.2	80.2	84.6	78.8	81.2	75.5	73.6	75.6	75.1	73.7	74.5	0.223	0.347	0.252	0.311	0.283	0.053	0.015	0.076
12:40	819	42.6	82.0	86.5	80.7	83.1	77.1	75.0	77.3	76.8	75.4	76.1	0.232	0.359	0.261	0.324	0.294	0.055	0.016	0.083
12:50	863	43.3	83.9	88.3	82.4	84.9	78.8	76.6	78.8	78.3	76.8	77.6	0.238	0.368	0.267	0.331	0.301	0.057	0.017	0.083
13:00	916	43.7	86.2	90.9	84.8	87.3	81.0	78.5	81.0	80.4	78.8	79.7	0.249	0.386	0.280	0.346	0.315	0.059	0.019	0.086
13:10	694	43.7	85.3	89.6	84.3	86.4	80.7	78.5	80.7	80.1	78.7	79.5	0.249	0.386	0.280	0.348	0.316	0.060	0.019	0.114
13:20	901	43.2	85.0	89.2	83.5	85.9	80.0	77.9	80.0	79.4	77.9	78.8	0.247	0.383	0.278	0.345	0.313	0.059	0.018	0.086
13:30	869	42.9	85.0	89.2	83.6	85.9	79.9	77.7	79.9	79.3	77.8	78.7	0.247	0.384	0.278	0.347	0.314	0.059	0.019	0.090
13:40	530	41.9	80.1	83.9	79.4	81.1	76.2	74.4	76.2	75.8	74.5	75.2	0.232	0.360	0.262	0.326	0.295	0.056	0.016	0.130
13:50	845	42.4	83.1	87.3	81.7	84.0	77.8	75.9	77.8	77.4	75.8	76.7	0.237	0.368	0.267	0.332	0.301	0.057	0.017	0.085
14:00	886	43.4	86.5	90.9	85.1	87.5	81.1	79.0	81.0	80.5	78.8	79.8	0.252	0.391	0.285	0.355	0.321	0.061	0.019	0.092
14:10	449	42.7	83.6	87.2	83.0	84.6	79.2	77.6	79.4	79.0	77.6	78.4	0.249	0.383	0.280	0.351	0.316	0.060	0.019	0.175
14:20	177	42.0	78.1	81.3	77.8	79.1	74.7	73.4	74.7	74.3	73.2	73.9	0.223	0.344	0.252	0.314	0.283	0.053	0.015	0.358
14:30	351	40.4	72.6	76.0	72.0	73.5	69.1	67.7	69.0	68.6	67.5	68.2	0.191	0.297	0.218	0.269	0.244	0.046	0.011	0.134
14:40	956	41.8	79.4	84.3	78.0	80.6	74.3	72.3	74.1	73.6	72.0	73.0	0.212	0.332	0.243	0.298	0.271	0.051	0.014	0.061
14:50	852	42.7	84.0	88.5	82.6	85.0	78.6	76.5	78.5	78.0	76.3	77.3	0.237	0.370	0.270	0.332	0.302	0.057	0.017	0.085
15:00	860	43.7	88.8	93.6	87.6	90.0	83.3	80.6	83.3	82.6	80.8	81.8	0.261	0.407	0.296	0.366	0.332	0.063	0.021	0.102
15:10	883	44.7	93.2	98.3	91.9	94.5	87.2	84.5	87.1	86.6	84.6	85.7	0.284	0.437	0.318	0.396	0.359	0.068	0.024	0.115
15:20	832	45.9	97.0	102.2	95.8	98.3	90.8	87.9	90.7	90.2	88.0	89.2	0.301	0.460	0.336	0.420	0.379	0.072	0.027	0.137
15:30	599	45.4	94.2	98.4	93.6	95.4	89.2	87.0	89.3	88.8	87.0	88.0	0.299	0.454	0.331	0.418	0.376	0.071	0.027	0.186
15:40	772	45.4	95.1	99.9	94.1	96.4	89.5	86.7	89.3	88.7	86.7	87.9	0.295	0.452	0.329	0.412	0.372	0.070	0.026	0.142
15:50	782	45.3	94.4	99.0	93.5	95.6	89.0	86.4	89.0	88.5	86.5	87.6	0.295	0.449	0.327	0.410	0.370	0.070	0.026	0.139
16:00	488	44.8	91.1	95.4	90.7	92.4	86.4	84.3	86.5	86.1	84.3	85.3	0.283	0.431	0.316	0.396	0.356	0.067	0.024	0.206
16:10	289	43.3	85.3	89.0	85.2	86.5	81.3	79.6	81.3	80.9	79.4	80.3	0.259	0.397	0.292	0.364	0.328	0.062	0.020	0.295
16:20	94	40.6	72.7	75.0	72.9	73.5	70.2	69.5	70.2	70.0	69.1	69.7	0.205	0.315	0.233	0.289	0.260	0.049	0.013	0.571
16:30	73	38.2	62.0	63.6	62.2	62.6	60.2	60.2	60.3	60.2	59.5	60.1	0.152	0.233	0.173	0.214	0.193	0.036	0.007	0.404
16:40	64	36.8	54.6	55.9	54.6	55.0	53.1	53.6	53.2	53.1	52.6	53.1	0.113	0.173	0.129	0.159	0.143	0.027	0.004	0.254
16:50	52	35.7	49.3	50.4	49.4	49.7	48.3	48.6	48.4	48.3	47.9	48.3	0.086	0.131	0.098	0.121	0.109	0.021	0.002	0.181
17:00	54	34.7	45.5	46.5	45.5	45.8	44.6	45.1	44.7	44.6	44.3	44.7	0.068	0.104	0.078	0.095	0.086	0.016	0.001	0.109

Table 2b: Raw Data of Run #2

Time	T _{h1}	T _{h2}	T _{h3}	T _{h4}	T _{h5}	T _{h6}	T _{h7}	T _{h8}	T _{h9}	T _{h10}	T _{h11}	T _{h12}	T _h	T _{c1}	T _{c2}	T _{c3}	T _{c4}	T _{c5}	T _{c6}	T _{c7}	T _{c8}	T _{c9}	T _{c10}	T _{c11}	T _{c12}	T _c
10:00	46.3	46.7	46.6	46.4	46.5	46.4	45.8	46.3	46.6	45.7	45.3	45.1	46.1	33.7	34.2	34.1	35.5	35.8	35.1	36.6	34.6	34.8	34.8	36.2	34.9	35.0
10:10	47.4	47.3	47.2	47.0	47.1	47.0	46.7	47.2	47.5	46.2	46.1	45.6	46.9	32.6	33.0	32.9	35.0	35.0	34.5	35.8	33.5	33.7	33.9	35.5	33.9	34.1
10:20	46.6	46.6	46.6	46.3	46.4	46.3	45.8	46.3	46.7	45.5	45.1	44.9	46.1	32.5	32.8	32.7	34.6	34.6	34.2	35.4	33.2	33.3	33.3	34.7	33.2	33.7
10:30	46.7	47.0	46.7	46.5	46.6	46.5	46.2	46.8	47.1	45.9	45.7	45.4	46.4	32.9	33.2	33.1	35.0	35.0	34.6	35.8	33.7	33.8	33.8	35.4	33.9	34.2
10:40	48.7	49.0	48.7	48.5	48.6	48.5	47.8	48.3	48.8	47.8	47.4	47.2	48.3	33.9	34.2	34.0	35.8	36.2	35.2	37.0	34.6	34.8	34.6	36.4	34.7	35.1
10:50	50.4	51.1	50.9	50.6	50.8	50.7	49.9	50.4	50.9	49.8	49.2	49.2	50.3	34.7	35.1	34.9	36.9	37.2	36.3	38.0	35.5	35.6	35.6	37.4	35.6	36.1
11:00	53.0	53.3	53.0	52.8	53.0	52.9	52.2	52.7	53.2	51.9	51.7	51.3	52.6	35.7	36.1	35.9	38.0	38.4	37.4	39.3	36.6	36.8	36.8	38.8	36.9	37.2
11:10	56.8	56.8	56.6	56.4	56.6	56.4	55.9	56.5	56.9	55.2	54.9	54.5	56.1	36.4	36.9	36.6	39.5	39.5	38.8	40.4	37.4	37.6	37.8	40.0	37.7	38.2
11:20	60.4	60.8	60.8	60.4	60.7	60.5	59.6	60.3	60.8	59.0	58.7	58.3	60.0	37.9	38.4	38.1	41.2	41.4	40.4	42.3	39.0	39.2	39.2	41.8	39.2	39.8
11:30	62.8	62.9	62.7	62.4	62.7	62.5	61.8	62.4	62.9	61.0	60.9	60.2	62.1	38.4	39.0	38.7	42.0	42.2	41.0	43.3	39.7	40.0	39.8	42.8	40.0	40.6
11:40	64.6	64.8	64.6	64.3	64.6	64.3	63.5	64.2	64.8	62.7	62.7	61.9	63.9	38.3	38.9	38.6	42.1	42.3	41.0	43.6	39.6	39.9	39.8	43.0	39.9	40.6
11:50	66.6	66.5	66.5	66.1	66.4	66.1	65.4	66.1	66.7	64.3	64.2	63.4	65.7	38.5	39.1	38.7	42.8	42.8	41.7	44.0	39.9	40.2	40.1	43.4	40.1	40.9
12:00	68.4	68.2	68.4	67.9	68.2	67.9	67.0	67.7	68.3	65.9	65.8	65.0	67.4	38.7	39.4	38.9	43.2	43.2	42.0	44.4	40.1	40.4	40.3	43.9	40.3	41.2
12:10	69.9	69.8	69.9	69.5	69.7	69.5	68.6	69.4	70.0	67.3	67.3	66.4	68.9	39.0	39.8	39.3	43.7	43.6	42.4	45.0	40.5	40.8	40.8	44.6	40.8	41.7
12:20	71.7	71.7	71.8	71.3	71.6	71.3	70.2	70.9	71.6	69.1	69.1	68.1	70.7	39.5	40.3	39.8	44.0	44.2	42.7	45.8	41.1	41.4	41.3	45.4	41.4	42.2
12:30	73.0	72.9	73.0	72.5	72.8	72.5	71.6	72.5	73.1	70.2	70.3	69.2	72.0	39.4	40.2	39.7	44.4	44.3	43.0	45.8	40.9	41.2	41.2	45.5	41.3	42.2
12:40	74.7	74.5	74.7	74.1	74.5	74.1	73.0	73.9	74.6	71.6	71.6	70.6	73.5	39.7	40.5	40.0	44.9	44.8	43.4	46.4	41.2	41.6	41.3	45.7	41.4	42.6
12:50	76.0	75.9	76.0	75.5	75.9	75.5	74.6	75.5	76.1	73.0	73.1	71.9	74.9	40.3	41.1	40.6	45.7	45.6	44.1	47.1	41.9	42.2	42.2	46.7	42.2	43.3
13:00	78.0	77.9	78.1	77.5	77.9	77.5	76.3	77.2	77.9	74.8	74.9	73.7	76.8	40.6	41.4	40.9	46.1	46.0	44.4	47.7	42.2	42.6	42.4	47.2	42.5	43.7
13:10	78.0	77.9	78.1	77.5	77.9	77.5	76.4	77.3	78.0	74.9	74.9	73.8	76.9	40.7	41.5	41.0	46.1	46.2	44.3	47.8	42.3	42.6	42.3	47.1	42.4	43.7
13:20	77.2	77.1	77.3	76.7	77.1	76.7	75.5	76.5	77.2	74.1	74.3	73.0	76.1	40.1	41.0	40.4	45.5	45.6	43.8	47.2	41.7	42.1	41.7	46.7	42.0	43.2
13:30	77.0	77.0	77.0	76.5	76.9	76.5	75.5	76.4	77.1	73.9	74.2	72.8	75.9	39.8	40.6	40.1	45.5	45.3	43.8	46.9	41.4	41.8	41.6	46.4	41.7	42.9
13:40	73.9	74.0	74.0	73.5	73.8	73.5	72.5	73.4	74.1	71.2	71.2	70.2	72.9	39.1	39.9	39.4	44.1	44.3	42.5	45.8	40.5	40.9	40.5	45.1	40.7	41.9
13:50	75.0	75.1	75.0	74.5	74.9	74.6	73.6	74.5	75.1	72.1	72.4	71.1	74.0	39.4	40.2	39.7	44.8	44.7	43.2	46.3	41.0	41.3	41.1	45.6	41.2	42.4
14:00	78.0	78.2	78.1	77.5	78.0	77.7	76.5	77.4	78.2	74.9	75.4	73.9	77.0	40.3	41.2	40.7	45.9	45.9	44.1	47.4	41.9	42.2	41.8	46.9	42.2	43.4
14:10	77.0	77.0	77.0	76.5	76.9	76.5	75.7	76.6	77.3	74.0	74.2	72.9	76.0	39.6	40.4	39.9	45.5	45.3	43.7	46.8	41.2	41.5	41.3	46.2	41.4	42.7
14:20	72.7	72.9	72.8	72.4	72.7	72.3	71.5	72.3	73.1	70.3	70.4	69.3	71.9	39.1	39.9	39.4	44.2	44.3	42.7	45.6	40.5	40.8	40.6	45.3	41.0	42.0
14:30	66.9	67.2	67.0	66.6	66.9	66.6	65.7	66.5	67.3	64.8	65.0	64.2	66.2	38.0	38.6	38.2	42.2	42.4	41.0	43.4	39.1	39.3	39.2	43.2	39.6	40.4
14:40	71.2	71.5	71.2	70.7	71.2	70.9	69.8	70.7	71.3	68.6	69.0	67.9	70.3	39.1	39.8	39.4	44.0	44.1	42.6	45.2	40.4	40.7	40.8	45.0	41.0	41.8
14:50	75.5	75.5	75.5	75.0	75.4	75.1	74.0	75.0	75.6	72.4	72.9	71.5	74.5	39.7	40.5	40.0	45.1	45.0	43.6	46.4	41.1	41.4	41.6	46.2	41.8	42.7
15:00	80.0	79.9	80.0	79.5	79.9	79.5	78.2	79.2	80.0	76.6	76.8	75.6	78.8	40.5	41.5	40.9	46.4	46.3	44.6	47.8	42.0	42.2	42.4	47.5	42.5	43.7
15:10	83.7	83.6	83.8	83.1	83.6	83.2	82.0	83.0	83.8	80.0	80.5	78.9	82.4	41.0	42.0	41.4	47.8	47.5	45.8	49.2	42.9	43.2	43.2	48.6	43.3	44.7
15:20	87.2	87.1	87.4	86.7	87.2	86.7	85.3	86.3	87.3	83.4	83.8	82.2	85.9	42.2	43.2	42.6	49.2	49.3	47.0	50.7	44.0	44.3	44.1	50.0	44.3	45.9
15:30	86.3	86.2	86.4	85.8	86.2	85.7	84.6	85.6	86.5	82.6	83.1	81.4	85.0	41.6	42.6	42.0	48.7	48.7	46.5	50.3	43.6	43.8	43.5	49.5	43.9	45.4
15:40	85.9	85.8	86.0	85.4	85.8	85.4	84.0	85.0	86.0	82.2	82.6	81.0	84.6	41.6	42.6	42.0	48.7	48.7	46.5	50.2	43.6	43.8	43.6	49.4	43.9	45.4
15:50	85.8	85.6	85.8	85.2	85.6	85.1	84.1	85.0	85.8	82.0	82.4	80.8	84.4	41.4	42.4	41.8	48.8	48.5	46.7	50.1	43.5	43.8	43.7	49.4	43.9	45.3
16:00	83.7	83.6	83.8	83.2	83.6	83.2	82.0	83.0	83.9	80.2	80.4	79.1	82.5	41.2	42.1	41.5	48.1	48.1	46.0	49.4	43.0	43.3	43.1	48.7	43.3	44.8
16:10	78.8	78.9	78.9	78.4	78.7	78.3	77.6	78.5	79.1	75.8	76.1	74.7	77.8	39.9	40.8	40.2	46.4	46.1	44.5	47.4	41.4	41.7	41.7	46.9	42.0	43.3
16:20	68.7	69.1	68.9	68.5	68.7	68.4	68.1	68.8	69.3	66.8	67.0	66.1	68.2	38.0	38.6	38.2	43.0	42.8	41.5	43.9	39.0	39.2	39.4	43.6	39.7	40.6
16:30	59.3	59.9	59.4	59.1	59.3	59.1	58.9	59.6	60.0	58.2	58.3	57.7	59.1	36.2	36.7	36.3	39.9	39.7	38.8	40.6	37.0	37.2	37.6	40.6	37.8	38.2
16:40	52.4	53.4	52.6	52.4	52.6	52.5	52.3	52.9	53.3	52.0	52.2	51.7	52.5	35.2	35.6	35.3	37.8	37.9	37.1	38.6	35.9	36.1	36.5	38.9	36.8	36.8
16:50	47.8	48.7	47.9	47.8	47.9	47.8	47.5	48.1	48.6	47.6	47.5	47.4	47.9	34.5	34.8	34.6	36.3	36.5	35.8	37.1	35.0	35.1	35.5	37.4	35.8	35.7
17:00	44.2	45.1	44.3	44.2	44.3	44.3	44.2	44.7	45.1	44.2	44.1	44.1	44.4	33.6	33.9	33.7	35.2	35.2	34.9	35.7	34.1	34.2	34.7	36.1	34.9	34.7

Table 3a: Raw Data of Run #3

Time	H	T _a	T _{e1}	T _{e2}	T _{e3}	T _{fm}	T _{ad}	T _{cond1}	T _{cond2}	T _{cond3}	T _{cond4}	T _{cond}	V _{L1}	V _{L2}	V _{L3}	V _{L4}	V _L	I _L	P _L	η _{TE}
10:10	425	27.6	46.7	39.6	34.0	40.1	33.5	32.7	33.2	33.2	32.3	32.9	0.028	0.043	0.032	0.039	0.036	0.007	0.000	0.002
10:20	600	28.3	44.6	46.5	42.7	44.6	42.0	41.6	42.1	42.2	41.2	41.8	0.079	0.116	0.088	0.114	0.099	0.019	0.002	0.013
10:30	610	28.3	47.3	49.6	45.7	47.5	44.8	44.5	44.9	45.1	44.0	44.6	0.094	0.137	0.105	0.136	0.118	0.022	0.003	0.018
10:40	446	28.6	49.3	51.7	47.9	49.6	46.8	46.3	46.9	47.1	46.0	46.6	0.106	0.154	0.118	0.154	0.133	0.025	0.003	0.031
10:50	583	29.3	51.8	54.5	50.4	52.2	49.1	48.2	49.3	49.4	48.2	48.8	0.115	0.168	0.129	0.167	0.145	0.027	0.004	0.028
11:00	692	30.3	53.8	56.6	52.3	54.2	50.8	50.4	50.9	51.1	49.8	50.6	0.125	0.183	0.140	0.182	0.157	0.030	0.005	0.028
11:10	721	29.9	56.3	59.1	54.8	56.7	53.1	52.6	53.1	53.4	51.9	52.8	0.134	0.197	0.151	0.195	0.170	0.032	0.005	0.032
11:20	733	30.5	58.9	61.9	57.4	59.4	55.5	54.7	55.6	55.7	54.2	55.1	0.144	0.210	0.163	0.210	0.182	0.034	0.006	0.036
11:30	760	30.5	61.6	64.7	60.0	62.1	58.0	56.9	58.0	58.2	56.6	57.4	0.155	0.224	0.175	0.226	0.195	0.037	0.007	0.039
11:40	777	31.4	64.1	67.4	62.5	64.7	60.4	58.8	60.4	60.7	59.0	59.7	0.166	0.247	0.188	0.242	0.211	0.040	0.008	0.045
11:50	787	32.4	66.4	69.9	64.8	67.0	62.6	60.9	62.5	62.8	61.1	61.8	0.176	0.262	0.199	0.257	0.224	0.042	0.009	0.050
12:00	819	32.4	68.6	72.3	67.0	69.3	64.7	63.0	64.5	64.9	63.0	63.9	0.186	0.278	0.211	0.271	0.236	0.045	0.011	0.054
12:10	844	32.0	70.7	74.5	69.0	71.4	66.4	64.8	66.3	66.6	64.7	65.6	0.197	0.294	0.223	0.287	0.250	0.047	0.012	0.059
12:20	854	32.7	72.9	76.8	71.2	73.6	68.5	66.8	68.3	68.7	66.6	67.6	0.208	0.309	0.235	0.303	0.264	0.050	0.013	0.064
12:30	866	34.9	74.9	79.0	73.2	75.7	70.3	68.5	70.1	70.5	68.3	69.4	0.217	0.323	0.246	0.316	0.275	0.052	0.014	0.069
12:40	873	34.8	76.8	81.0	75.1	77.6	72.1	70.2	71.8	72.3	70.0	71.1	0.227	0.336	0.256	0.329	0.287	0.054	0.016	0.075
12:50	890	33.6	78.6	82.9	76.8	79.4	73.7	71.7	73.4	73.8	71.5	72.6	0.236	0.351	0.267	0.343	0.299	0.056	0.017	0.079
13:00	885	32.9	80.3	84.7	78.5	81.2	75.2	73.1	74.9	75.4	72.9	74.1	0.246	0.367	0.277	0.356	0.311	0.059	0.018	0.087
13:10	895	35.4	81.8	86.2	79.9	82.6	76.6	74.3	76.2	76.7	74.2	75.4	0.253	0.376	0.284	0.365	0.319	0.060	0.019	0.090
13:20	907	34.6	83.4	87.9	81.6	84.3	78.1	75.8	77.6	78.2	75.6	76.8	0.261	0.388	0.292	0.377	0.329	0.062	0.020	0.095
13:30	901	35.1	84.8	89.3	83.0	85.7	79.5	77.0	78.9	79.5	76.8	78.1	0.269	0.399	0.301	0.388	0.339	0.064	0.022	0.101
13:40	909	35.5	86.2	90.8	84.4	87.1	80.8	78.2	80.3	80.9	78.1	79.4	0.276	0.409	0.308	0.398	0.348	0.066	0.023	0.105
13:50	900	35.3	87.4	92.2	85.7	88.4	81.9	79.3	81.3	82.0	79.2	80.5	0.283	0.419	0.315	0.407	0.356	0.067	0.024	0.111
14:00	895	36.4	88.4	93.2	86.7	89.4	83.0	80.2	82.3	83.1	80.1	81.4	0.287	0.425	0.320	0.413	0.361	0.068	0.025	0.115
14:10	885	34.7	89.3	94.2	87.7	90.4	83.9	81.1	83.2	83.9	80.9	82.3	0.292	0.433	0.325	0.421	0.368	0.069	0.026	0.121
14:20	851	34.8	90.0	94.8	88.4	91.1	84.6	81.7	83.9	84.6	81.6	83.0	0.296	0.439	0.329	0.426	0.372	0.070	0.026	0.129
14:30	872	36.1	90.6	95.5	89.0	91.7	85.0	82.2	84.4	85.0	82.0	83.4	0.299	0.444	0.332	0.430	0.376	0.071	0.027	0.128
14:40	838	35.8	91.1	96.0	89.5	92.2	85.5	82.7	84.9	85.5	82.5	83.9	0.302	0.447	0.335	0.434	0.379	0.072	0.027	0.136
14:50	836	35.6	91.8	96.8	90.2	92.9	86.2	83.3	85.4	86.1	83.1	84.5	0.306	0.451	0.339	0.439	0.384	0.072	0.028	0.139
15:00	818	36.1	92.0	97.0	90.5	93.2	86.4	83.5	85.6	86.3	83.3	84.7	0.307	0.455	0.340	0.441	0.386	0.073	0.028	0.144
15:10	787	36.1	92.2	97.1	90.7	93.3	86.6	83.7	85.8	86.6	83.5	84.9	0.308	0.454	0.341	0.442	0.386	0.073	0.028	0.150
15:20	774	36.1	92.0	96.9	90.6	93.2	86.5	83.5	85.6	86.4	83.4	84.7	0.307	0.451	0.340	0.440	0.385	0.073	0.028	0.151
15:30	732	35.5	91.8	96.7	90.4	93.0	86.2	83.5	85.5	86.3	83.3	84.7	0.307	0.453	0.340	0.441	0.385	0.073	0.028	0.160
15:40	715	35.0	90.7	95.5	89.4	91.9	85.3	82.5	84.6	85.3	82.4	83.7	0.302	0.442	0.334	0.433	0.378	0.071	0.027	0.158
15:50	711	35.9	90.0	94.8	88.8	91.2	84.8	81.9	84.0	84.7	81.7	83.1	0.298	0.440	0.330	0.427	0.374	0.071	0.026	0.155
16:00	693	35.1	89.6	94.5	88.5	90.9	84.4	81.6	83.7	84.4	81.5	82.8	0.295	0.437	0.328	0.424	0.371	0.070	0.026	0.157
16:10	696	35.3	88.7	93.6	87.7	90.0	83.8	80.8	82.9	83.7	80.7	82.0	0.290	0.429	0.323	0.417	0.365	0.069	0.025	0.151
16:20	625	35.3	88.5	93.2	87.4	89.7	83.5	80.8	82.7	83.5	80.6	81.9	0.290	0.428	0.323	0.417	0.364	0.069	0.025	0.168
16:30	581	36.4	87.2	91.8	86.4	88.5	82.4	79.7	81.6	82.3	79.5	80.8	0.284	0.420	0.316	0.410	0.358	0.067	0.024	0.174
16:40	566	35.5	85.8	90.4	85.1	87.1	81.1	78.6	80.4	81.1	78.3	79.6	0.278	0.411	0.309	0.400	0.349	0.066	0.023	0.171
16:50	515	35.7	84.3	88.7	83.7	85.6	79.8	77.5	79.1	79.7	77.1	78.4	0.271	0.400	0.301	0.391	0.340	0.064	0.022	0.178
17:00	481	36.0	82.8	87.1	82.2	84.0	78.3	76.2	77.7	78.3	75.8	77.0	0.263	0.389	0.293	0.380	0.331	0.062	0.021	0.180

Table 3b: Raw Data of Run #3

Time	T _{h1}	T _{h2}	T _{h3}	T _{h4}	T _{h5}	T _{h6}	T _{h7}	T _{h8}	T _{h9}	T _{h10}	T _{h11}	T _{h12}	T _h	T _{e1}	T _{e2}	T _{e3}	T _{e4}	T _{e5}	T _{e6}	T _{e7}	T _{e8}	T _{e9}	T _{e10}	T _{e11}	T _{e12}	T _e
10:10	32.1	32.1	31.9	31.9	32.0	31.9	31.5	31.8	32.1	31.6	31.6	31.3	31.8	27.4	27.6	27.6	28.3	28.3	28.2	28.8	28.0	28.4	27.9	28.1	28.1	28.1
10:20	41.1	41.1	41.0	40.8	40.9	40.8	40.3	40.8	41.2	40.2	40.0	39.6	40.7	28.7	29.2	29.0	30.8	31.2	30.5	31.9	29.7	30.8	29.3	29.7	29.5	30.0
10:30	43.9	44.2	44.0	43.8	43.9	43.8	43.2	43.7	44.2	43.2	42.8	42.5	43.6	29.4	29.9	29.6	31.7	32.2	31.3	33.1	30.4	31.8	29.8	30.4	30.1	30.8
10:40	45.9	46.0	45.9	45.7	45.8	45.6	45.3	45.9	46.1	44.8	44.5	44.1	45.5	29.3	29.7	29.4	32.3	32.4	31.9	33.3	30.3	31.8	30.1	30.6	30.1	30.9
10:50	48.1	48.2	48.2	47.9	48.1	47.9	47.0	47.6	48.1	46.9	46.1	46.1	47.5	30.1	30.5	30.2	32.9	33.4	32.5	34.3	31.0	32.7	30.4	31.0	30.5	31.6
11:00	49.6	49.8	49.6	49.4	49.6	49.4	48.9	49.5	50.0	48.4	48.2	47.6	49.2	30.3	30.8	30.5	33.6	34.1	33.1	35.0	31.6	33.4	30.9	31.6	31.3	32.2
11:10	51.7	51.9	51.8	51.5	51.7	51.5	51.0	51.7	52.1	50.4	50.2	49.5	51.3	30.8	31.4	31.1	34.5	34.9	34.0	35.9	32.3	34.2	31.6	32.2	31.9	32.9
11:20	54.0	54.0	54.0	53.7	53.9	53.7	53.1	53.8	54.2	52.4	52.1	51.4	53.4	31.4	32.0	31.6	35.6	35.8	35.1	36.6	32.7	34.6	32.2	32.8	32.4	33.6
11:30	56.3	56.2	56.2	55.9	56.1	55.9	55.2	56.0	56.4	54.5	54.2	53.4	55.5	32.2	32.8	32.3	36.7	36.9	36.2	37.6	33.4	35.6	32.8	33.5	33.1	34.4
11:40	58.8	58.5	58.9	58.4	58.7	58.4	57.4	58.0	58.6	56.7	56.0	55.6	57.8	32.9	33.5	33.0	37.1	37.3	36.3	38.6	34.1	36.4	33.5	34.0	33.4	35.0
11:50	60.8	60.8	60.9	60.5	60.8	60.5	59.4	60.0	60.7	58.9	57.9	57.7	59.9	33.8	34.4	33.5	37.9	38.1	37.1	39.4	34.7	37.1	34.0	34.5	34.0	35.7
12:00	62.7	62.7	62.8	62.4	62.7	62.4	61.3	61.9	62.7	60.6	59.9	59.5	61.8	34.3	34.7	34.4	38.7	39.3	37.8	40.7	35.7	38.2	34.5	35.2	34.7	36.5
12:10	64.4	64.3	64.4	64.0	64.3	64.0	63.2	63.9	64.4	62.1	61.6	60.8	63.5	34.3	35.0	34.5	39.4	39.5	38.4	41.0	35.7	38.5	35.0	35.5	34.9	36.8
12:20	66.3	66.2	66.4	65.9	66.2	65.9	65.0	65.9	66.3	63.8	63.4	62.6	65.3	34.7	35.4	34.8	40.1	40.3	39.1	41.7	36.2	39.0	35.2	35.8	35.2	37.3
12:30	68.0	67.9	68.1	67.6	67.9	67.6	66.7	67.5	68.0	65.4	65.0	64.1	67.0	35.1	35.8	35.2	40.7	40.9	39.6	42.3	36.6	39.6	35.6	36.2	35.6	37.8
12:40	69.7	69.5	69.7	69.3	69.6	69.2	68.3	69.1	69.6	67.0	66.5	65.6	68.6	35.4	36.2	35.5	41.3	41.4	40.1	42.8	36.9	40.0	35.9	36.5	35.8	38.2
12:50	71.1	71.0	71.2	70.7	71.1	70.7	69.7	70.6	71.1	68.3	67.9	66.9	70.0	35.4	36.3	35.6	41.6	41.7	40.3	43.2	37.0	40.3	36.0	36.7	36.0	38.3
13:00	72.6	72.4	72.7	72.1	72.5	72.1	71.1	71.9	72.5	69.6	69.2	68.1	71.4	35.4	36.4	35.6	41.7	41.7	40.3	43.5	37.1	40.5	36.1	36.7	36.0	38.4
13:10	73.8	73.6	73.9	73.4	73.7	73.2	72.3	73.2	73.8	70.7	70.4	69.2	72.6	35.8	36.7	35.9	42.2	42.2	40.8	44.0	37.4	40.9	36.4	37.1	36.3	38.8
13:20	75.2	75.0	75.3	74.7	75.1	74.6	73.6	74.5	75.2	72.0	71.7	70.5	74.0	36.0	37.0	36.2	42.6	42.7	41.2	44.5	37.7	41.3	36.6	37.4	36.6	39.2
13:30	76.4	76.3	76.5	75.9	76.3	75.8	74.8	75.8	76.4	73.1	72.9	71.6	75.2	36.1	37.1	36.2	43.0	43.0	41.4	44.8	37.9	41.6	36.7	37.5	36.7	39.3
13:40	77.7	77.5	77.8	77.2	77.6	77.0	76.0	77.0	77.6	74.2	74.0	72.7	76.4	36.3	37.3	36.5	43.4	43.4	41.8	45.2	38.1	41.9	36.9	37.7	36.9	39.6
13:50	78.7	78.6	78.9	78.2	78.6	78.1	77.0	78.0	78.7	75.2	75.0	73.6	77.4	36.4	37.5	36.5	43.7	43.7	42.1	45.5	38.2	42.1	37.0	37.8	37.0	39.8
14:00	79.7	79.5	79.8	79.2	79.6	79.0	77.9	79.0	79.7	76.1	75.9	74.5	78.3	36.6	37.7	36.8	44.1	44.1	42.4	46.0	38.5	42.5	37.3	38.1	37.2	40.1
14:10	80.5	80.3	80.6	80.0	80.4	79.8	78.7	79.8	80.5	76.8	76.7	75.2	79.1	36.7	37.8	36.9	44.3	44.2	42.6	46.2	38.6	42.7	37.4	38.2	37.3	40.2
14:20	81.1	80.9	81.3	80.6	81.0	80.4	79.3	80.4	81.1	77.4	77.2	75.8	79.7	36.8	37.9	37.0	44.4	44.4	42.7	46.4	38.7	42.8	37.5	38.3	37.5	40.4
14:30	81.6	81.4	81.7	81.1	81.5	80.9	79.8	80.9	81.6	77.9	77.8	76.3	80.2	36.9	37.9	37.0	44.5	44.5	42.7	46.5	38.8	42.9	37.5	38.3	37.5	40.4
14:40	82.1	82.0	82.2	81.6	82.0	81.4	80.3	81.4	82.1	78.4	78.3	76.8	80.7	36.9	37.9	37.0	44.7	44.6	42.9	46.6	38.9	43.1	37.6	38.4	37.6	40.5
14:50	82.6	82.5	82.8	82.2	82.6	82.0	80.9	82.0	82.7	78.8	78.8	77.2	81.3	37.0	38.0	37.1	44.9	44.9	43.1	46.8	38.9	43.2	37.7	38.6	37.7	40.7
15:00	82.9	82.8	83.0	82.4	82.8	82.2	81.1	82.2	83.0	79.1	79.1	77.5	81.5	36.9	38.0	37.1	44.9	44.7	43.0	46.8	38.9	43.2	37.7	38.5	37.7	40.6
15:10	83.1	83.0	83.2	82.6	83.0	82.4	81.3	82.4	83.1	79.2	79.2	77.7	81.7	37.0	38.1	37.2	45.1	45.1	43.3	46.9	39.0	43.3	37.8	38.7	37.8	40.8
15:20	83.0	82.9	83.1	82.5	82.9	82.2	81.2	82.3	83.1	79.2	79.1	77.6	81.6	37.0	38.1	37.2	45.3	45.2	43.5	47.0	39.1	43.4	37.9	38.7	37.9	40.9
15:30	82.8	82.7	83.0	82.4	82.8	82.1	81.1	82.2	82.9	79.0	79.0	77.4	81.5	36.9	37.9	37.0	45.1	45.0	43.2	46.8	38.9	43.2	37.7	38.6	37.7	40.7
15:40	81.9	81.9	82.0	81.5	81.9	81.2	80.2	81.3	82.0	78.3	78.2	76.7	80.6	36.8	37.9	36.9	45.0	45.0	43.2	46.7	38.9	43.1	37.6	38.5	37.7	40.6
15:50	81.3	81.3	81.4	80.8	81.2	80.6	79.6	80.7	81.4	77.7	77.6	76.1	80.0	36.8	37.8	36.9	44.6	44.5	42.7	46.5	38.8	43.0	37.6	38.4	37.6	40.4
16:00	81.0	81.0	81.2	80.6	81.0	80.3	79.4	80.4	81.2	77.4	77.3	75.9	79.7	36.7	37.8	36.9	44.6	44.6	42.8	46.4	38.8	42.9	37.6	38.4	37.6	40.4
16:10	80.2	80.3	80.4	79.8	80.2	79.5	78.6	79.7	80.4	76.8	76.7	75.3	79.0	36.8	37.8	36.9	44.5	44.5	42.7	46.2	38.7	42.7	37.6	38.4	37.6	40.4
16:20	80.1	80.1	80.2	79.7	80.1	79.4	78.5	79.6	80.3	76.6	76.6	75.2	78.9	36.7	37.6	36.8	44.5	44.4	42.7	46.1	38.5	42.6	37.4	38.3	37.5	40.3
16:30	79.1	79.2	79.2	78.7	79.1	78.4	77.6	78.6	79.3	75.8	75.6	74.3	77.9	36.5	37.5	36.6	44.2	44.1	42.4	45.8	38.4	42.3	37.2	38.0	37.3	40.0
16:40	77.9	78.0	78.0	77.5	77.9	77.2	76.5	77.5	78.1	74.7	74.6	73.3	76.8	36.3	37.2	36.4	43.8	43.7	42.1	45.5	38.2	42.0	37.0	37.8	37.0	39.8
16:50	76.7	76.9	76.9	76.4	76.7	76.1	75.4	76.4	77.0	73.7	73.6	72.3	75.7	36.1	37.0	36.3	43.5	43.4	41.8	45.1	38.0	41.7	36.9	37.7	37.0	39.5
17:00	75.4	75.6	75.6	75.1	75.4	74.8	74.1	75.0	75.7	72.5	72.3	71.2	74.4	35.9	36.8	36.0	43.0	43.0	41.4	44.7	37.8	41.4	36.6	37.4	36.7	39.2

Table 4a: Raw Data of Run #4

Time	H	T _a	T _{e1}	T _{e2}	T _{e3}	T _m	T _{ad}	T _{cond1}	T _{cond2}	T _{cond3}	T _{cond4}	T _{cond}	V _{L1}	V _{L2}	V _{L3}	V _{L4}	V _L	I _L	P _L	Π _{TE}
10:10	456	27.9	36.3	58.8	38.8	44.6	30.3	29.4	29.5	29.6	29.1	29.4	0.007	0.012	0.009	0.008	0.009	0.002	0.000	0.0001
10:20	492	28.3	51.3	44.6	40.6	45.5	39.9	38.6	39.6	39.7	38.4	39.1	0.063	0.095	0.071	0.088	0.079	0.015	0.001	0.0101
10:30	554	29.5	46.4	48.6	45.0	46.7	44.1	43.3	44.1	44.2	43.2	43.7	0.088	0.128	0.097	0.124	0.109	0.021	0.002	0.0170
10:40	587	30.5	48.6	51.1	47.4	49.0	46.2	45.6	46.2	46.4	45.3	45.9	0.099	0.145	0.110	0.140	0.123	0.023	0.003	0.0205
10:50	596	29.6	51.3	54.0	50.2	51.8	48.8	47.9	48.8	49.0	47.8	48.4	0.108	0.159	0.121	0.154	0.136	0.026	0.003	0.0245
11:00	603	29.9	53.4	56.2	52.2	53.9	50.7	50.1	50.7	50.8	49.6	50.3	0.118	0.173	0.132	0.168	0.147	0.028	0.004	0.0285
11:10	637	30.0	55.8	58.6	54.5	56.3	52.8	52.3	52.8	53.0	51.7	52.5	0.127	0.186	0.143	0.181	0.159	0.030	0.005	0.0315
11:20	682	31.4	58.1	61.1	56.8	58.7	55.0	53.9	55.0	55.2	53.7	54.5	0.136	0.202	0.153	0.194	0.171	0.032	0.006	0.0341
11:30	690	30.6	60.9	64.0	59.5	61.5	57.6	56.7	57.6	57.9	56.3	57.1	0.147	0.219	0.165	0.209	0.185	0.035	0.006	0.0392
11:40	694	32.2	62.9	66.1	61.4	63.5	59.4	58.4	59.3	59.5	57.9	58.8	0.156	0.233	0.177	0.223	0.197	0.037	0.007	0.0443
11:50	712	32.0	65.3	68.6	63.8	65.9	61.6	60.1	61.6	61.8	60.1	60.9	0.166	0.247	0.187	0.237	0.209	0.039	0.008	0.0486
12:00	735	33.1	67.2	70.7	65.8	67.9	63.5	62.2	63.5	64.0	62.2	63.0	0.175	0.260	0.198	0.250	0.221	0.042	0.009	0.0525
12:10	740	31.0	69.4	72.9	67.9	70.1	65.4	63.8	65.3	65.7	63.8	64.7	0.185	0.274	0.210	0.266	0.234	0.044	0.010	0.0584
12:20	745	33.3	70.5	74.1	69.0	71.2	66.5	65.1	66.4	66.8	64.9	65.8	0.191	0.282	0.216	0.274	0.241	0.045	0.011	0.0616
12:30	755	33.6	71.7	75.4	70.2	72.4	67.5	66.5	67.4	67.8	65.8	66.9	0.198	0.291	0.224	0.283	0.249	0.047	0.012	0.0649
12:40	757	33.5	73.8	77.7	72.2	74.6	69.4	67.4	69.2	69.7	67.6	68.5	0.205	0.301	0.232	0.293	0.258	0.049	0.013	0.0695
12:50	751	34.3	75.3	79.2	73.7	76.1	70.8	68.7	70.6	71.1	69.0	69.9	0.213	0.311	0.240	0.304	0.267	0.050	0.013	0.0751
13:00	761	33.0	76.3	80.2	74.7	77.1	71.7	69.8	71.5	71.9	69.8	70.8	0.220	0.321	0.249	0.315	0.276	0.052	0.014	0.0792
13:10	729	33.3	77.3	81.3	75.7	78.1	72.7	70.9	72.5	73.0	70.7	71.8	0.226	0.328	0.255	0.323	0.283	0.053	0.015	0.0869
13:20	768	33.4	77.9	82.0	76.3	78.7	73.2	71.3	73.0	73.4	71.2	72.2	0.230	0.332	0.259	0.328	0.287	0.054	0.016	0.0849
13:30	822	34.1	80.2	84.5	78.4	81.0	75.1	73.1	74.9	75.4	73.0	74.1	0.239	0.343	0.270	0.341	0.298	0.056	0.017	0.0856
13:40	821	34.3	82.0	86.4	80.2	82.9	76.7	74.6	76.4	77.0	74.5	75.6	0.248	0.353	0.279	0.354	0.308	0.058	0.018	0.0917
13:50	802	34.0	84.0	88.4	82.2	84.9	78.5	76.3	78.2	78.8	76.2	77.4	0.259	0.364	0.290	0.368	0.320	0.060	0.019	0.1010
14:00	770	34.2	84.4	88.7	82.7	85.3	79.1	76.8	78.8	79.4	76.8	78.0	0.262	0.368	0.292	0.373	0.324	0.061	0.020	0.1078
14:10	776	35.4	83.9	88.0	82.3	84.7	78.7	76.5	78.4	79.0	76.4	77.6	0.260	0.362	0.289	0.369	0.320	0.060	0.019	0.1044
14:20	769	34.4	85.6	89.9	84.0	86.5	80.2	77.9	79.8	80.5	77.8	79.0	0.269	0.372	0.297	0.381	0.329	0.062	0.020	0.1117
14:30	761	34.1	85.6	89.8	84.0	86.5	80.3	77.9	79.9	80.5	77.9	79.1	0.269	0.368	0.298	0.382	0.329	0.062	0.020	0.1126
14:40	714	34.7	86.1	90.3	84.6	87.0	80.8	78.5	80.4	81.1	78.4	79.6	0.273	0.370	0.301	0.387	0.333	0.063	0.021	0.1227
14:50	726	34.7	86.0	90.2	84.5	86.9	80.8	78.4	80.4	81.0	78.3	79.5	0.272	0.370	0.300	0.386	0.332	0.063	0.021	0.1203
15:00	664	34.5	86.3	90.5	84.8	87.2	81.0	78.6	80.6	81.3	78.6	79.8	0.273	0.369	0.301	0.388	0.333	0.063	0.021	0.1319
15:10	688	34.2	86.1	90.4	84.7	87.1	80.8	78.6	80.5	81.2	78.5	79.7	0.272	0.367	0.299	0.387	0.331	0.062	0.021	0.1261
15:20	693	35.0	86.5	90.8	85.0	87.4	81.3	78.9	80.8	81.5	78.8	80.0	0.273	0.368	0.299	0.388	0.332	0.063	0.021	0.1259
15:30	643	35.5	86.8	91.1	85.4	87.8	81.6	79.2	81.2	81.8	79.1	80.3	0.276	0.372	0.300	0.391	0.335	0.063	0.021	0.1379
15:40	570	34.6	85.2	89.3	84.1	86.2	80.5	78.3	80.1	80.7	78.1	79.3	0.271	0.368	0.293	0.383	0.329	0.062	0.020	0.1500
15:50	433	33.9	82.9	86.8	82.0	83.9	78.4	76.5	78.1	78.7	76.3	77.4	0.261	0.353	0.283	0.370	0.317	0.060	0.019	0.1833
16:00	522	33.6	81.0	85.1	80.0	82.0	76.5	74.7	76.3	76.7	74.5	75.6	0.249	0.341	0.273	0.354	0.304	0.057	0.017	0.1402
16:10	314	34.1	78.4	82.2	77.7	79.4	74.4	72.9	74.3	74.7	72.6	73.6	0.239	0.329	0.263	0.340	0.293	0.055	0.016	0.2162
16:20	551	33.7	77.7	81.7	76.7	78.7	73.4	71.8	73.1	73.6	71.4	72.5	0.231	0.320	0.256	0.329	0.284	0.054	0.015	0.1157
16:30	531	34.6	77.9	81.9	76.9	78.9	73.6	71.7	73.3	73.7	71.5	72.6	0.232	0.321	0.255	0.329	0.284	0.054	0.015	0.1204
16:40	550	34.5	79.0	83.3	78.0	80.1	74.6	72.6	74.2	74.7	72.3	73.5	0.236	0.330	0.259	0.336	0.290	0.055	0.016	0.1212
16:50	506	34.7	79.1	83.3	78.2	80.2	74.8	72.9	74.5	74.9	72.7	73.8	0.239	0.334	0.261	0.339	0.293	0.055	0.016	0.1343
17:00	438	34.8	79.3	83.5	78.5	80.4	75.1	73.2	74.7	75.2	73.0	74.0	0.240	0.352	0.261	0.341	0.299	0.056	0.017	0.1611

Table 4b: Raw Data of Run #4

Time	T _{h1}	T _{h2}	T _{h3}	T _{h4}	T _{h5}	T _{h6}	T _{h7}	T _{h8}	T _{h9}	T _{h10}	T _{h11}	T _{h12}	T _h	T _{c1}	T _{c2}	T _{c3}	T _{c4}	T _{c5}	T _{c6}	T _{c7}	T _{c8}	T _{c9}	T _{c10}	T _{c11}	T _{c12}	T _c
10:10	28.9	29.3	28.9	28.9	28.9	28.9	28.7	29.1	29.3	29.1	28.9	29.1	29.0	27.8	27.9	27.9	27.7	28.1	27.9	28.3	28.1	28.2	27.8	28.1	28.2	28.0
10:20	38.2	38.2	38.1	37.9	38.0	37.9	37.4	37.9	38.1	37.3	37.0	36.8	37.7	28.2	28.4	28.2	29.8	29.9	29.5	30.6	28.8	29.9	28.9	29.2	28.8	29.2
10:30	43.1	43.1	43.1	42.8	42.9	42.3	42.0	42.5	43.1	42.1	41.7	41.4	42.5	29.4	29.7	29.5	31.3	31.8	31.1	32.7	30.2	31.8	29.9	30.4	30.3	30.7
10:40	45.1	45.4	45.1	44.9	45.1	44.7	44.3	44.9	45.4	44.3	43.8	43.5	44.7	29.4	30.0	30.0	32.2	32.7	32.0	33.7	30.9	32.6	30.5	31.1	30.8	31.3
10:50	47.6	47.7	47.4	47.4	47.5	46.8	46.6	47.1	47.6	46.5	46.0	45.6	47.0	30.3	31.1	30.8	33.3	33.8	33.0	34.8	31.7	33.6	31.3	31.9	31.6	32.3
11:00	49.4	49.5	49.4	49.2	49.3	49.1	48.7	49.2	49.5	48.1	48.0	47.2	48.9	31.0	31.4	31.1	34.2	34.4	33.7	35.4	32.1	34.3	32.1	32.7	32.3	32.9
11:10	51.5	51.5	51.4	51.2	51.4	51.1	50.7	51.2	51.6	50.1	50.0	49.1	50.9	31.6	32.1	31.7	35.2	35.3	34.6	36.3	32.8	35.3	32.8	33.4	33.1	33.7
11:20	53.6	53.6	53.6	53.2	53.5	53.2	52.6	53.3	53.6	52.0	51.5	51.0	52.9	32.3	32.9	32.5	35.9	36.0	35.2	37.2	33.4	35.9	33.4	33.9	33.3	34.3
11:30	56.1	56.3	56.1	55.9	56.1	55.5	54.9	55.9	56.3	54.6	54.2	53.6	55.5	33.1	33.9	33.7	36.8	37.4	36.3	38.7	34.7	37.2	34.2	34.9	34.6	35.5
11:40	57.7	57.8	57.7	57.4	57.7	57.4	56.8	57.5	57.8	56.1	55.8	55.0	57.1	33.6	34.2	33.7	37.6	37.8	36.9	39.1	34.8	37.7	34.8	35.3	34.8	35.9
11:50	59.9	59.9	60.0	59.6	59.8	59.2	58.6	59.5	60.0	58.0	57.4	56.8	59.1	34.1	34.8	34.3	38.4	38.6	37.6	39.9	35.4	38.5	35.3	35.9	35.2	36.5
12:00	62.0	62.0	62.1	61.7	62.0	61.1	60.6	61.5	62.1	60.0	59.3	58.9	61.1	35.4	35.8	35.1	39.3	39.6	38.5	40.9	36.1	39.3	36.0	36.6	35.9	37.4
12:10	63.6	63.5	63.6	63.2	63.4	62.8	62.1	62.8	63.6	61.4	60.8	60.1	62.6	35.6	35.7	35.2	39.8	40.2	38.9	41.4	36.3	39.8	36.0	36.7	36.0	37.6
12:20	64.6	64.7	64.7	64.3	64.6	63.9	63.1	63.9	64.7	62.5	62.1	61.3	63.7	35.5	36.2	35.6	40.2	40.8	39.4	42.0	36.9	40.3	36.2	36.9	36.5	38.0
12:30	65.6	65.6	65.6	65.2	65.5	65.1	64.4	65.2	65.7	63.3	63.3	62.0	64.7	35.5	36.2	35.7	40.8	41.2	39.9	42.3	37.1	40.5	36.6	37.4	37.0	38.4
12:40	67.3	67.3	67.4	66.9	67.2	66.4	65.7	66.5	67.2	64.9	64.1	63.5	66.2	36.8	36.8	36.2	41.3	41.8	40.4	42.9	37.4	41.1	36.9	37.6	36.8	38.8
12:50	68.6	68.6	68.7	68.2	68.5	67.8	66.9	67.7	68.6	66.1	65.4	64.7	67.5	35.9	37.1	36.4	41.8	42.3	40.9	43.3	37.6	41.5	37.1	37.8	37.0	39.1
13:00	69.4	69.5	69.5	69.1	69.4	69.0	68.1	69.0	69.5	66.9	66.4	65.4	68.4	36.0	36.8	36.1	42.3	42.5	41.2	43.4	37.5	41.4	37.2	37.9	37.1	39.1
13:10	70.4	70.4	70.5	70.0	70.3	69.9	69.0	69.9	70.4	67.7	67.3	66.2	69.3	36.1	36.9	36.3	42.7	42.9	41.7	43.6	37.7	41.7	37.3	37.9	37.2	39.3
13:20	70.9	70.9	70.9	70.4	70.8	70.4	69.5	70.4	70.9	68.1	67.8	66.6	69.8	36.2	36.9	36.2	42.9	43.1	41.7	43.7	37.6	41.8	37.2	37.9	37.1	39.4
13:30	72.6	72.6	72.7	72.2	72.5	72.1	71.1	72.0	72.6	69.7	69.4	68.1	71.5	36.5	37.3	36.6	43.7	43.9	42.6	44.4	38.0	42.3	37.6	38.3	37.6	39.9
13:40	74.1	74.1	74.2	73.7	74.0	73.6	72.6	73.6	74.1	71.1	70.9	69.5	73.0	36.7	37.5	36.8	44.5	44.6	43.2	44.8	38.3	42.7	37.8	38.5	37.7	40.3
13:50	75.8	75.8	75.9	75.4	75.7	75.3	74.2	75.2	75.9	72.7	72.4	71.0	74.6	36.9	37.7	37.0	45.3	45.5	44.0	45.4	38.6	43.2	38.0	38.8	37.9	40.7
14:00	76.4	76.4	76.5	76.0	76.3	75.8	74.8	75.8	76.4	73.2	72.9	71.5	75.2	37.0	37.9	37.1	45.5	45.6	44.1	45.7	38.8	43.4	38.1	38.8	38.0	40.8
14:10	76.0	76.0	76.1	75.6	76.0	75.5	74.5	75.5	76.1	72.9	72.7	71.2	74.8	37.0	37.9	37.0	45.7	45.8	44.3	45.6	38.8	43.4	38.1	38.9	38.1	40.9
14:20	77.4	77.4	77.4	77.0	77.3	76.8	75.8	76.8	77.4	74.1	73.9	72.4	76.1	37.1	38.0	37.2	46.3	46.4	44.9	46.2	39.2	43.9	38.4	39.1	38.3	41.3
14:30	77.4	77.4	77.5	77.1	77.4	77.0	75.9	76.9	77.5	74.2	74.0	72.5	76.2	37.1	38.0	37.2	46.8	46.9	45.4	46.2	39.2	44.0	38.3	39.0	38.2	41.4
14:40	78.0	78.0	78.1	77.6	78.0	77.5	76.5	77.4	78.1	74.7	74.5	72.9	76.8	37.1	38.0	37.2	47.1	47.2	45.7	46.4	39.3	44.1	38.3	39.1	38.2	41.5
14:50	77.9	77.9	78.0	77.5	77.9	77.4	76.3	77.3	78.0	74.6	74.5	72.9	76.7	37.1	38.0	37.2	47.0	47.2	45.7	46.3	39.3	44.0	38.3	39.1	38.3	41.5
15:00	78.2	78.3	78.3	77.8	78.1	77.7	76.6	77.6	78.3	74.9	74.7	73.2	77.0	37.3	38.2	37.4	47.4	47.6	46.1	46.6	39.5	44.3	38.4	39.2	38.3	41.7
15:10	78.1	78.1	78.2	77.7	78.1	77.6	76.5	77.6	78.2	74.8	74.7	73.1	76.9	37.3	38.2	37.3	47.6	47.7	46.2	46.6	39.6	44.4	38.4	39.2	38.3	41.7
15:20	78.4	78.4	78.5	78.0	78.4	77.9	76.8	77.8	78.5	75.1	75.0	73.4	77.2	37.5	38.4	37.5	47.7	47.9	46.4	47.0	39.9	44.6	38.6	39.4	38.6	42.0
15:30	78.7	78.8	78.8	78.3	78.7	78.2	77.2	78.2	78.9	75.4	75.3	73.7	77.5	37.4	38.3	37.5	47.7	47.9	46.4	47.1	40.1	44.9	38.7	39.5	38.7	42.0
15:40	77.7	77.8	77.8	77.4	77.7	77.2	76.3	77.3	77.9	74.5	74.5	72.8	76.6	37.2	38.2	37.4	47.0	47.3	45.7	46.9	40.1	44.7	38.6	39.4	38.5	41.8
15:50	76.0	76.1	76.1	75.7	76.0	75.5	74.7	75.6	76.3	73.0	72.9	71.3	74.9	37.0	37.8	37.1	46.5	46.7	45.3	46.3	39.5	44.0	38.2	38.9	38.2	41.3
16:00	74.1	74.3	74.3	73.8	74.1	73.6	72.8	73.8	74.4	71.3	71.2	69.8	73.1	36.7	37.6	36.9	45.7	45.9	44.5	45.6	39.2	43.4	37.9	38.7	38.0	40.8
16:10	72.3	72.5	72.4	72.0	72.3	71.8	71.2	72.1	72.7	69.7	69.6	68.2	71.4	36.4	37.1	36.5	44.8	45.0	43.7	44.8	38.5	42.7	37.6	38.3	37.6	40.3
16:20	71.1	71.4	71.1	70.7	71.1	70.6	69.9	70.8	71.4	68.5	68.5	67.1	70.2	36.3	37.0	36.4	44.4	44.6	43.4	44.4	38.4	42.4	37.5	38.2	37.5	40.0
16:30	71.2	71.4	71.3	70.9	71.2	70.7	70.0	70.9	71.5	68.6	68.4	67.2	70.3	36.4	37.0	36.4	44.4	44.6	43.3	44.6	38.6	42.6	37.5	38.2	37.5	40.1
16:40	71.9	72.1	72.0	71.6	71.9	71.5	70.7	71.6	72.2	69.2	69.1	67.7	71.0	36.5	37.2	36.5	44.5	44.7	43.3	44.9	38.8	42.8	37.7	38.4	37.6	40.2
16:50	72.3	72.4	72.4	72.0	72.2	71.8	71.1	71.9	72.5	69.5	69.4	68.0	71.3	36.5	37.3	36.6	44.5	44.7	43.3	45.1	38.9	43.0	37.7	38.4	37.7	40.3
17:00	72.6	72.7	72.7	72.2	72.5	72.0	71.4	72.3	72.8	69.8	69.8	68.3	71.6	36.6	37.4	36.6	43.2	43.4	42.0	45.3	39.2	43.2	37.8	38.5	37.8	40.1

Table 5a: Raw Data of Run #5

Time	H	T _a	T _{e1}	T _{e2}	T _{e3}	T _{in}	T _{ad}	T _{cond1}	T _{cond2}	T _{cond3}	T _{cond4}	T _{cond}	V _{L1}	V _{L2}	V _{L3}	V _{L4}	V _L	I _L	P _L	η _{TE}
10:30	719	30.2	42.7	43.2	40.3	42.1	40.0	38.6	40.1	40.0	39.3	39.5	0.053	0.083	0.059	0.075	0.068	0.013	0.001	0.0050
10:40	736	30.5	44.5	45.9	43.0	44.5	42.4	41.5	42.6	42.5	41.9	42.1	0.072	0.113	0.079	0.102	0.091	0.017	0.002	0.0089
10:50	760	32.1	46.5	48.2	45.1	46.6	44.3	43.5	44.5	44.4	43.7	44.0	0.081	0.128	0.090	0.115	0.104	0.020	0.002	0.0112
11:00	769	32.8	48.7	50.7	47.3	48.9	46.3	45.5	46.5	46.5	45.7	46.1	0.092	0.146	0.103	0.131	0.118	0.022	0.003	0.0143
11:10	811	32.1	51.3	53.5	49.8	51.5	48.6	47.6	48.8	48.8	47.8	48.3	0.105	0.164	0.116	0.149	0.134	0.025	0.003	0.0174
11:20	805	32.7	53.9	56.2	52.3	54.1	50.8	49.8	51.1	51.1	50.0	50.5	0.118	0.186	0.131	0.168	0.151	0.028	0.004	0.0224
11:30	829	33.0	56.4	58.9	54.9	56.7	53.2	52.0	53.5	53.5	52.2	52.8	0.130	0.206	0.146	0.184	0.167	0.031	0.005	0.0265
11:40	676	34.1	57.3	59.5	56.0	57.6	54.2	53.0	54.5	54.5	53.3	53.8	0.139	0.219	0.155	0.198	0.178	0.034	0.006	0.0370
11:50	678	34.2	59.6	62.5	58.3	60.1	56.3	54.8	56.5	56.5	55.2	55.8	0.151	0.237	0.168	0.214	0.192	0.036	0.007	0.0432
12:00	940	32.9	62.1	65.1	60.3	62.5	58.3	56.6	58.6	58.5	57.0	57.7	0.161	0.252	0.179	0.228	0.205	0.039	0.008	0.0354
12:10	939	32.4	65.6	68.6	63.5	65.9	61.4	59.4	61.6	61.6	59.9	60.6	0.176	0.277	0.197	0.250	0.225	0.042	0.010	0.0427
12:20	922	35.6	67.4	70.3	65.2	67.6	62.9	60.8	63.0	63.1	61.3	62.1	0.187	0.293	0.209	0.264	0.238	0.045	0.011	0.0486
12:30	922	33.3	69.3	72.4	67.0	69.6	64.6	62.4	64.7	64.8	63.0	63.7	0.197	0.310	0.220	0.279	0.252	0.047	0.012	0.0543
12:40	795	33.6	70.4	73.3	68.2	70.6	65.7	63.5	65.9	65.9	64.1	64.9	0.207	0.324	0.231	0.293	0.264	0.050	0.013	0.0691
12:50	949	33.2	71.2	74.5	68.8	71.5	66.2	63.8	66.4	66.4	64.5	65.3	0.207	0.326	0.232	0.293	0.264	0.050	0.013	0.0582
13:00	947	33.5	75.1	78.5	72.5	75.4	69.7	66.9	69.7	69.8	67.7	68.5	0.225	0.351	0.251	0.319	0.286	0.054	0.015	0.0685
13:10	968	34.0	78.2	81.8	75.5	78.5	72.4	69.4	72.4	72.6	70.4	71.2	0.242	0.379	0.270	0.341	0.308	0.058	0.018	0.0775
13:20	1001	34.2	81.2	85.2	78.5	81.6	75.0	71.9	75.2	75.3	72.8	73.8	0.256	0.402	0.287	0.362	0.327	0.062	0.020	0.0844
13:30	1066	36.5	84.2	88.2	81.7	84.7	78.1	74.6	78.1	78.3	75.7	76.7	0.273	0.426	0.304	0.384	0.347	0.065	0.023	0.0892
13:40	1050	34.4	80.5	84.0	78.6	81.0	75.4	72.2	75.3	75.4	73.1	74.0	0.260	0.406	0.290	0.367	0.330	0.062	0.021	0.0823
13:50	577	33.5	75.9	79.2	74.6	76.6	71.6	69.0	71.7	71.8	69.8	70.6	0.237	0.372	0.266	0.335	0.302	0.057	0.017	0.1254
14:00	690	34.6	69.7	72.8	68.5	70.3	66.0	63.7	66.0	66.0	64.3	65.0	0.203	0.319	0.228	0.286	0.259	0.049	0.013	0.0768
14:10	1011	34.5	69.0	72.2	67.5	69.6	64.9	62.7	65.0	65.0	63.1	64.0	0.196	0.307	0.220	0.276	0.250	0.047	0.012	0.0488
14:20	981	33.9	68.7	72.1	66.9	69.2	64.4	62.1	64.4	64.4	62.5	63.4	0.190	0.300	0.215	0.268	0.244	0.046	0.011	0.0478
14:30	907	34.3	77.0	80.8	74.6	77.5	71.3	68.4	71.4	71.5	69.0	70.1	0.229	0.359	0.258	0.324	0.292	0.055	0.016	0.0744
14:40	910	35.2	83.1	87.1	80.6	83.6	76.9	73.5	76.9	77.1	74.4	75.5	0.263	0.412	0.295	0.371	0.335	0.063	0.021	0.0977
14:50	220	35.7	84.4	87.9	83.1	85.1	79.3	76.3	79.3	79.5	77.2	78.1	0.283	0.438	0.313	0.399	0.358	0.068	0.024	0.4613
15:00	176	34.5	74.5	77.2	74.1	75.3	71.1	69.2	71.2	71.3	69.7	70.4	0.236	0.368	0.264	0.335	0.301	0.057	0.017	0.4063
15:10	909	36.1	72.9	76.8	71.3	73.7	68.4	65.7	68.3	68.3	66.1	67.1	0.212	0.334	0.239	0.299	0.271	0.051	0.014	0.0640
15:20	142	34.5	70.4	72.9	69.9	71.1	67.2	65.5	67.3	67.4	66.0	66.6	0.212	0.331	0.238	0.300	0.270	0.051	0.014	0.4064
15:30	795	37.1	76.7	80.8	74.9	77.5	71.5	68.5	71.5	71.5	69.1	70.2	0.232	0.363	0.260	0.328	0.296	0.056	0.016	0.0870
15:40	196	34.4	73.8	76.6	73.3	74.6	70.3	68.4	70.4	70.5	68.9	69.6	0.231	0.360	0.258	0.328	0.294	0.056	0.016	0.3497
15:50	185	34.2	65.1	67.4	64.9	65.8	62.5	61.3	62.7	62.7	61.6	62.1	0.187	0.290	0.208	0.265	0.237	0.045	0.011	0.2411
16:00	336	35.1	62.9	65.7	62.4	63.7	60.1	58.6	60.1	60.1	58.8	59.4	0.167	0.261	0.187	0.236	0.213	0.040	0.009	0.1063
16:10	286	35.4	60.9	63.5	60.3	61.6	58.2	56.8	58.2	58.2	57.0	57.6	0.156	0.243	0.174	0.221	0.198	0.037	0.007	0.1087
16:20	267	34.0	63.0	66.0	62.5	63.8	60.1	58.6	60.2	60.2	58.9	59.5	0.169	0.264	0.188	0.239	0.215	0.041	0.009	0.1368
16:30	659	34.9	66.6	70.5	65.5	67.5	62.7	60.4	62.6	62.6	60.8	61.6	0.181	0.284	0.203	0.256	0.231	0.044	0.010	0.0640
16:40	584	35.2	70.8	74.6	69.9	71.8	66.7	64.3	66.7	66.8	64.8	65.7	0.209	0.327	0.234	0.295	0.266	0.050	0.013	0.0959
16:50	385	33.6	73.1	76.7	72.3	74.0	69.0	66.5	69.0	69.1	67.1	67.9	0.224	0.351	0.250	0.318	0.286	0.054	0.015	0.1678
17:00	453	34.1	75.4	79.3	74.5	76.4	71.0	68.3	70.9	71.0	68.8	69.8	0.237	0.371	0.264	0.336	0.302	0.057	0.017	0.1592

Table 5b: Raw Data of Run #5

Time	T _{h1}	T _{h2}	T _{h3}	T _{h4}	T _{h5}	T _{h6}	T _{h7}	T _{h8}	T _{h9}	T _{h10}	T _{h11}	T _{h12}	T _h	T _{e1}	T _{e2}	T _{e3}	T _{e4}	T _{e5}	T _{e6}	T _{e7}	T _{e8}	T _{e9}	T _{e10}	T _{e11}	T _{e12}	T _e
10:30	33.0	39.0	39.0	38.7	38.9	38.8	38.4	38.8	39.0	38.6	38.0	38.4	38.2	30.9	31.4	30.9	31.4	31.8	31.5	31.3	31.3	31.0	31.0	31.2	31.0	31.2
10:40	33.7	41.6	41.7	41.3	41.6	41.5	41.1	41.6	41.8	41.3	40.7	40.9	40.7	30.5	31.2	30.5	31.1	31.6	31.4	31.0	31.1	30.8	31.0	31.3	31.1	31.1
10:50	34.8	43.4	43.6	43.2	43.5	43.4	43.1	43.5	43.8	43.3	42.6	42.9	42.6	30.9	31.6	30.9	31.6	32.2	31.9	31.5	31.6	31.2	31.6	31.9	31.8	31.6
11:00	35.7	45.5	45.6	45.2	45.5	45.5	45.0	45.5	45.8	45.2	44.5	44.7	44.5	31.1	31.9	31.1	31.9	32.6	32.3	31.8	31.9	31.5	32.1	32.4	32.2	31.9
11:10	36.1	47.6	47.7	47.3	47.7	47.6	47.1	47.7	48.0	47.3	46.5	46.8	46.5	31.5	32.5	31.5	32.4	33.2	32.7	32.2	32.3	31.9	32.6	32.9	32.7	32.4
11:20	36.8	49.8	49.9	49.5	49.9	49.8	49.3	49.9	50.2	49.4	48.5	48.8	48.5	31.5	32.6	31.5	32.6	33.5	33.0	32.4	32.5	32.1	32.7	33.1	32.9	32.5
11:30	37.1	52.0	52.2	51.7	52.2	52.1	51.4	52.1	52.5	51.5	50.6	50.9	50.5	31.8	33.0	31.9	33.0	34.0	33.5	32.8	32.9	32.5	33.2	33.6	33.3	33.0
11:40	38.0	53.1	53.3	52.8	53.2	53.1	52.5	53.1	53.6	52.5	51.5	51.8	51.5	31.7	33.0	31.7	32.9	34.0	33.4	32.7	32.8	32.3	33.0	33.4	33.1	32.8
11:50	39.0	54.9	55.1	54.6	55.0	54.9	54.2	54.9	55.3	54.2	53.1	53.4	53.2	31.9	33.4	31.9	33.2	34.3	33.7	33.0	33.1	32.5	33.2	33.7	33.3	33.1
12:00	38.7	56.8	57.0	56.4	56.8	56.7	55.9	56.6	57.1	55.9	54.8	55.1	54.8	32.3	33.8	32.3	33.7	34.9	34.2	33.4	33.6	32.9	33.6	34.1	33.7	33.5
12:10	40.4	59.7	59.9	59.2	59.8	59.6	58.7	59.4	59.9	58.6	57.5	57.7	57.5	32.9	34.6	33.0	34.5	35.8	35.0	34.2	34.3	33.6	34.3	34.8	34.4	34.3
12:20	40.6	61.1	61.3	60.6	61.1	60.9	60.1	60.8	61.3	59.9	58.8	59.0	58.8	32.8	34.6	32.9	34.5	35.9	35.0	34.2	34.3	33.7	34.3	34.7	34.3	34.3
12:30	40.9	62.7	62.9	62.1	62.8	62.5	61.6	62.3	62.9	61.4	60.2	60.4	60.2	33.0	34.8	33.0	34.6	36.1	35.2	34.3	34.5	33.7	34.4	35.0	34.5	34.4
12:40	40.6	63.8	64.0	63.3	63.9	63.6	62.7	63.4	64.1	62.4	61.2	61.5	61.2	32.7	34.7	32.8	34.5	36.0	35.1	34.2	34.3	33.5	34.2	34.8	34.3	34.3
12:50	40.5	64.2	64.4	63.6	64.2	64.0	62.9	63.7	64.3	62.7	61.5	61.8	61.5	33.0	34.9	33.0	34.8	36.3	35.3	34.4	34.5	33.7	34.3	35.0	34.5	34.5
13:00	41.9	67.4	67.6	66.7	67.4	67.1	66.0	66.8	67.5	65.7	64.4	64.6	64.4	33.8	35.9	33.8	35.8	37.4	36.3	35.2	35.4	34.4	35.1	35.7	35.2	35.3
13:10	42.0	69.9	70.2	69.2	70.0	69.7	68.4	69.3	70.0	68.0	66.7	66.9	66.7	33.7	35.9	33.7	35.8	37.5	36.5	35.3	35.4	34.5	35.2	35.8	35.3	35.4
13:20	42.4	72.4	72.7	71.7	72.4	72.1	70.8	71.7	72.4	70.4	69.0	69.1	68.9	34.0	36.4	34.0	36.2	38.0	36.9	35.7	35.8	34.8	35.6	36.2	35.6	35.8
13:30	45.0	75.3	75.6	74.5	75.3	74.9	73.6	74.5	75.3	72.9	71.5	71.7	71.7	34.6	37.2	34.6	36.9	38.8	37.6	36.3	36.5	35.4	36.2	36.8	36.2	36.4
13:40	44.7	72.8	73.1	72.1	72.8	72.5	71.3	72.2	72.9	70.7	69.3	69.5	69.5	34.0	36.5	34.1	36.3	38.1	36.9	35.7	35.9	34.9	35.6	36.2	35.6	35.8
13:50	42.7	69.5	69.7	68.8	69.5	69.2	68.1	69.0	69.7	67.7	66.3	66.5	66.4	33.8	36.1	33.9	35.9	37.6	36.6	35.4	35.6	34.6	35.3	35.9	35.4	35.5
14:00	41.4	64.0	64.2	63.5	64.1	63.8	62.9	63.7	64.2	62.6	61.4	61.7	61.5	33.4	35.3	33.4	35.2	36.5	35.7	34.7	34.8	34.1	34.7	35.3	34.9	34.8
14:10	41.7	62.9	63.1	62.3	62.9	62.7	61.8	62.5	63.1	61.6	60.5	60.7	60.5	33.4	35.2	33.4	35.1	36.4	35.6	34.7	34.8	34.1	34.8	35.3	34.9	34.8
14:20	39.9	62.2	62.4	61.7	62.3	62.1	61.1	61.9	62.5	61.0	60.0	60.2	59.8	33.4	35.1	33.4	35.0	36.3	35.6	34.6	34.8	34.1	34.8	35.3	35.0	34.8
14:30	42.3	68.7	68.9	68.0	68.8	68.5	67.3	68.1	68.8	67.0	65.8	66.0	65.7	34.4	36.5	34.4	36.5	38.1	37.0	35.8	36.0	35.1	35.9	36.5	36.1	36.0
14:40	44.4	74.1	74.3	73.3	74.1	73.8	72.4	73.4	74.1	71.9	70.6	70.7	70.6	34.6	37.1	34.6	37.0	38.8	37.7	36.4	36.5	35.5	36.3	37.0	36.4	36.5
14:50	45.8	76.8	77.1	76.1	76.8	76.5	75.2	76.2	76.9	74.5	73.1	73.2	73.2	34.8	37.5	34.8	37.3	39.3	38.0	36.6	36.8	35.7	36.5	37.2	36.6	36.8
15:00	44.0	69.4	69.7	68.9	69.5	69.2	68.3	69.1	69.8	67.8	66.5	66.7	66.6	34.0	36.3	34.0	36.1	37.8	36.7	35.6	35.7	34.8	35.5	36.2	35.7	35.7
15:10	42.8	65.8	66.1	65.2	65.9	65.7	64.6	65.4	66.0	64.4	63.3	63.5	63.2	33.9	35.8	33.8	35.7	37.2	36.4	35.2	35.4	34.6	35.4	36.0	35.6	35.4
15:20	42.7	65.6	66.0	65.2	65.8	65.5	64.8	65.6	66.1	64.4	63.2	63.4	63.2	33.8	35.8	33.8	35.8	37.1	36.3	35.2	35.3	34.5	35.3	35.9	35.5	35.4
15:30	44.1	68.8	69.0	68.1	68.9	68.6	67.4	68.2	68.9	67.1	65.9	66.1	65.9	34.1	36.3	34.1	36.2	37.8	36.8	35.6	35.8	34.9	35.7	36.3	35.8	35.8
15:40	43.4	68.6	68.8	68.1	68.6	68.4	67.5	68.3	68.9	67.1	65.8	66.0	65.8	34.0	36.1	34.0	36.1	37.7	36.7	35.5	35.6	34.7	35.5	36.1	35.6	35.6
15:50	41.9	61.3	61.6	61.0	61.4	61.2	60.7	61.4	61.9	60.4	59.4	59.6	59.3	33.2	35.0	33.2	34.9	36.1	35.5	34.5	34.6	33.9	34.6	35.2	34.8	34.6
16:00	41.0	58.5	58.8	58.2	58.7	58.5	57.9	58.6	59.1	57.8	56.8	57.2	56.8	33.3	34.8	33.3	34.9	35.9	35.3	34.4	34.5	33.9	34.6	35.2	34.9	34.6
16:10	40.6	56.7	57.0	56.4	56.9	56.7	56.1	56.8	57.3	56.1	55.2	55.5	55.1	33.1	34.5	33.1	34.5	35.5	35.0	34.2	34.3	33.7	34.4	34.9	34.6	34.3
16:20	40.5	58.6	58.9	58.3	58.8	58.6	57.9	58.6	59.1	57.8	56.8	57.1	56.8	33.0	34.6	33.0	34.5	35.7	35.1	34.2	34.3	33.7	34.5	35.0	34.6	34.4
16:30	41.2	60.4	60.7	60.0	60.6	60.4	59.4	60.2	60.7	59.4	58.4	58.6	58.3	33.1	34.7	33.1	34.7	35.9	35.2	34.3	34.4	33.7	34.5	35.0	34.7	34.4
16:40	42.1	64.5	64.7	64.0	64.6	64.3	63.3	64.1	64.7	63.1	61.9	62.2	62.0	33.1	35.0	33.1	34.9	36.3	35.5	34.4	34.6	33.8	34.6	35.2	34.7	34.6
16:50	42.5	66.8	67.0	66.2	66.9	66.6	65.6	66.4	67.0	65.2	64.1	64.3	64.1	33.2	35.2	33.2	35.2	36.7	35.8	34.6	34.8	33.9	34.7	35.3	34.8	34.8
17:00	43.6	68.5	68.8	67.9	68.6	68.3	67.2	68.0	68.7	66.8	65.6	65.8	65.7	33.0	35.3	33.0	35.1	36.8	35.8	34.6	34.8	33.8	34.6	35.3	34.8	34.7

Table 6: Summary of Run #1

Time	H	T _a	T _{wi}	T _{fin}	T _{cond}	T _h	T _c	T _{wo}	ΔT _w	V _{NL}
	w/m ²	°C	°C	°C	°C	°C	°C	°C	°C	V
9:32	399	29.3	30.1	41.9	37.7	36.8	32.4	32.1	2.0	0.059
9:56	505	30.1	31.0	45.8	43.7	42.9	34.9	34.1	3.1	0.112
10:38	598	32.5	33.3	57.7	54.4	53.2	38.8	37.1	3.8	0.202
11:12	703	33.7	33.9	66.7	62.2	60.7	41.0	38.7	4.8	0.285
12:04	800	35.1	34.3	78.6	72.7	70.5	44.1	41.1	6.8	0.392
15:05	801	38.2	35.1	100.4	92.0	88.9	49.2	44.8	9.7	0.598
15:55	701	36.9	35.0	98.7	90.6	87.7	48.7	44.5	9.5	0.586
16:09	598	37.2	35.0	97.2	89.7	86.9	48.5	44.4	9.4	0.574
16:46	504	36.7	34.5	89.0	82.5	80.1	46.6	43.3	8.8	0.496
17:03	399	36.4	34.2	82.3	76.6	74.6	44.9	41.9	7.7	0.439

Table 7: Summary of Run #2

Time	H	T _a	T _{wi}	T _{fin}	T _{cond}	T _h	T _c	T _{wo}	ΔT _w	V _L	I _L	P _L	η _{TE}
	w/m ²	°C	°C	°C	°C	°C	°C	°C	°C	V	A	W	%
09:35	397	29.2	29.5	42.0	40.2	39.5	32.0	31.1	1.6	0.067	0.013	0.001	0.009
09:58	498	31.3	31.1	49.5	46.5	45.4	34.8	33.7	2.6	0.098	0.018	0.002	0.015
10:58	594	31.9	32.1	56.8	53.1	51.8	36.9	35.2	3.1	0.139	0.026	0.004	0.026
11:11	697	32.5	33.2	62.8	58.2	56.5	38.5	36.2	3.0	0.168	0.032	0.005	0.032
12:25	800	35.0	33.0	80.3	73.8	71.3	42.1	38.6	5.6	0.278	0.052	0.015	0.076
14:01	904	35.5	33.4	88.0	80.2	77.2	43.3	39.5	6.1	0.323	0.061	0.020	0.091
15:22	798	37.3	34.0	98.7	89.6	86.3	45.9	41.4	7.4	0.382	0.072	0.028	0.145
15:30	599	36.1	33.5	95.4	88.0	85.0	45.4	40.9	7.4	0.376	0.071	0.027	0.186
16:02	496	35.1	33.4	91.3	84.4	81.5	44.4	40.3	6.9	0.351	0.066	0.023	0.197

Table 8: Summary of Run #3

Time	H	T _a	T _{wi}	T _{fin}	T _{cond}	T _h	T _c	T _{wo}	ΔT _w	V _L	I _L	P _L	η _{TE}
	w/m ²	°C	°C	°C	°C	°C	°C	°C	°C	V	A	W	%
10:25	599	28.9	27.2	46.2	43.4	42.3	30.4	29.13	1.93	0.11	0.021	0.00	0.0160
11:05	709	29.9	28.3	55.9	51.9	50.3	32.3	30.05	1.75	0.16	0.031	0.005	0.0299
11:55	799	33.2	30.6	68.2	62.9	60.9	36.3	33.28	2.68	0.23	0.043	0.01	0.0522
14:00	895	36.4	32.0	89.4	81.4	78.3	40.1	35.43	3.43	0.36	0.068	0.025	0.1155
15:07	797	35.9	32.3	93.3	84.9	81.7	40.8	35.65	3.35	0.39	0.073	0.028	0.1482
15:48	702	35.3	32.2	91.3	83.2	80.0	40.4	35.70	3.50	0.37	0.071	0.026	0.1577
16:23	607	35.2	32.1	89.5	81.7	78.7	40.2	35.63	3.53	0.36	0.069	0.025	0.1719
16:58	505	34.8	31.8	84.4	77.3	74.7	39.3	35.00	3.20	0.33	0.063	0.021	0.1740

Table 9: Summary of Run #4

Time	H	T _a	T _{wi}	T _{fin}	T _{cond}	T _h	T _c	T _{wo}	ΔT _w	V _L	I _L	P _L	η _{TE}
	w/m ²	°C	°C	°C	°C	°C	°C	°C	°C	V	A	W	%
10:21	496	28.9	26.9	43.5	40.1	39.0	29.7	28.6	1.7	0.085	0.016	0.001	0.012
10:59	605	29.6	29.1	54.1	50.4	49.0	32.9	30.8	1.7	0.146	0.028	0.004	0.028
11:44	703	31.1	31.3	64.6	59.8	58.1	36.3	33.6	2.3	0.202	0.038	0.008	0.046
14:02	800	35.2	32.9	85.5	78.0	75.4	40.9	36.6	3.7	0.325	0.061	0.020	0.104
14:43	701	35.0	33.2	87.0	79.5	76.9	41.6	37.1	3.9	0.333	0.063	0.021	0.125
15:45	606	34.4	33.4	85.4	78.3	75.8	41.5	37.2	3.8	0.323	0.061	0.020	0.136
16:49	498	34.3	33.0	80.1	73.6	71.3	40.3	36.4	3.4	0.293	0.055	0.016	0.136

Table 10: Summary of Run #5

PM	H	T _a	T _{wi}	T _{fin}	T _{cond}	T _h	T _c	T _{wo}	ΔT _w	T _{glass}	V _L	I _L	P _L	η _{TE}
	w/m ²	°C	°C	°C	°C	°C	°C	°C	°C	°C	V	A	W	%
10:24	702	30.6	32.3	39.8	34.9	34.4	32.5	32.4	0.1	36.7	0.016	0.003	0.000	0.000
11:19	800	32.3	31.4	53.8	50.3	49.3	32.6	31.5	0.1	41.9	0.149	0.028	0.004	0.022
12:09	900	33.2	32.2	65.6	60.3	58.8	34.3	32.6	0.3	45.5	0.222	0.042	0.009	0.043
13:15	1000	34.1	32.9	80.1	72.5	70.1	35.7	33.3	0.4	49.7	0.317	0.060	0.019	0.079
14:32	900	35.5	33.4	79.0	71.4	69.0	36.0	33.7	0.3	50.7	0.304	0.057	0.017	0.081
15:14	695	34.6	33.3	75.7	69.3	67.3	36.0	33.8	0.5	46.9	0.287	0.054	0.016	0.094
15:33	799	35.6	33.0	79.7	72.0	69.7	36.0	33.6	0.6	53.6	0.310	0.058	0.018	0.095
16:13	496	35.1	32.8	63.5	58.7	57.3	34.4	32.8	0.0	46.8	0.206	0.039	0.008	0.068
16:51	397	34.4	32.1	74.2	68.0	66.1	34.7	32.5	0.4	47.5	0.286	0.054	0.015	0.163